Hematopoietic Stem Cell-Derived Chimeric Antigen Receptor Expressing Cells Traffic to HIV Reservoir Sites in SHIV-Infected Non-Human Primates

Isaac M. Barber-Axthelm

A thesis

submitted in partial fulfillment of the

requirements of the degree of

Master of Science

University of Washington

2019

Committee:

Hans-Peter Kiem

Brian M. Iritani

Robert D. Murnane

Donald L. Sodora

Program Authorized to Offer the Degree:

Department of Comparative Medicine

University of Washington

Abstract

Hematopoietic Stem Cell-Derived Chimeric Antigen Receptor Expressing Cells Traffic to HIV Reservoir Sites in SHIV-Infected Non-Human Primates

Isaac M. Barber-Axthelm

Chair of the Supervisory Committee:

Hans-Peter Kiem

Department of Medicine

Department of Pathology

The successful treatment of 2 HIV^+ individuals with allogeneic stem cell transplantations has garnered much interest in its utility as a therapy for HIV. However, there are significant limitations that prevent allogeneic stem cell transplantation from being a viable therapy for HIV infection, including toxicity due to Graft-versus-host disease, and the limited availability of donors who are homozygous for the CCR5Δ32 mutation. One viable option to circumvent these limitations and provide a functional cure, through immune-mediated elimination of the virus, is with chimeric antigen receptor (CAR) immunotherapy. By introducing the CAR engineered to target HIV infected cells into hematopoietic stem cells, we have the potential to generate a self-

renewing population of CAR T-cells, thus circumventing some of the limitations with longevity that are seen with CAR T-cells. Here, we report trafficking of hematopoietic stem and progenitor (HSPC)-derived CAR^+ cells to HIV tissue reservoir sites, in a pigtail macaque model of HIV infection. CAR^+ cells were identified in the lymphoid germinal centers, the parenchyma of the central nervous system, and the gastrointestinal tract by immunohistochemistry, almost 2 years after initial engraftment with lentiviral modified HSPCs. Multilineage engraftment of CAR^+ cells were identified in lymphoid germinal centers and the gastrointestinal tract, consisting of T-cells, B-cells, and myeloid lineage cells. CAR^+ B-cells in the germinal centers were also actively replicating, characterized by robust Ki-67 expression. No difference was observed in trafficking, engraftment, and cell cycle activity between CAR animals and control animals that carry a "tailless" CAR which lacks the cytoplasmic signal transduction domain. These results show the HSPC-derived CAR^+ cells will traffic to, and persist in, HIV tissue reservoir sites, with multilineage engraftment of CAR^+ cells. The method could be used as a platform for immunotherapeutic delivery treatment of HIV infection, as well as a variety of other medical conditions.

Acknowledgement

This study was supported by funds from: amfAR ARCHE Awards (108688-54-RGRL, 108929-56-RGRL; Kitchen-PI), NIH U19 and UM1 grants (AI117941, AI126623), and a California Institute of Regenerative Medicine (CIRM) Quest Discovery grant (DISC2-10748). All primate work was completed at the Washington National Primate Research Center (WaNPRC), which is supported by U42 (U42OD011123) and P51 (P51OD010425) grants through the NIH Office of Research Infrastructure Programs (ORIP). All multiplex immunohistochemistry staining, slide scanning, and brightfield quantitative analysis were completed by the Experimental Histopathology Shared Resource of the Fred Hutch/University of Washington Cancer Consortium. This consortium is supported by a P30 Cancer Center Support Grant through NCI (P30 CA015704).

I would like to thank Dr. Charles Frevert, Dr. Brian Johnson, Dr. Stephen Hewitt, Dr. Michael Axthelm, Dr. Jake Estes, and Dr. Robert Murnane for providing their immunohistochemistry expertise for this project.

Thank you also to Dr. Savanh Chanthaphavong, Tracy Goodpaster, Li-Ya Huang, Paul Kong, Kimberley Smythe, and Dr. Robert Pierce for their assistance with the multiplex immunohistochemistry assays and the quantitative image analysis.

Thank you to Valerie Barber-Axthelm for her support with the multiplex quantitative image analysis, and thank you to Kelvin Sze for his assistance with the analysis validation.

Finally, thank you to my mentors, Dr. Hans-Peter Kiem and Dr. Christopher Peterson, for their continued support and guidance throughout this project.

Dedication

This thesis is dedicated to my loving wife, Val, for her constant support and encouragement… I could not have done this without you.

Table of Contents

List of Figures

List of Abbreviations

AIDS- Acquired immunodeficiency syndrome
BBB- Blood-brain-barrier
BMI1- BMI1 Polycomb Ring Finger Oncogene
bNAbs- Broadly neutralizing antibody
cART- Combination antiretroviral therapy
CAR- Chimeric antigen receptor
CCND2- Cyclin D2
CCR5- C-C chemokine receptor type 5
CCR5Δ32- A mutant CCR5 allele that contains a 32 base pair deletion in the second extracellular loop
$CCR5^{(\Delta32/\Delta32)}$- An individual that is homozygous for the CCR5Δ32 mutation
CD4CAR- Chimeric antigen receptor consisting of a CD4 extracellular and transmembrane domain, with a CD3ζ signal transduction domain
CD4CARΔζ- Chimeric antigen receptor consisting of a CD4 extracellular and transmembrane domain
CD3ζ- CD3 zeta chain of the T-cell receptor-CD3 complex
CNS- Central nervous system
CTL- Cytotoxic T-lymphocytes
CXCR4- C-X-C chemokine receptor type 4
DAB- 3,3’ diaminobenzidine
DPBS- Dulbecco's phosphate-buffered saline
Dual-tropic- HIV strains that can use either CCR5 or CXCR4 as a coreceptor to facilitate membrane fusion and viral entry
EGFR- Epidermal growth factor receptor
FDC- Follicular dendritic cell
FcRγ- Fc receptor gamma chain
γc chain- The common gamma chain
GIT- Gastrointestinal tract
GALT- Gastrointestinal lymphoid tissue
GvHD- Graft-versus-host disease
HDACi- Histone deacetylase inhibitor
HIER- Heat-induced epitope retrieval
HER2- Human epidermal growth factor receptor 2
HIV- Human Immunodeficiency Virus
HOXB4- Homeobox B4
HRP- Horseradish peroxidase
HSPC- Hematopoietic stem and progenitor cell
IHC- Immunohistochemistry
IV- Intravenous
Lck- Tyrosine-protein kinase Lck
LMO2- LIM domain-only 2
mIHC- Multiplex immunohistochemistry
PBMC- Peripheral blood mononuclear cells
P.O.- *per os*

q24h- Every 24 hours
q12h- Every 12 hours
R5-tropic- HIV strains that can use CCR5 as a coreceptor to facilitate membrane fusion and viral entry
Rag2- Recombinase activating gene-2
ROI- Region of Interest
S.C.- Subcutaneously
SHIV- Simian/Human Immunodeficiency Virus
SIV- Simian Immunodeficiency Virus
TDL- Thoracic duct lymph
X4-tropic- HIV strains that can use CXCR4 as a coreceptor to facilitate membrane fusion and viral entry
ZO-1- Zonula occludens-1

Introduction

Hematopoietic stem and progenitor cell (HSPC) transplantation has emerged as a promising approach to achieve a functional HIV cure, in large part due to the functional cure of 2 chronically infected HIV^+ patients with allogeneic stem cell transplantations: Timothy Ray Brown (aka. the "Berlin Patient"), and the "London Patient."[1–4] In both clinical cases, the patients received HSPCs from donors who were homozygous for a 32 base pair deletion in the second extracellular loop of the CCR5 gene ($CCR5^{\Delta 32/\Delta 32}$) that introduces a premature stop codon, resulting in a truncated protein that is not expressed on the cell surface.[5–8] The successful eradication of the virus in these 2 patients is hypothesized to have occurred due to a combination Graft-versus-Host Disease (GvHD) mediated elimination of host-derived HIV^+ cells (frequently referred to as "Graft-versus-Virus" or "Graft-versus-Reservoir"), and rapid and high-level engraftment of donor derived cells [9–13]. The GvHD mediated removal of latently infected host cells is similar to what has been observed in leukemia patients treated with allogeneic stem cell transplantations (referred to as "Graft-versus-Leukemia"), where prolonged periods of remission were observed in individuals who developed acute and or chronic GvHD, indicating an antileukemic effect of GvHD.[14–15] Because CCR5 is the major co-receptor for viral envelope fusion,[16–11] individuals with a $CCR5^{(\Delta 32/\Delta 32)}$ genotype have improved resistance to HIV infection compared to individuals with a $CCR5^{(WT/WT)}$ genotype, and those with $CCR5^{(\Delta 32/WT)}$ heterozygosity show slower decreases in peripheral CD4 T-cell counts and longer timer periods to the development of AIDS compared to $CCR5^{(WT/WT)}$ individuals.[19] The generation of HIV-resistant cell populations through reconstitution with $CCR5^{(\Delta 32/\Delta 32)}$ HSPCs is believed to be an important component to the functional cure observed in the Berlin and London patients. This is

supported by the results of the "Boston Patients," where HIV recrudescence was observed in 2 chronically infected patients following allogeneic stem cell transplantation with $CCR5^{(WT/WT)}$ HSC's, following a prolonged period of remission.[20]

Despite the success seen with the "Berlin Patient" and the "London Patient," there are multiple limitations that prevent allogenic stem cell transplantation from being a viable therapy for HIV patients. The principle concern is the risk of serious complications associated with the allogeneic HSPC transplant, including but not limited to graft-versus-host disease (GvHD), opportunistic infections, and toxicities associated with the pre-transplantation conditioning regimen and post-transplantation immunosuppressive regimens. [21,22] The treatment of HIV^{+} patients poses additional risks, due to the potential for interactions between the immunosuppressive agents necessary to allow engraftment and prevent GvHD and cART, resulting in additional toxicities.[23] Both the Berlin and London patients underwent allogeneic stem cell transplantations to treat hematological neoplasms that were refractory to first- and second-line treatments. It is unlikely that allogeneic stem cell transplantation will be a viable option for treatment of HIV infections, due to the significant risk associated with the procedure. Additionally, the prevalence of individuals with a $CCR5^{(\Delta32/\Delta32)}$ genotype range from 0-3.1% of the population, with significant variation dependent on geography and ancestry.[24–30] Because of this low frequency of individuals that are homozygous for the CCR5 mutation, it is unlikely that suitable donors could be identified for the approximately 36.9 million people worldwide who are infected with HIV (Source: World Health Organization). Additionally, individuals who are $CCR5\Delta32^{(\Delta32/\Delta32)}$ have a 21% increase in all-cause mortality rates compared to $CCR5^{(WT/WT)}$ and $CCR5\Delta32^{(\Delta32/WT)}$ individuals, suggesting the homozygous mutations may have deleterious physiologic effects, which could preclude its usage in bone marrow transplantation.[31] Finally,

there is evidence that the virus is able to circumvent the CCR5Δ32 mutation via a shift in tropism from CCR5 to CXCR4, and mount an infection.[31,33] While use of allogeneic stem cell transplantation with CCR5Δ32$^{(\Delta32/\Delta32)}$ donors is not a viable option as an HIV therapy, what we have learned from the Berlin and London patients can be applied to alternative approaches which are less toxic, can be utilized to treat a large patient population including individuals in developing nations, and achieves comparable levels of immune-mediated viral elimination as was seen with the Berlin and London patients. One viable option to accomplish this is through autologous immunotherapeutic approaches.

HIV-1 adaptation to CCR5 mutations via shift in viral tropism (R5-tropic HIV to predominately X4-tropic HIV) has been observed in humans following allogenic stem cell transplantation with CCR5$^{(\Delta32/\Delta32)}$ donor HSPCs,[32,33] or treatment with Maraviroc (Pfizer Global R&D, Sandwich, UK), a CCR5 antagonist.[34,35] It is likely that the patients that experienced viral rebound following CCR5$^{(\Delta32/\Delta32)}$ allogenic stem cell transplantation carried a small population of R4-tropic virions prior to transplantation, which expanded post-transplantation due to selective pressure from the CCR5$^{(\Delta32/\Delta32)}$ engrafted cells. The usage of alternative chemokine co-receptors has also been observed in HIV infected individuals who naturally carry the CCR5$^{(\Delta32/\Delta32)}$, where the predominant viral variants were X4-tropic, dual-tropic, or utilized alternative chemokine co-receptors. [36,37] Due to the potential of HIV circumventing the usage of CCR5 as a co-receptor, a more universal method should be considered to block viral infection.

One such approach is the C46 fusion-inhibitory peptide. [38,39] This peptide is derived from the C-terminal heptad repeat of the HIV gp41 transmembrane glycoprotein, and is hypothesized to block fusion of the viral envelope with the plasma membrane by disrupting the α-helical structure of the leucine-zipper-like domain of gp41.[40] This α-helical structure of the HIV gp41 is

highly conserved: amino acid substitutions result in impaired viral infectivity.[41–44] This structure has been used as a target for pharmaceutical fusion inhibitors, as part of a cART regimen.[45–47] Previous clinical trials have shown that autologous T-cells transduced with C46 persisted throughout the 1 year period that the patients were followed, with no clinical evidence of toxicity.[48] The evidence supporting C46, combined with its mechanism of targeting a highly conserved, tropism-independent region of the virus, makes C46 an ideal candidate to generate HIV-resistant cell populations.

The use of chimeric antigen receptors (CARs), which originally demonstrated efficacy in achieving remission of various malignancies by redirecting cytotoxic T-lymphocytes to recognize and destroy neoplastic cells in vivo,[49–59] has yielded positive results as a potential curative HIV therapy. Primary human $CD8^+$ T-cells transduced with an HIV-specific CAR consisting of a CD4 extracellular and transmembrane domain fused to the CD3ζ signal transduction domain (CD4CAR) effectively lyse HIV infected immortalized cell lines and primary human cell lines *in vitro*.[60,61] This CAR recognizes the CD4 binding domain of the HIV Env protein when it is expressed on the plasma membrane of infected cells. The permits CAR T-cells to mediate lysis of HIV infected cells independent of MHC presentation of viral epitopes, circumventing the viral mediated downregulation of MHC I.[62,63] Additionally, four clinical trials have demonstrated safety and long-term engraftment of autologous and syngeneic T-lymphocytes engineered to express the CD4CAR via *ex vivo* retroviral vector transduction, through PCR-based quantitation from PBMCs and rectal biopsies.[64–67] The reported *in vivo* antiviral efficacy of CD4CAR transduced T-cells is mixed: 2 trials reported limited clinical efficacy (transiently reduced plasma viral load, reductions in replication competent virions isolated from the blood, and reductions in proviral DNA and viral RNA in rectal biopsy

specimens in CD4CAR treated patients).[64,67] One study reported no evidence of *in vivo* antiviral activity following CD4CAR T-cell administration.[63]

Current data suggests CAR T-cell therapy for HIV-1 is limited by the need for significant *ex vivo* expansion of gene modified T-lymphocytes to reach a therapeutic amount, which in turn may limit the persistence of cells *in vivo*.[50,68–71] These barriers could be circumvented with the use of genetically modified HSPCs transduced with a CAR, which allows continuous production of CAR T-cells that undergo normal physiologic development, increasing the potential for immunologic memory without the need for significant *ex vivo* expansion.[68,70,71] Genetically modifying HSPC's also permits multilineage engraftment of CAR-modified cells. HSPC's transduced with CD4, CD19, and HER2 CARs have been shown to generate CAR expressing B-cells, myeloid cells, and NK cells *in vivo*.[68,72–74]Additionally, NK cells and neutrophils have been shown to have CAR specific cytolytic activity mediated by CD4, CD19, CD33, and epidermal growth factor receptor (EGFR) CARs *in vitro* and *ex vivo*.[68,75–80] CD4-CAR transduced immortalized NK Cells (NK3.3 cell line) show CAR directed cytolytic activity when co-cultured with HIV-1 IIIB-infected immortalized human T-cells (CEM.NKR cell line), demonstrating cytolytic efficacy against HIV infected cells.[75] Similarly, EGFR-CAR transduced immortalized NK cells (NK-92 cell line) have been shown to reduce tumor burden and improve survival, compared to mock-transduced NK-cells and untreated control animals in a murine orthotopic glioblastoma model.[79] Multilineage CAR-mediated cytotoxicity, which can be generated through transduction of HSPCs with CARs, could be beneficial in the setting of an HIV infection, by generating a multilineage pool of CAR^+ cells that could identify and lyse HIV-infected cells.

Zhen, Peterson, et al. (2017) previously evaluated the efficacy of HSPC-derived CD4CAR T-cells in a pigtail macaque HIV model.[73] The protocol for the HSPC transplantation

and the experimental timeline are depicted in Figure 1. The C46 fusion inhibitor was included in the lentiviral vector in addition to the CAR, to prevent SHIV infection of gene modified cells through CD4CAR binding. CD4CAR-C46 transduced Jurkat cells were resistant to HIV infection *in vitro*, compared to cells transduced with only the CD4CAR, confirming that the addition of the C46 construct confers resistance to HIV infection. All animals maintained multilineage engraftment of CAR expressing cells in peripheral blood and in lymphoid and non-lymphoid tissues for the ~1.8-year duration of the study. Macaques that received the CD4CAR had increased gene marking in the peripheral blood with expansion of the peripheral CAR^+ effector T-cell population during periods of active viral replication, compared to control animals that received a CD4 CAR that lacked the CD3ζ signal transduction domain. The expansion of CAR^+ cells is believed to be viral antigen mediated as the increase in peripheral blood gene marking correlated with increases in plasma viral load. Compared to control animals, CAR animals had significantly lower lymphoid, CNS, and GIT tissue viral loads, suggesting a CAR-mediated reduction in active viral replication in these tissue sites. Notably, CAR animals also had a lower rebound plasma viremia post cART withdrawal compared to control animals but did not achieve complete viral suppression. One possible explanation for incomplete viral suppression is that HSPC-derived CAR T-cells are not migrating to physiological reservoir sites.

The ability of CAR-modified cells to traffic to, and persist in, HIV tissue reservoir sites where target cells reside is a central consideration for any CAR immunotherapy. Multiple tissue sites have been identified as potential HIV reservoirs, including but not limited to lymphoid germinal centers (GC's), [81-87,104-107] central nervous system (CNS), [86,88-93] and gastrointestinal tract (GIT).[86,87,94-103] The physiologic properties that allow these sites to function as HIV reservoirs vary, and include: i) persistence of detectable proviral DNA and viral RNA after

prolonged periods of complete cART-dependent suppression of plasma viremia, ii) resident cell populations that support latent viral infection and/or active viral replication after prolonged cART, iii) resident cells that retain infectious virions for prolonged periods of time, and iv) the immune privileged sites which potentially exclude effectors that are necessary for viral clearance. For a CAR therapy to control viral replication in the absence of cART (terms such as "functional cure" and "functional remission" are frequently used interchangeably), CAR^+ must traffic to HIV tissue reservoir sites, recognize, and kill infected cells. In the present study, we ask if HSPC-derived, CAR-expressing cells traffic and persist in HIV tissue reservoir sites, via immunohistochemistry-based assays, evaluating macaque tissues originally reported in *Zhen, Peterson, et al*.[73] We show that HSPC-derived, CAR-expressing cells traffic to and persist long term in, lymphoid GCs, CNS tissue, and GIT. Additionally, we show multilineage engraftment, and evidence of active proliferation, of engrafted CAR^+ cells.

Materials and Methods

Autologous HSPC transplantation

NHP studies were conducted as described previously.[73] Juvenile male pigtail macaques were utilized for these studies. Animals were primed with granulocyte colony stimulating factor and stem cell factor for 4 days prior to collection of bone marrow aspirates and bead-based sorting for $CD34^+$ HSPCs. Stem cells were cultured *ex vivo* for 48 hours, during which time the cells were transduced twice with lentiviral vectors at a multiplicity of infection of 5-10. Table 1 summarizes the experimental manipulations for each study macaque.

NHPs were transplanted with autologous, lentiviral modified HSPCs following myeloablative conditioning consisting of a fractionated dose of 1020cGy total body irradiation over a 2-day period. Two experimental animals (CAR 1 and CAR 2) were transplanted with HSPCs that were transduced with lentiviral vectors expressing the membrane fusion inhibitor c46[38,108], and a CAR consisting of a human CD4 extracellular and transmembrane domain with a CD3ζ signaling domain (CD4CAR).[60,61,72,73] control animals (control 1 and control 2) were transplanted with HSPCs that expressed c46 and a "tailless" CD4CAR which lacks the cytoplasmic signal transduction domain, rendering the CAR incapable of signaling when bound to antigen. This study was conducted as a pilot, and no statistical methods were used to pre-determine NHP group size.

Animals recovered for at least 200 days following HSPC transplantation, before SHIV challenge. NHPs were challenged IV with 500µl of SHIV1157ipd3n4, a replication competent, CCR5 tropic SHIV.[109,110] The stock was determined to have a titer of 1.9×10^4 $TCID_{50}$/ml in TZM-bl cells *in vitro*, prior to *in vivo* administration. cART, consisting of Tenofovir (20mg/kg)

+ Emtricitabine (40mg/kg) S.C. q24h, and Raltegravir (150mg P.O. q12h), was initiated approximately 24 weeks post viral challenge, to model treatment of a chronically infected HIV patient. cART was administered for 28 weeks, and the NHPs were monitored for approximately 15 weeks post-cART withdrawal to simulate viral rebound.

At the time of necropsy, representative lymphoid, CNS, and GIT tissues were preserved in 4% paraformaldehyde diluted (15714; Electron Microscopy Science, Hatfield, PA) in DPBS (14190-144; Thermo Fisher Scientific, Waltham, MA) for 24 hours at room temperature at a minimum ratio 1:10 tissue: fixative. Tissues were subsequently transferred to 80% ethanol and stored at 4°C for approximately 48-96 hours prior to processing and paraffin embedding.

Representative tissues from macaques that did not receive a CAR transgene were utilized as controls. CAR negative animals consisted of NHPs that were transplanted with HSPCs transduced with lentiviral vectors expressing the membrane fusion inhibitor c46.[111] Representative tissues were collected, preserved, and processed in an identical manner as the tissues from the CAR and control animals.

All animal studies were conducted in accordance with the Guide for the Care and Use of Laboratory Animals and the Public Health Assurance Policy, and were approved by the Institutional Animal Care and Use Committees of the Fred Hutchinson Cancer Research Center and the University of Washington (Protocol #'s 3235-01). The Fred Hutchinson Cancer Research Center and the University of Washington are full AAALAC accredited institutions.

Brightfield Immunohistochemistry

Single label immunohistochemical staining against human CD4 was utilized to identify CAR expressing cells in NHP tissues. Paraformaldehyde-fixed paraffin-embedded tissues were

sectioned at 4µm onto positively charged slides and baked for 1 hour at 60°C. Sections were deparaffinized in xylene and rehydrated through a graded ethanol series followed by deionized water. HIER was accomplished by incubating the section in Tris-EDTA buffer (0.01M Trizma base, 0.001M EDTA, 0.05% Tween-20 [pH 9.0]) for 20 minutes at approximately 95°C- 97°C in a commercial rice cooker, with an additional 20 minutes to allow the buffer to cool prior to rinsing the sections. Endogenous peroxidase activity was quenched with a 15-minute incubation of 3% hydrogen peroxide at ambient temperature. The sections were incubated for 1 hour at ambient temperature in a humidified chamber with rabbit anti-CD4 antibody (clone: SP35) (MA5-16338 or MA1-39582, 1:50 dilution; Thermo Fisher Scientific, Waltham, MA) following a 20-minute protein block at ambient temperature (X0909; Dako, Carpinteria, CA). The primary antibody was diluted to an appropriate working concentration with a commercial antibody diluent (559148; Becton Dickinson, Franklin Lakes, NJ). A horse anti-rabbit IgG poly-HRP (MP-7401; Vector Laboratories, Burlingame, CA) was utilized for secondary antibody labeling, and antigen-antibody complexes were visualized with DAB (550880; Becton Dickinson, Franklin Lakes, NJ). Slides were counterstained with hematoxylin (S3302; Dako, Carpinteria, CA), dehydrated through a graded ethanol series followed by xylene, and mounted with Permount mounting media (SP15-100; Fisher Scientific, Hampton, NH). Sections were washed for 5 minutes twice in TBST (0.02M Trizma base, 0.15M NaCl, 0.1% Tween-20 [pH 7.6]) at ambient temperature after being incubated with the 3% hydrogen peroxide, the primary antibody, and the secondary antibody. Controls consisted of sections of human tonsil and lymphoid tissues from pigtail macaques that did not receive a CAR that were processed in an identical manner, as well as sections labeled with non-specific, isotype-matched rabbit antibody (08-6199; Invitrogen, Carlsbad, CA).

Multiplex Fluorescent Immunohistochemistry

Fluorescent multiplex IHC (mIHC) of lymphoid and GIT sections was accomplished utilizing the OPAL labeling method.[112] Tables 2-4 outline each fluorescent mIHC panel utilized with the antibodies, fluorophores, and their respective positions in each mIHC panel. Paraformaldehyde-fixed paraffin-embedded tissues were sectioned at 4µm onto positively charged slides and baked for 1 hour at 60°C. The sections were then deparaffinized and stained on a Leica BOND Rx stainer (Leica, Buffalo Grove, IL) using Leica Bond reagents for dewaxing (Dewax Solution; AR9222), antigen retrieval and antibody stripping (Epitope Retrieval Solution 2; AR9640), and rinsing after each step (Bond Wash Solution; AR9590). A high stringency wash was performed after the secondary and tertiary applications using high-salt TBST solution (0.05M Trizma base, 0.3M NaCl, 0.1% Tween-20 [pH 7.2-7.6]). OPAL Polymer HRP Mouse plus Rabbit (ARH1001EA; PerkinElmer, Hopkington, MA) was used for all secondary antibody applications.

Antigen retrieval and antibody elution steps were performed at 100°C with all other steps at ambient temperature. Endogenous peroxidase was blocked with 3% H_2O_2 for 8 minutes followed by protein blocking with TCT buffer (0.05M Tris, 0.15M NaCl, 0.25% Casein, 0.1% Tween 20 [pH 7.5-7.7]) for 30 minutes. The first primary antibody (position 1) was applied for 60 minutes followed by the secondary antibody application for 10 minutes and the application of the tertiary TSA-amplification reagent (OPAL fluorophores; PerkinElmer, Hopkington, MA) for 10 minutes. The primary and secondary antibodies were eluted via incubation with the retrieval solution for 20 minutes before repeating the process with the second primary antibody (position 2) starting with a new application of 3% H_2O_2. The process was repeated until all positions for the respective panel were completed; however, there was no stripping step after the last position.

Slides were removed from the stainer and stained with Spectral DAPI (FP1490; PerkinElmer, Hopkington, MA) for 3 minutes, rinsed for 5 minutes, and coverslipped with Prolong Gold Antifade reagent (P10144; Invitrogen/Life Technologies, Grand Island, NY). Slides were cured for 24 hours at room temperature prior to digital image acquisition.

Brightfield Image Analysis

Slides were scanned in Brightfield at a 20x objective using an Aperio ScanScope AT Imaging System (Leica Biosystems, Wetzlar, Germany). Digital images were imported into HALO software (Indica Labs, Albuquerque, NM) for analysis. Regions of interest (ROIs) were manually drawn around relevant areas, and the Indica Labs' Area Quantification module (Version 1.0) was utilized to determine the percentage area of CAR marking in each ROI. The software was trained to differentiate DAB-positive staining versus DAB-negative hematoxylin-positive staining based on threshold values for individual pixels, and the images were batch processed using these configurations. The output values (Total area, DAB-positive area, DAB-negative hematoxylin-positive area), were transferred to Microsoft Excel (Microsoft Corporation, Redmond, WA) and used to calculate a ratio of CAR marking to tissue area within the ROIs for lymphoid and CNS tissues, as has been previously described.[113] Aperio ScanScope digital images were imported into QuPath (version 0.2.0-m2), and regions of interest were annotated and exported to Fiji (ImageJ).[114–117] Figures were subsequently generated using FigureJ.[111]

Fluorescent Image Analysis

For lymphoid section, representative images were acquired on a Vectra 3.0 Automated Imaging System at a 20x objective (PerkinElmer, Hopkington, MA). Images were spectrally

unmixed using PerkinElmer inForm software (PerkinElmer, Hopkington, MA) and exported to Fiji (ImageJ) as multi-image TIFFs for colocalization analysis.[115–117]

For GIT sections, slides were scanned at a 20x objective using an Aperio ScanScope FL Imaging System (Leica Biosystems, Wetzlar, Germany). Aperio ScanScope digital images were imported into QuPath (version 0.2.0-m2), and regions containing GALT were annotated and exported to Fiji (ImageJ) for colocalization analysis.[114–117] Individual regions were appended together to facilitate image binarization and analysis using a custom built, Eclipse-compiled plugin that is compatible with ImageJ (Eclipse Foundation, Inc. Ottawa, Ontario, Canada) (Plugin Name: Append Images; Web Address: https://github.com/circuitBreaker7/Append_Images). The plugin stitches individual multi-channel fluorescent images together independent of individual image dimensions, and without altering individual pixel fluorescent intensities.

All mIHC images were analyzed for colocalization in an identical manner, using an area analysis approach to determine the percent area occupied by each phenotypic marker, following individual marker binarization; like the approach utilized for singleplex brightfield area analysis.[113,119] Overlapping binarized phenotypic markers indicates marker colocalization. All image analysis was performed using Fiji.[115–117] The image binarization protocol is based on binarization methods described for Automated Quantitative Analysis (AQUA).[120] The protocol for fluorescent image binarization and colocalization analysis is depicted in Figure 2. Briefly, individual lymphoid images and appended GALT images were separated into individual fluorescent channels using the "Stack to Images" macro. The channels were renamed with the corresponding animal ID, tissue site, image number, and phenotypic marker. Each channels was subsequently binarized using the following process: 1) Rolling-Ball background correction

(Rolling-ball radius: 50 pixels);[121] 2) Threshold using the thresholding macro, followed by conversion to an 8-bit binary image; 3) Remove outlying pixels with the Remove Outliers macro (Radius: 2 pixels; Threshold: 50 pixels; Remove bright outliers). Automatic thresholds for each channel were generated using the Ostu thresholding plugin.[122] Automatically thresheld images were reviewed by an observer, and adjustments to the thresholds were made as needed. Individual channels for each image were subsequently stacked together using the "Images to Stacks" tool. Regions of interest were defined around germinal centers and GALT in lymphoid and GIT sections respectively, using the Freehand selection tool, and saved using the ROI manager. Individual macros were written to expedite the image binarization process. Figures 3 and 4 show the macro code used for binarizing the lymphoid and GIT mIHC images.

Colocalization analysis of binarized mIHC stacks was completed using a custom built, Eclipse-compiled plugin that is compatible with ImageJ (Eclipse Foundation, Inc. Ottawa, Ontario, Canada) (Plugin Name: Multiplex Pixel Colocalization; Web Address: https://github.com/circuitBreaker7/Multiplex_Pixel_Colocalization). Briefly, the plugin creates a list of 2^n potential outcomes, where n represents the number of slices in each image stack, indicating the number of fluorescent channels in the image. As an example, the GIT sections were labeled with a 3-color mIHC assay (CD4CAR, CD3, CD20), and have 4 slices in each stack (CD4CAR, CD3, CD20, DAPI). Therefore, there are $2^4=16$ potential outcomes when analyzing these images. At each pixel coordinate, the plugin generates a binary number based on the pixel intensity of each slice at the same position; where a 0 represents a pixel that has 0 intensity, and 1 represents a pixel that has an intensity above the threshold. For 8-bit binarized images, the intensities above the threshold are automatically set to 255. The binary number generated from each pixel position are used to index an array that represents the 2^n potential outcomes, and

increment the appropriate count based on the binary number. Figure 5 depicts the process for image colocalization. The output is a pixel count for the number of pixel positions that fulfilled each potential outcome, where pixel positions with phenotypic markers above the threshold were considered colocalized. The plugin also requests ROI information prior to the colocalization analysis and adjusts intensity of pixel positions outside of the ROIs to *0* prior to colocalization analysis. A subset of binarized image stacks were utilized to validate the plugin, with the ImageJ Image Calculator Macro. Stacks of known colocalization were generated by multiplying binary slices to each other for full colocalization, or 1 slice was multiplied by the reciprocal of another slice to generate an image with no colocalization. The slices were subsequently recombined into stacks and analyzed using the Multiplex Pixel Colocalization plugin, and the results were reviewed to confirm consistency with the known outcomes.

The pixel counts for each potential outcome were transferred to Microsoft Excel and used to calculate a ratio of CAR marking to tissue area, as well as the percentage of CAR colocalization with different phenotypic markers. Tissue area was determined by the number of pixels that had an intensity above the threshold for at least one fluorescent marker or DAPI, similar to what has been previously described for brightfield area analysis with hematoxylin counterstain.[113] The percentage of CAR colocalization with different phenotypic markers was determined by the percentage of different phenotypic marker combinations within the GALT and germinal centers that were colocalized with the CD4CAR marker. Different combinations of phenotypic markers colocalizing at the same pixel position were used to determine the expected cell phenotypes. Table 5 illustrates what different phenotypic marker combinations correlated to different cell types. The presence of CAR^+ cells were based on the CD4CAR IHC marker colocalizing with different phenotypic markers. The pixel aspect ratios and the pixel/μm

conversion factor from the Aperio ScanScope FL and the Vectra 3.0 Imaging Systems were used to calculate the areas occupied by different fluorescent markers, based on the pixel counts.

Binarized images of $CAR^{+}CD3^{+}$ and $CAR^{+}CD3^{+}CD8^{+}$ pixels from representative images were generated to qualitatively evaluate CAR colocalization with T-cells, using the Image Calculator Macro in Fiji.[115–117] This was accomplished by sequentially combining binarized images from a stack using the multiply function. By multiplying an image with a second image or the inverse of a second image (denoted as [*phenotypic marker]*$^{-1}$), colocalized or non-colocalized pixels can be sequentially selected. For T-cells, the following pixel selection parameters were utilized: $[CD4CAR][CD3][CD8]^{+/-}[CD20]^{-1}[CD68/CD163]^{-1}$. The resulting binarized images were overlayed on the original fluorescence images, to qualitatively evaluate phenotypic T-cell marker colocalization with the CD4CAR marker. A subset of fluorescent images were utilized as a test set to evaluate the analysis method, by comparing pixel counts from individual and appended binarized regions for consistency, along with manual cell counts from an independent observer (Figure 6).

Results

CD4CAR specific IHC assay specifically labels CD4CAR-modified cells

The first goal in this study was to identify an antibody reagent that would label the human CD4 extracellular domain of CD4CAR, without also labeling the closely related endogenous pigtail macaque CD4 protein. We identified a monoclonal anti-CD4 antibody (Clone: SP35) that satisfied these criteria. Lymphoid tissues from animals that received CAR-transduced HSPCs show immunoreactivity for the CD4 (SP35) antibody (Figure 7. CAR specific immunoreactivity was seen in tissues from both CAR and control animals, indicating the CD4 (SP35) antibody could bind to the CD4CAR and the CD4CARΔζ constructs. In contrast, lymphoid tissues from pigtail macaques that did not receive CD4CAR transduced cells did not display any CD4 (SP35) specific immunoreactivity. Lymphoid tissues from CAR-transduced and non-transduced pigtail macaques show no immunoreactivity when the CD4 antibody was substituted for a rabbit isotype control antibody. Additionally, sections of human tonsil showed CD4 (SP35) specific immunoreactivity predominately in the parafollicular T-cell zones (i.e. was recognizing human CD4+ T-cells), supporting that the antibody was binding to the human CD4 antigen in the CAR modified animals. This data shows that the CD4 immunoreactivity observed in tissues from CAR transduced animals is due to specific CAR labeling, and not due to cross-reactivity with the endogenous macaque CD4 antigen or non-specific binding from the secondary antibody.

HSPC-derived CAR expressing cells traffic to lymphoid germinal centers

To evaluate HSPC-derived, CAR^+ cell trafficking to lymphoid germinal centers, paraffin-embedded sections from central and peripheral lymph nodes along with spleen and tonsil from CAR and control animals were stained with the monoclonal antibody against the CD4CAR (anti-

CD4, Clone: SP35). Immunoreactivity to the CAR was observed in the germinal centers of all tissue sites evaluated, and from all 4 macaques (CD4CAR and CD4CARΔζ controls). The amount of CAR marking in the germinal centers ranged from 1.4-62.6% of the total germinal center tissue area, with the most robust CD4CAR marking observed in tissues from CAR 1 and both control animals (Figure 8). A mosaic germinal center staining pattern was observed within individual tissues; the amount of CD4CAR immunoreactivity ranging from absent to occupying almost the entire area in an individual germinal center (Figure 8A). CD4CAR marking was observed in lymphoid germinal centers in CAR 2, but the frequency of CD4CAR marking was markedly decreased relative to the frequency observed in the other 3 animals. Multiple germinal centers in the second CAR animal had CD4CAR staining restricted to the periphery of the germinal center, at the margin with the mantle (Figure 9). This marginal CD4CAR staining pattern was also observed in a small percentage of germinal centers from the first CAR animal but was not observed in either of the control animals. Brightfield quantification could not be performed on tissue sections from the control 1 Iliac LN, due to accumulations of endogenous brown pigment in the section, which interfered with the area analysis. The brown pigment is suspected to be hemosiderin accumulations, due to regional hemorrhage secondary to multiple femoral vein blood collections. By comparison, tissues from macaques that did not receive a CAR had a 0.0031% average germinal center CAR marking; which was used as a threshold for CAR specific marking. No differences were observed in the frequency of germinal center CD4CAR staining between CAR and control animals, aside from the overall reduced CAR marking in tissues from CAR 2. However, all 4 animals had CAR marking frequencies above the threshold set by the unmodified control tissues, in all tissues that were analyzed. This data

indicates that HSPC-derived CAR$^+$ cells traffic to central and peripheral lymphoid germinal centers, in both CAR and control animals.

HSPC-derived CAR expressing cells traffic to CNS tissues

To evaluate if HSPC-derived CAR$^+$ cells traffic to the CNS, paraffin-embedded sections from 5 representative CNS tissue sites (parietal cortex, hippocampus, basal ganglia, thalamus, cerebellum) were stained with the SP35 monoclonal antibody against the CD4CAR. Immunoreactivity to the CD4CAR antibody was observed in both white and gray matter in both CAR and control sections (Figure 10). For semi-quantitative analysis, whole sections were analyzed for the ratio of CD4CAR marking over the combined white and gray matter tissue area (Figure10B). Tissues from macaques that did not receive a CAR had a 0.040% average CAR marking. This was used as the threshold for CAR specific marking in the CNS, like our evaluation method for the lymphoid GCs. CAR specific staining, above the threshold, was observed in the parietal cortex and hippocampal sections of both CAR and control macaques. Only CAR2 and control 2 had CAR marking above the threshold in the basal ganglia, and all animals except CAR 1 had CAR marking above the threshold frequency in the thalamus. All 4 macaques had CAR staining frequencies below the threshold in the cerebellum, indicating minimal to no trafficking of gene modified cells to this site. In contrast to findings in lymphoid GCs, control 2 consistently had a higher frequency of CAR staining in all CNS tissue sites except for the cerebellum, compared to the other animals. CAR 2 tended to have higher CAR marking frequencies compared to CAR 1, for respective tissues sites. This is consistent with gene marking data previously published in *Zhen, Peterson, et al*, which showed that CAR 2 and control 2 tended to have higher levels of lentiviral gene marking in the CNS.[66] Aside for the aforementioned patterns, no differences were observed in the frequency of CNS CD4CAR

marking between CAR and control animals. This data indicates that HSPC-derived CAR^+ cells traffic to CNS tissues in both CAR and control animals, with levels of CAR marking comparable to previously published observations.

HSPC-derived CAR expressing cells traffic to GIT tissues

To evaluate if HSPC-derived CAR+ cells traffic to the GIT, paraformaldehyde-fixed paraffin-embedded sections from 6 representative GIT tissue sites (duodenum, jejunum, ileum, cecum, colon, rectum) were stained with the monoclonal antibody against the CD4CAR, either with a brightfield singleplex assay or with a fluorescent 3-plex mIHC (Table 3). Immunoreactivity to the CD4CAR antibody was observed in the GALT and the lamina propria of both CAR and control GIT sections (Figure 11). We performed semi-quantitative analysis of CAR tissue marking within the GALT and adjacent submucosa, using GIT sections that were stained with the 3-plex fluorescent mIHC protocol. The ratio of CAR marking: total tissue area was determined by the amount of CAR marking using binarized fluorescent images, divided by the amount of binarized CAR and DAPI marking in the identical images. Tissues from macaques that did not receive a CAR had 0.013% average CAR marking, which was utilized as the threshold for CAR specific marking as described earlier. CAR specific immunoreactivity, above the threshold, was observed in all GIT section from CAR 2 and control 1. CAR specific immunoreactivity was observed in all GIT tissues except the duodenum in control 2. CAR marking was observed in all CAR 2 GIT tissues, but the marking in the ileum, cecum, and rectum were below the threshold frequency. CAR marking could not be evaluated in rectal tissue from control 1, due to a lack of GALT in the sections that were evaluated. CAR 2 consistently had lower frequencies of CAR immunoreactivity compared to the other 3 animals, in all GIT tissue sites. Compared to the marking in the lymphoid germinal centers, CAR marking was

significantly reduced in all GIT sections in both CAR and control animals. No other differences were observed in staining frequency between the 4 macaques. This data indicates that HSPC-derived CAR^+ cells traffic to the GIT in both CAR and control animals.

Multilineage engraftment of HSPC-derived CAR expressing cells within lymphoid germinal centers

Our data clearly demonstrates that HSPC-derived CAR^+ cells traffic to lymphoid germinal centers. Next, we were asked what cell phenotypes were expressing the CD4CAR at these sites. Because the CAR lentiviral vector was introduced into HSPC's, the CAR^+ cells could theoretically be any hematopoietic cell lineage. Although B-cells often outnumber T-cells following hematopoietic stem cell transplantation,[123] lymphoid germinal centers contain an extremely heterogenous population of hematopoietic lineages including lymphoid cells, and myeloid cells such as monocytes and macrophages. We phenotyped the CAR^+ cells within the germinal centers with an area analysis approach, evaluating fluorescent mIHC stained sections of central and peripheral lymphoid tissues from CAR and control macaques. An exclusion colocalization approach was used to determine different cell phenotypes, as depicted in Table 5. Pixels with phenotypic colocalization patterns outside of the defined sets were considered "mixed colocalization," and not included in any of the individual cell phenotype counts. This approach was utilized as a form of "watershedding," to remove pixels from junctions where neighboring cells of different phenotypes are adjacent to, or overlapping with, each other.

The majority of the CD4CAR immunoreactivity within the germinal centers colocalized with the B-cell marker CD20 (Range: 28.3-65.9% of the total CAR^+ pixels) (Figure 12). CD4CAR colocalization was seen in 0.5-49.6% of the total $CD20^+$ B-cell area within the lymphoid germinal centers (Figure 12A). The CD4CAR marker also colocalized with $CD3^+$ T-

cells (0.8-5.2% of the total CAR^+ area; 0.19-11.5% of the total $CD3^+$ T-cell area), $CD3^+CD8^+$ CTLs (0.02-0.74% of the total CAR^+ area; 0.08-9.7% of the total $CD3^+CD8^+$ CTL area), and $CD68/CD163^+$ macrophages (0.05-3.1% of the total CAR^+ area; 0.27-5.7% of the total $CD68/CD163^+$ macrophage area) (Figure 12A and B). CD4 could not be utilized as a phenotypic marker for T_H cells, due the potential for cross reactivity with the CD4CAR. Because of this, T-cell phenotypes were defined as $CD3^+$ and $CD3^+CD8^+$. Between 26.2-66.6% of the total CAR^+ area within the germinal centers did not colocalize with any of the phenotypic markers. This could be due to insufficient phenotypic antigen availability in portions of the germinal centers or CAR expression in additional cell types (ex. Myeloid or lymphoid progenitors) that do not express the phenotypic markers utilized in the multiplex panel. An anti-CD35 antibody was included in the panel to label follicular dendritic cells (FDC's). The anti-CD35 immunoreactivity to FDCs was used to aid in the identification of lymphoid germinal centers but was not included in the colocalization analysis due to marked inter-slide variability in CD35 staining quality. A higher frequency of mixed colocalization was observed in the submandibular lymph nodes, spleen, and tonsil from control 1. No significant difference in the phenotypic colocalization with the CAR, or the frequency of the different phenotypic markers, within the germinal centers was observed between CAR and control NHP's. In summary, this data demonstrates multilineage engraftment of HSPC-derived CAR^+ cells within lymphoid GC's, with the majority of CAR^+ cells being $CD20^+$ B-cells.

In addition to quantifying the amount of CAR colocalization with our T-cell phenotypic markers, CAR^+ T-cells were also visualized qualitatively utilizing the binarized mIHC image stacks as described in the *Materials and Methods section* (Figure 13). In agreement with the quantitative colocalization data, HSPC-derived CAR^+ $CD3^+$ T-cells and $CD3^+CD8^+$ CTLs, the

target cell population for the CAR, were identified in lymphoid germinal centers. This data supports the quantitative colocalization data and indicates that HSPC-derived CAR^+ T-cells do traffic to lymphoid germinal centers.

Multilineage engraftment of HSPC-derived CAR expressing cells within the GIT

Similar to our analysis of the GCs, we evaluated the phenotypes of CAR^+ cells in the GIT through colocalization analysis of fluorescent mIHC stained GIT sections from CAR and control animals. An exclusion colocalization approach similar to the GC evaluation was employed to evaluate HSPC-derived CAR^+ cell differentiation, utilizing a lymphoid-focused phenotypic panel (Table 3). Tissues that were determined to have CD4CAR marking below threshold for specific detection we excluded from further phenotypic analysis. Additionally, the CAR 2 jejunal section was excluded from phenotypic analysis due to a low CAR marking, with a low CAR binarized pixel count (CAR Jejunum CAR pixel count: 242); which clustered near the pixel counts for the sections that were excluded due to being below the threshold for specific CAR marking. The percent CAR marking in the CAR2 jejunal section was also marginally above the threshold established from analyzing GIT tissues from CAR^- macaques.

CD4CAR immunoreactivity predominately colocalized with the T-cell marker CD3 in all sections of the GIT. CD3/CAR colocalization was observed in 0.02-1.5% (CAR animals: 0.02-0.9%; control animals: 0.07-1.5%) of the total $CD3^+$ tissue area (Figure 14A), and accounted for 16.7-56.5% (CAR animals: 16.7-56.5%; control animals: 25.8-49.4%) of the total CD4CAR immunoreactivity (Figure 14B), across all 6 tissue sites. The CD4CAR marker also colocalized with CD20+ B-cells (0-0.7% of the total CD20+ area [CAR animals: 0.005-0.7%; control animals: 0-0.5%]; 0-41.9% of the total CD4CAR+ area [CAR animals: 4.3-41.9%; control animals: 0-29.1%]), with the ileum sections from CAR 1 and control 2 having higher frequencies

of CAR colocalization with CD20, compared to CD3 colocalization. Between 5.4-55.8% of the total CAR+ area did not colocalize with either CD3 or CD20. Similar to what was observed in the lymphoid germinal centers, the lack of colocalization in these subsets of pixels is unknown, but may be due to insufficient CD3 and/or CD20 antigen expression in these subsets of cells, or HSPC-derived non-lymphoid cell lineages that are expressing the CAR in these tissues (ex. myeloid cell lineages). The frequency of CD20 and CD3 marking was relatively consistent for both CAR and control animals, across all tissues that were evaluated (Figure 14C). HSPC-derived CAR^+ $CD3^+$ T-cells and CAR^+ $CD20^+$ B-cells we also visualized in GIT sections, utilizing the binarized mIHC image stacks as described in the *Materials and Methods* section, and was utilized in the lymphoid sections (Figure 15). These results show that HSPC-derived CAR^+ T-cells and B-cells traffic to, and persist in, the GIT.

HSPC derived CAR expressing cells are actively dividing within the lymphoid germinal centers of CAR and control animals

To assess whether HSPC-derived CAR+ cells in GCs were active/proliferating, we employed a fluorescent mIHC assay, using Ki-67 as a marker of cell cycle activation. Ki-67^+CAR^+ cells were readily identified in germinal centers from both CAR and control macaques (Figure 16). There was no qualitative difference in the level of Ki-67^+CAR^+ cells between the CAR and control animals, aside from the reduced frequency of CAR marking observed in tissues from CAR 2. Consistent with what was observed with the phenotypic mIHC analysis, the Ki-67^+CAR^+ cells predominately colocalized with CD20, indicating they are predominately B-cells. As the germinal centers are a site of active B-cell proliferation, these findings are consistent with normal B-cells within the germinal centers, as part of affinity maturation.[124,125] While Ki-67+ in itself does not indicate B-cell functionality, these results provide evidence that expression of a

CD4CAR does not disrupt B-cell functionality within the germinal centers. This data supports that HSPC-derived CAR^+ B-cells are actively proliferating within the lymphoid germinal centers, consistent with normal physiologic function.

No significant clinical toxicities or postmortem pathologic findings associated with lentiviral modified HSPC

No clinical signs, adverse events, or toxicities were observed during the ~1.8-year timespan of the study. All 4 animals experienced transient weight loss (Range: 2.5-14.7% from baseline), with a transient thrombocytopenia and leukopenia following total-body irradiation (TBI). These findings are consistent with side-effects associated with TBI. All 4 macaques developed transient bouts of diarrhea that were managed with antibiotics and/or symptomatic treatment. *Campylobacter sp.* and *Shigella sp.* were cultured from rectal swabs in a subset of these diarrhea cases and were believed to be the cause for the diarrhea in these instances. The remaining cases of diarrhea were suspected to be due to other factors; most notably due to inflammatory bowel disease (otherwise known as food allergy/hypersensitivity/dietary intolerance), with other possible causes including but not limited to stress-associated diarrhea, and inflammation in the GIT associated with chronic SHIV infection. CAR 2 developed mild, chronic diarrhea approximately 1.5 years post HSPC transplantation, which was managed with Tylosin. All 4 macaques developed transient, mild anemias, which were suspected to be due to anemia of chronic disease associated with chronic SHIV infection. There were no clinical abnormalities associated with the anemia. CAR 2 developed a prolonged period of thrombocytopenia starting ~5 months post-SHIV inoculation and was managed with long-term oral Clopidogrel. We suspect the thrombocytopenia is related to the SHIV infection, analogous to HIV-related thrombocytopenia in humans.[126] Thrombocytopenia has also been observed in

SIV infected macaques, during both acute and chronic stages of infection.[127] All 4 NHP's gained body weight over the course of the study (Range: 76.6-85.8% from baseline weights taken prior to TBI), and all reached their planned study endpoint.

Table 6 illustrates the major gross and histopathological findings for both the CAR and control macaques. All 4 macaques had diffuse testicular hypoplasia that was due to previous TBI. Diffuse, eosinophilic, lymphoplasmacytic, and gastro-entero-colitis was also seen histologically in all 4 macaques, and is consistent with inflammatory bowel disease (otherwise known as food allergy/hypersensitivity/dietary intolerance) that is seen in most captive-raised macaques. A renal adenoma was identified histologically in CAR 1, which is suspected to be an incidental finding of idiopathic origin. control 2 developed sub-clinical mild granulomatous meningoencephalitis, which is suspected to be due to chronic SHIV infection. This data shows that CAR based gene therapies can be safely delivered via HSPC transduction, with no clinical pathologic evidence of toxicity.

Discussion

In the present study, we have demonstrated that HSPC-derived CD4CAR expressing cells readily traffic to, and persist in, lymphoid GC's, the CNS, and the GIT, in particular GALT. Additionally, we have demonstrated multilineage engraftment of HSPC-derived CAR^+ cells in GCs and GIT tissues, with evidence of cell cycle activity in CAR^+ cells in the GCs. Lastly, we demonstrate successful engraftment of lentiviral transduced HSPC's into HIV tissue reservoir sites, with no evidence of toxicity related to the transplantation or the lentiviral insert over the ~1.8-year duration of the study. This study has broad implications for the use of HSPC-based immunotherapies targeting HIV, as well as a variety of other diseases.

One major concern with the usage of lentiviral modified HSPC's, is the potential for insertional mutagenesis resulting in a malignant transformation. Notable examples of these events occurring include the development of T-cell acute lymphocytic leukemia in 4 individuals previously treated with a retroviral vector containing a copy of the common gamma (γc) chain, to correct a form of X-linked severe combined immunodeficiency.[128–140] The cause of the malignant transformations have been speculated to be due to a combination of aberrant activation of proto-oncogenes (LMO2, CCND2, BMI1) associated with insertional mutagenesis by the viral vector, along with acquired somatic mutations.[129,130,132,137,138] Additionally, expression of the γc chain transgene may have contributed to the malignant transformation through a synergistic effect with the previously described mutations [139]. Myelodysplasia has been observed in pigtail macaques following experimental autologous HSPC transplantation with gammaretroviral vector modified stem cells. The dysplasia likely occurred due to a combination of vector mediated insertional mutagenesis resulting in overexpression of HOXB4, with subsequent acquired somatic mutations. [140] A variety of methods of been employed to reduce the risk of lentiviral vector

associated insertional mutagenesis, including but not limited to, the development of self-inactivating vectors that lack promoter and enhancer activity at the 3' LTR, incorporation of chromatin insulators, modification to the 3' polyadenylation sequence to reduce transcriptional read-through, and modifications to the vector dose to achieve therapeutic efficacy while reducing the number of transduced cells infused back into the patient.[133,141,142] More than 100 patients have been treated with lentiviral-modified HSPCs, with no evidence of insertional mutagenesis or neoplastic transformation related to the vector.[143-155] While future studies may require longer durations to insure safety, the results from this study support that CAR lentiviral modified HSPCs can engraft safely, without clinical evidence of insertional mutagenesis and neoplastic transformation.

The frequency of CAR immunoreactivity in GCs, the CNS, and the GIT were roughly equal between CAR and CAR-tailless control animals. This suggests that CAR signaling is not necessary for CAR^+ cell trafficking to the HIV tissue reservoir sites evaluated in this study. While the transgenes may have contributed to trafficking through non-signaling mechanisms, the observation of HSPC-derived CAR^+ cells in the examined HIV tissue reservoir sites is likely due to cell trafficking post-transplantation. Donor HSPC-derived cells have been shown to traffic to lymphoid GCs,[156] CNS tissues,[157–159] and GIT tissues[160,161] in rodent animal models, following TBI. Donor HSPC-derived cells have been shown to traffic to the small intestinal lamina propria and submucosa, as well as donor HSPC-derived T_{FH} cells in GCs, in mice following total body irradiation.[160,161] Additionally, germinal centers have been shown to have an oligoclonal development pattern in rats who received syngeneic thoracic duct lymph (TDL) following lethal total body irradiation.[156] This manifested as germinal centers containing varying frequencies of donor- and recipient TDL derived B-cells within the germinal centers, identical to the mosaic

staining pattern of CAR^+ and CAR^- cells within the germinal centers of the CAR and control animals. Based on our findings, along with previously published findings concerning distribution of donor derived cells post-HSPC transplantation, we hypothesize that the CAR^+ cell trafficking observed in the GCs and GIT tissues of CAR and control animals is the result of distribution of lentiviral transduced HSPC derived CAR^+ cells to these tissue sites as a part of cellular reconstitution post-myeloablative conditioning, and is independent of CAR signaling.

Trafficking of CAR^+ cells to the CNS is likely enhanced due to TBI-mediated disruption of the blood-brain-barrier (BBB), allowing for trafficking of HSPC-derived cells to this tissue site in the immediate post-irradiation period. Maintenance of the myeloid glial cell population in a homeostatic state occurs predominately through self-renewal, with minimal trafficking of bone marrow derived myeloid cells into the CNS parenchyma, although this normal trafficking may contribute to CAR cells being present in the CNS.[162,163] Trafficking of donor HSPC-derived cells to the CNS parenchyma has been observed in rodents following myeloablative conditioning by TBI.[157,164,165] In contrast, rodents receiving HSPC-transplantations following busulfan conditioning, delivery of donor cells through parabiosis, or HSPC-transplantation with TBI conditioning with the brain shielded, resulted in minimal to no trafficking of donor derived cells into the CNS parenchyma.[158,159,163,165–169] HSPC-derived cell trafficking to the CNS parenchyma following TBI is believed to occur due to TBI-mediated disruption of the BBB, which has been demonstrated through increased permeability of the BBB to various intravenous soluble markers following TBI, along with endothelial cell loss and reduction in tight junction protein immunoreactivity (ZO-1 and occluding) following TBI.[170–173] Based on our findings, along with previously published findings concerning distribution of donor derived cells post-HSPC transplantation and TBI, we hypothesize that the CAR^+ cell trafficking to the CNS in CAR and

control animals is due early post-transplantation localization, through TBI-mediated disruption of the BBB barrier.

One important consideration for the introduction of CD4-based CAR's into HSPC's, is the potential for interactions between the CAR and endogenous MHC II, which could affect T-cell differentiation and maturation. Over expression of CD4 during thymopoiesis significantly inhibits positive selection of $CD8^+$ thymocytes in mice,[174] and can drive $CD4^+CD8^+$ development and 100-fold expansion in mice lacking a functional recombinase activating gene-2 ($Rag2^{-/-}$).[175] Thyomocyte maturation arrests at the $CD4^-CD8^-$ stage in $Rag2^{-/-}$ mice that do not overexpress CD4, as well as $MHCII^{-/-}Rag2^{-/-}$ mice that overexpress CD4, indicating that the interaction between CD4 and MHCII drives thymocyte development and expansion, through signaling and activation of Lck associated with the cytoplasmic tail of CD4. Additionally, early developmental arrest of T-cells is seen in mice transplanted with CD4CAR transduced HSPCs carrying CD3ζ or FcRγ signal transduction domains.[176] This attenuation is dependent of signaling through the CAR, as T-cell developmental arrest is not observed in mice transduced with CD4CARs lacking a signal transduction domain. T-cell development was also rescued when CD4CAR transduced HSPCs were transplanted into mice deficient in MHC II, indicating the developmental arrest is dependent of CD4CAR binding with MHC II. The CD4CAR development arrest is also specific for T-cell lineages, as no attenuation is seen in CAR^+ myeloid cells, NK cells, and B-cells. Figure 17 illustrates an interspecies comparison of the amino acid sequences for previously defined CD4 coreceptor binding domains on the MHC class II α2, β1, and β2 chains, via NCBI protein BLAST.[177–180] The results show relatively high homology between humans, mice, and pigtail macaques, with the β1 chain binding site having the largest interspecies variation in primary protein sequences (68.8% homology between mice and humans; 60% homology

between mice and pigtail macaques). In all protein chains, the human sequences are more analogous to the macaque protein sequences, compared to the mouse sequences. The results of the CD4 binding site analysis on MHC II, combined with the evidence that a human based CD4CAR interacts with murine MHC II, suggest that the human CD4CAR will likely bind the pigtail macaque MHC II antigen. In contrast to what has been shown in mice expressing the HSPC-derived CD4CAR, previously published data from these animals shows $CD4CAR^+$ naïve, memory, and effector T-cell populations in the peripheral blood of both CAR and control animals, over the course of the study.[73] While there is likely binding between the CD4CAR and the macaque MHC II antigen, this interaction does not appear to arrest T-cell development or impair $CD8^+$ T-cell positive, compared to what's been documented with murine models.

While CAR-mediated cytolytic activity has been previously demonstrated with NK cells and neutrophils, it is unknown if the CAR B-cells observed in the GCs and GIT can exert any sort of CAR directed cytotoxicity. To the authors knowledge, no studies have evaluated the function of CAR-expressing B-cells. B-cells are capable of expressing granzyme B, and have been postulated to have antiviral functions, early tumor immunosurveillance functions, and regulatory functions through granzyme B mediated degradation of CD3ζ.[181–184] Granzyme B+ B-cells have also been shown to exert granzyme-mediated cytolytic activity against tumor cell lines *in vitro*.[185] While additional studies are necessary to demonstrate CAR-directed cytotoxicity by B-cells, in addition to what has been shown with CAR-NK cells and CAR-neutrophils, previous data shows that B-cells are capable of expressing granzyme B, and perform granzyme-mediated cytolytic functions.

Limitations from this study include the small sample size, rendering us unable to reach any statistically significant conclusions between the CAR and control animals. Nevertheless, the

findings show long-term, multilineage engraftment of HSPC-derived CAR^+ cells in HIV tissue reservoir sites, in a large animal model. Additionally, we demonstrate safe delivery of an immunotherapeutic CAR to these tissue sites, without evidence of toxicity associated with the CAR lentiviral vector. Refinements to this model could be implemented to improve efficacy and applicability to a broad spectrum of individuals; including the implementation of 2nd, 3rd, and 4th generation CARs to improve cytolytic activity,[69,186–191] addition of latency reversing agents to drive latent provirus into active replication, making the infected cells susceptible to CAR-mediated cytotoxicity, and incorporating genes encoding bNAbs as a method of additive immunotherapy to block ongoing viral infection.[192–194] Additionally, safe delivery and maintenance of CAR-modified cells in these tissue sites has the potential for therapies outside of HIV, including various forms of neoplasia and autoimmune disorders.[176]

Conclusions

We show evidence of HSPC-derived CD4CAR$^+$ cell engraftment in GCs, CNS tissue, and GIT tissue, following myeloablative conditioning by TBI. We demonstrated multi-lineage engraftment of HSPC-derived CAR$^+$ cells in lymphoid GCs and GIT, with CD3$^+$ T-cells being the predominate CAR$^+$ lineage in GIT, and CD20$^+$ B-cells being the predominate lineage in GCs. Cell cycle activity is maintained with CAR expression in cells within the GCs, as evidence by Ki-67 expression of CAR$^+$ cells. And CAR$^+$ cells are maintained for prolonged periods of these tissue sites, with no evidence of toxicity associated with the CAR vector. This HSPC-based immunotherapeutic technique has broad implications as a potential therapy for a wide array of diseases, including but not limited to infectious diseases, neoplasia, and autoimmune/inflammatory mediated disorders.

Figures

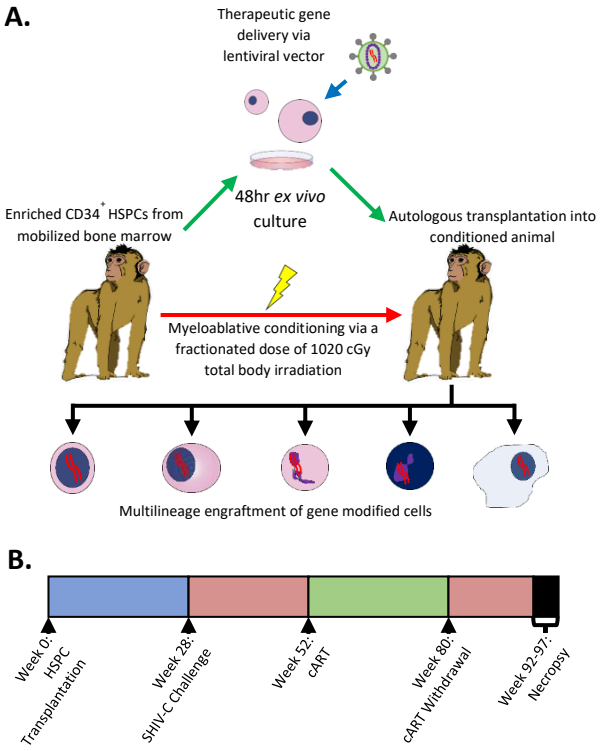

Figure 1. Schematic for HSPC-derived CAR HIV immunotherapy. A) $CD34^+$ HSPC's were isolated from G-CSF primed bone marrow aspirates. Following 48-hour *ex vivo* culture, during which time they were transduced twice with lentiviral vectors containing the C46 fusion inhibitor and either CD4CAR or CD4CARΔζ, the HSPC's were infused into the autologous animal (Schematic modified from Peterson et al 2016). **B)** Twenty-eight weeks post autologous HSPC transplantation, NHP's were challenged with SHIV-1157ipd3N4 intravenously. cART was initiated 24 weeks post-SHIV challenge and was maintained for 28 weeks. Following cART withdrawal, animals were monitored for an additional 15 weeks prior to necropsy. (Adapted from Peterson et al 2016)[194]

	CAR 1	CAR 2	Control 1	Control 2
Lentiviral transduction: Multiplicity of infection	5	10	10	10
% lentiviral gene marking in necropsy PBMC's	6.79	9.67	5.13	1.13
# of Lymphoid tissue sites evaluated	7	7	7	7
# of Germinal centers analyzed/ tissue site: Average (range)	57 (24-78)	56 (19-162)	41 (15-84)	107 (54-146)
Germinal center area evaluated (μm^2): Average (Range)	4,659,512 (2,449,374-10,634,438)	2,538,516 (671,454-6,334,436)	1,993,011 (793,486-3,641,349)	8,117,001 (5,715,385-10,406,826)
Average Germinal Center Size (μm^2/GC)	80461	50839	57673	81079
# of CNS tissue sites evaluated	5	5	5	5
CNS Area evaluated (μm^2): Average (Range)	$2.02E^8$ ($8.88E^7$-$3.44E^8$)	$9.40E^7$ ($1.68E^7$-$1.57E^7$)	$1.19E^8$ ($7.09E^7$-$2.08E^8$)	$1.55E^8$ ($1.06E^8$-$2.10E^8$)
# of GIT tissue sites evaluated	6	6	5	6
GIT Area evaluated (μm^2): Average (Range	7,049,196 (136,292-10,925,854)	1,054,112.188 (200,110.316-2,533,296.948)	3,568,626 (134,003-13,100,956)	1,247,516 (375,378-4,646,763)

Table 1. Summary of paraformaldehyde-fixed paraffin-embedded tissue analysis by IHC. Summary of the tissue sites evaluated for CAR^+ cell distribution in the lymphoid GC's, CNS, and GIT.

Position	Primary Antibody	Clone / Host; Primary Antibody	Company / Item; Primary Antibody	Dilution; Primary Antibody	Secondary Antibody	OPAL Fluor
1	CD20	Polyclonal - Rabbit	Thermo - PA5-16701	1:2000	OPAL Ms/Rbt Secondary	540
2	CD3	Polyclonal - Rabbit	Dako - A0452	1:800	OPAL Ms/Rbt Secondary	570
3	CD68	Polyclonal - Rabbit	Thermo - PA5-32330	1:200	OPAL Ms/Rbt Secondary	690
	CD163	EP324 - Rabbit	BioSB - BSB3276	1:2000	OPAL Ms/Rbt Secondary	
4	CD4	SP35 - Rabbit	Cell Marque - 104R-16	1:100	OPAL Ms/Rbt Secondary	520
5	CD8	EP334 - Rabbit	BioSB - BSB2849	1:2000	OPAL Ms/Rbt Secondary	650
6	CD35	polyclonal - Rabbit	Sigma - HPA049348	1:1000	OPAL Ms/Rbt Secondary	620

Table 2. Summary of the OPAL fluorescent mIHC utilized for phenotypic colocalization analysis of CAR^{+} cells in the lymphoid GC's. Tissue sections were sequentially stained with each primary antibody series, using the OPAL labeling method.[112] The positions represent the order the primary antibodies were applies applied to the tissue sections, with position 1 being applied 1st and position 6 being applies last.

Position	Primary Antibody	Clone / Host; Primary Antibody	Company / Item; Primary Antibody	Dilution; Primary Antibody	Secondary Antibody	OPAL Fluor
1	CD20	L26 / Mouse	Dako #M0755	1:10K	Opal Ms/Rbt Secondary	540
2	CD4	SP35 / Rbt	Cell Marque 104R-16	1:200	Opal Ms/Rbt Secondary	620
3	CD3	SP7 / Rbt	Thermo RM-9107	1:200	Opal Ms/Rbt Secondary	690

Table 3. Summary of the OPAL fluorescent mIHC utilized for phenotypic colocalization analysis of CAR^{+} cells in the GIT. Tissue sections were sequentially stained with each primary antibody series, using the OPAL labeling method.[112] The positions represent the order the primary antibodies were applies applied to the tissue sections, with position 1 being applied 1st and position 6 being applies last.

Position	Primary Antibody	Clone / Host; Primary Antibody	Company / Item; Primary Antibody	Dilution; Primary Antibody	Secondary Antibody	OPAL Fluor
1	CD20	L26 / Mouse	Dako #M0755	1:10K	Opal Ms/Rbt Secondary	520
2	Ki-67	D3B5	Cell Signaling 12202S	1:500	Opal Ms/Rbt Secondary	620
3	CD4	SP35 / Rbt	Cell Marque 104R-16	1:200	Opal Ms/Rbt Secondary	540
4	CD3	SP7 / Rbt	Thermo RM-9107	1:200	Opal Ms/Rbt Secondary	690

Table 4. Summary of the OPAL fluorescent mIHC utilized to evaluate Ki-67 expression in CAR^{+} cells in lymphoid germinal centers. Tissue sections were sequentially stained with each primary antibody series, using the OPAL labeling method.[112] The positions represent the order the primary antibodies were applies applied to the tissue sections, with position 1 being applied 1st and position 6 being applies last.

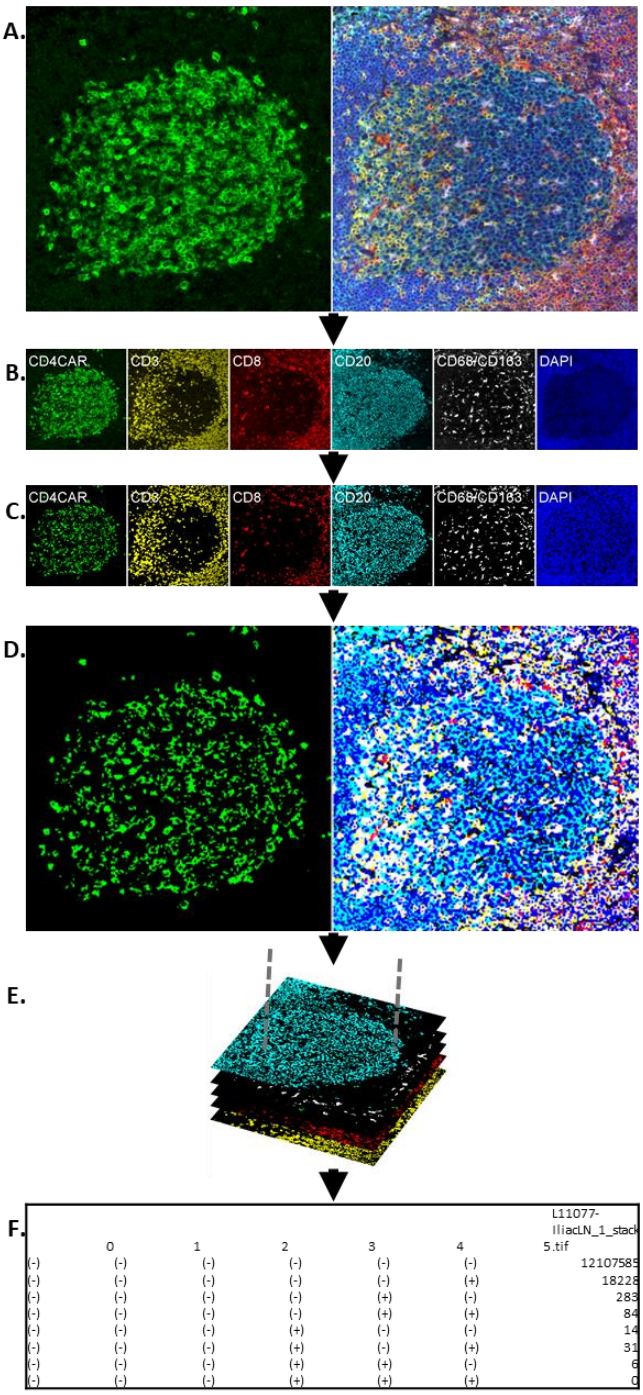

Figure 2. Schematic for mIHC image processing and colocalization analysis. Individual fluorescent mIHC photomicrographs (**A**; *i*: CD4CAR IHC, *ii*: phenotypic mIHC) are initially separated into individual fluorescent channels (**B**). Each channel is individually thresheld and binarized (**C**), and the individual binarized fluorescent channels are recombined into a stack (**D**; *i*: binarized CD4CAR IHC, *ii*: binarized phenotypic mIHC). Binarized stacks were analyzed with the Multiplex Pixel Colocalization plugin (**E**), which generated a list of different fluorescent marker colocalization data based on the colocalization of different markers at each pixel coordinate (**F**). The data was subsequently used determine CAR^{+} cell phenotypes in lymphoid GC's and GALT.

```
var basename = ""
var folder = "C:/Users/Isaac/OneDrive - UW/Research- Kiem/Experimental Histopathology Requests/Slide Scanning-
Analysis/Fluorescence/Multiplex IHC_GCs/AmFAR 6plex Images/";
var stacknames = newArray("Stack-0002", "Stack-0003", "Stack-0004", "Stack-0001", "Stack-0005", "Stack-0006", "Stack-0008", "Stack-0007");
var marker = newArray("_CD4CAR", "_CD20", "_CD3", "_CD35", "_CD8", "_CD68-163", "_Autofluorescence", "_DAPI");
var color = newArray("Green", "Cyan", "Yellow", "Magenta", "Red", "Grays", "Grays", "Blue");
Dialog.create("Enter the name of the image base");
Dialog.addString("Basename of Image:", basename, 200);
Dialog.show();
basename = Dialog.getString();
var stackname = basename + "_stack.tif";
var remove1 = 3;
var remove2 = 6;
run("Arrange Channels...", "new=41235678");
run("Stack to Images");
run("Images to Stack", "name=Stack title=[]");
run("Stack to Images");
var i = 0;
for(i = 0; i < 8; i++)
{
  if ((i == remove1) || (i == remove2))
  {
    selectWindow(stacknames[i]);
    close(stacknames[i]);
  }
  else {
  var newname = basename + marker[i];
  selectWindow(stacknames[i]);
  rename(newname);
  if(i == 7)
  {
    run("Duplicate...", "title=_DAPI-ROI");
    selectWindow(newname);
  }
  run("Subtract Background...", "rolling=50");
  run("Measure");
  selectWindow(newname);
  //run("Threshold...");
  setAutoThreshold("Otsu");
  setOption("BlackBackground", false);
  call("ij.plugin.frame.ThresholdAdjuster.setMode", "Over/Under");
  waitForUser("Record the automatic threshold value, then hit OK");
  run("Convert to Mask");
  run("Invert");
  run(color[i]);
  selectWindow(newname);
  run("Remove Outliers...", "radius=2 threshold=50 which=Bright");
  saveAs("Tiff", folder + newname + ".tif");
  if (i == 6)
  {
    close(newname + ".tif");
  }
  }
}
selectWindow("_DAPI-ROI");
//run("Brightness/Contrast...");
run("Enhance Contrast", "saturated=0.35");
run("Cyan");
run("ROI Manager...");
roiManager("Show All");
roiManager("Show All with labels");
setTool("freehand");
waitForUser("Annotate and save ROI's using the ROI Manager, and close any channels you do not want to include in the stack; then hit OK");
close("_DAPI-ROI");
run("Images to Stack", "name=Stack title=[] use");
saveAs("Tiff", folder + stackname);
close(stackname);
```

Figure 3. Macro code for image binarization of fluorescent mIHC lymph node, spleen, and tonsil sections. Binarized stacks of mIHC lymphoid photomicrographs were generated for mIHC colocalization analysis.

```
var basename = ""
var folder = "C:/Users/Isaac/OneDrive - UW/Research- Kiem/Experimental Histopathology Requests/Slide Scanning-
Analysis/Fluorescence/Multiplex IHC_GIT/";
var stacknames = newArray("Stack-0001", "Stack-0002", "Stack-0003", "Stack-0004");
var marker = newArray("_CD4CAR", "_CD20", "_CD3", "_DAPI");
var color = newArray("Green", "Cyan", "Yellow", "Blue");
Dialog.create("Enter the name of the image base");
Dialog.addString("Basename of Image:", basename, 200);
Dialog.show();
basename = Dialog.getString();
var stackname = basename + "_stack.tif";
run("Stack to Images");
run("Images to Stack", "name=Stack title=[]");
run("Stack to Images");
var i = 0;
for(i = 0; i < 4; i++)
{

  {
  var newname = basename + marker[i];
  selectWindow(stacknames[i]);
  rename(newname);
  run("Subtract Background...", "rolling=50");
  run("Measure");
  selectWindow(newname);
  //run("Threshold...");
  setAutoThreshold("Otsu");
  setOption("BlackBackground", false);
  call("ij.plugin.frame.ThresholdAdjuster.setMode", "Over/Under");
  waitForUser("Record the automatic threshold value, then hit OK");
  run("Convert to Mask");
  run("Invert");
  run(color[i]);
  selectWindow(newname);
  run("Remove Outliers...", "radius=2 threshold=50 which=Bright");
  saveAs("Tiff", folder + newname + ".tif");
  if (i == 4)
  {
    close(newname + ".tif");
  }
  }
}
waitForUser("Annotate and save ROI's using the ROI Manager, and close any channels you do not want to include in the stack; then hit OK");
close("_DAPI-ROI");
run("Images to Stack", "name=Stack title=[] use");
saveAs("Tiff", folder + stackname);
close(stackname);
```

Figure 4. Macro code for image binarization of fluorescent mIHC GIT sections. Binarized stacks of appended mIHC GALT photomicrographs were generated for mIHC colocalization analysis.

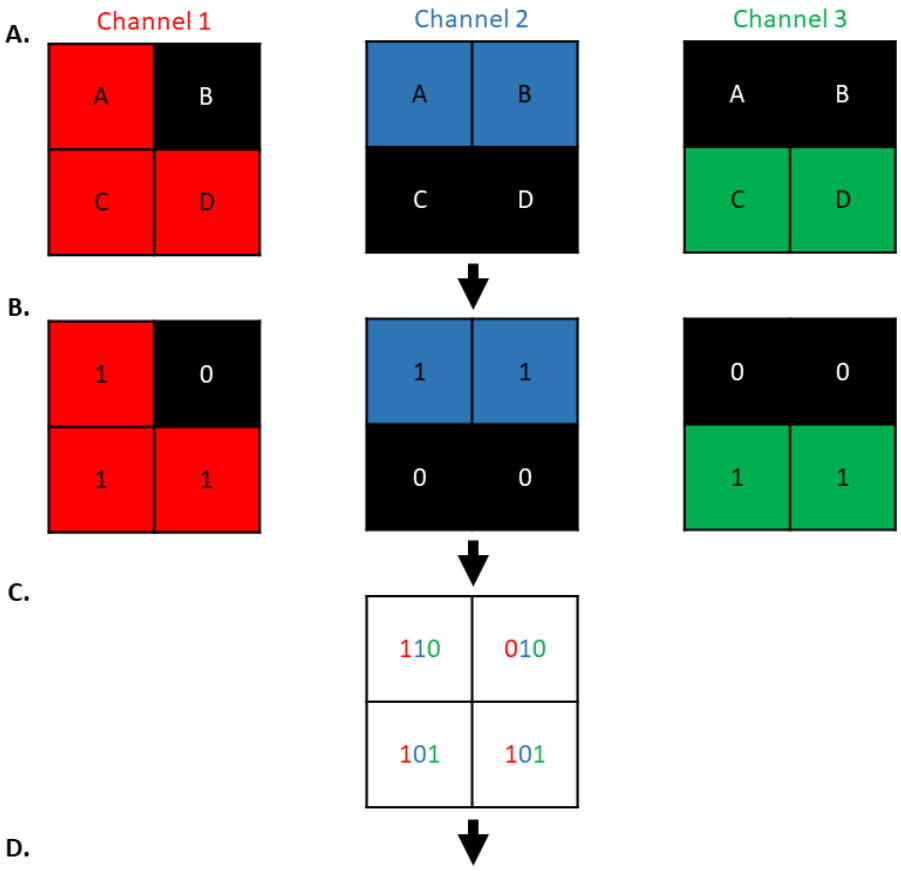

Binary Number (Array Index)	Colocalization Pattern (Channels)	Pixel Count (Array)
000	None	0
001	3	0
010	2	1
011	3,2	0
100	1	0
101	1,3	2
110	1,2	1
111	1,2,3	0

Figure 5. Conceptual schematic for the binarized pixel colocalization that is performed by the Multiplex Pixel Colocalization plugin. Example analysis for a hypothetical, binarized, 3 channel photomicrograph **(A).** Pixels in each channel are assigned either a "1" or a "0" based on the presence (1) or absence (0) of fluorescent signal in that pixel **(B).** Binary numbers are generated from each pixel position based on assigned number in each channel **(C)**, which are used to increment the count in an array of 2^n potential outcomes; where n is the number of channels being evaluated for colocalization **(D).**

	Phenotypic Markers				
Cell Types	**CD3**	**CD8**	**CD20**	**CD68/CD163**	**CD4CAR**
T-cells	+	+/-	-	-	-
CAR+ T-cells	+	+/-	-	-	+
CTLs	+	+	-	-	-
CAR+ CTLs	+	+	-	-	+
B-cells	-	-	+	-	-
CAR+ B-cells	-	-	+	-	+
Monocytes/Macrophages	-	-	-	+	-
CAR+ Monocytes/Macrophages	-	-	-	+	+

Table 5. Expected cell phenotypes from pixel-based phenotypic marker colocalization. Summary of the colocalization patterns that were used to define different cell phenotypes in fluorescent mIHC photomicrographs. Other phenotypic marker combinations were defined as "mixed colocalization."

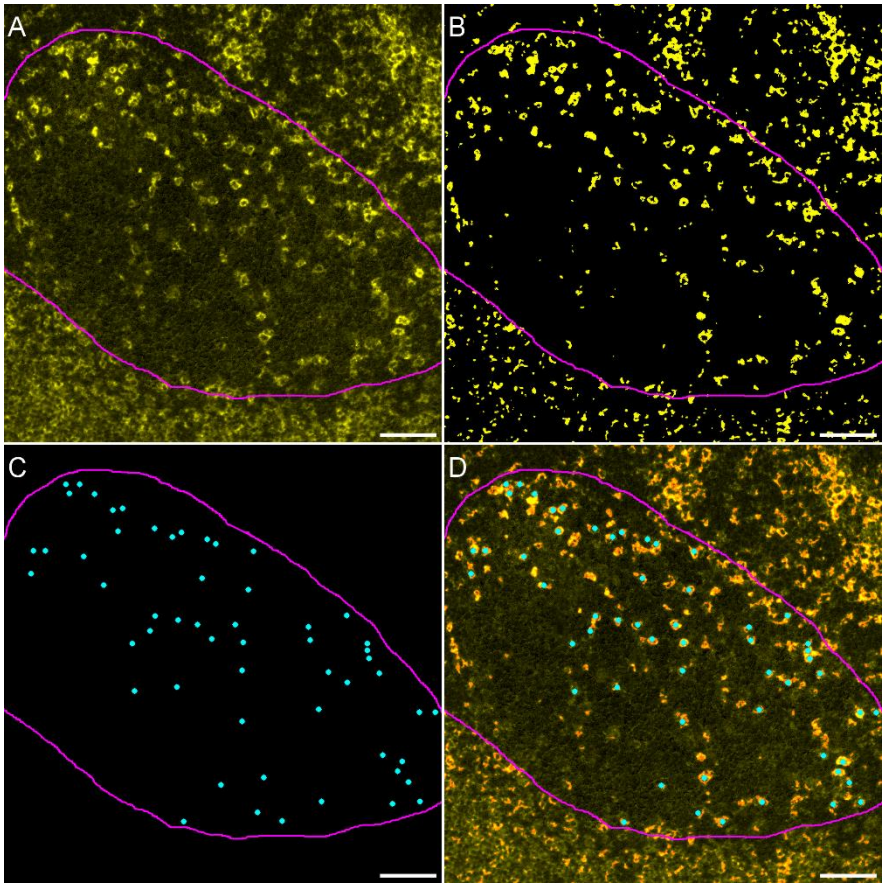

Figure 6. Binarized images are uniform with specific marking in fluorescent images. Binarized CD3 fluorescent images (**B**) compared to the original fluorescent image (**A**) and a manual $CD3^{+}$ cell count (**C**) within a germinal center, by an independent observer to evaluate the specificity of the binarized image. The magenta circle outlines the germinal center. The blue markers (**C** and **D**) illustrate the manual CD3+ cell counts. The binarized image is shown to be very sensitive and specific for CD3 marking in the lymphoid germinal center, shown by the presence of orange marking in the overlay image (**D**), which illustrates overlap of the binarized and original fluorescent images. Scale: 50μm.

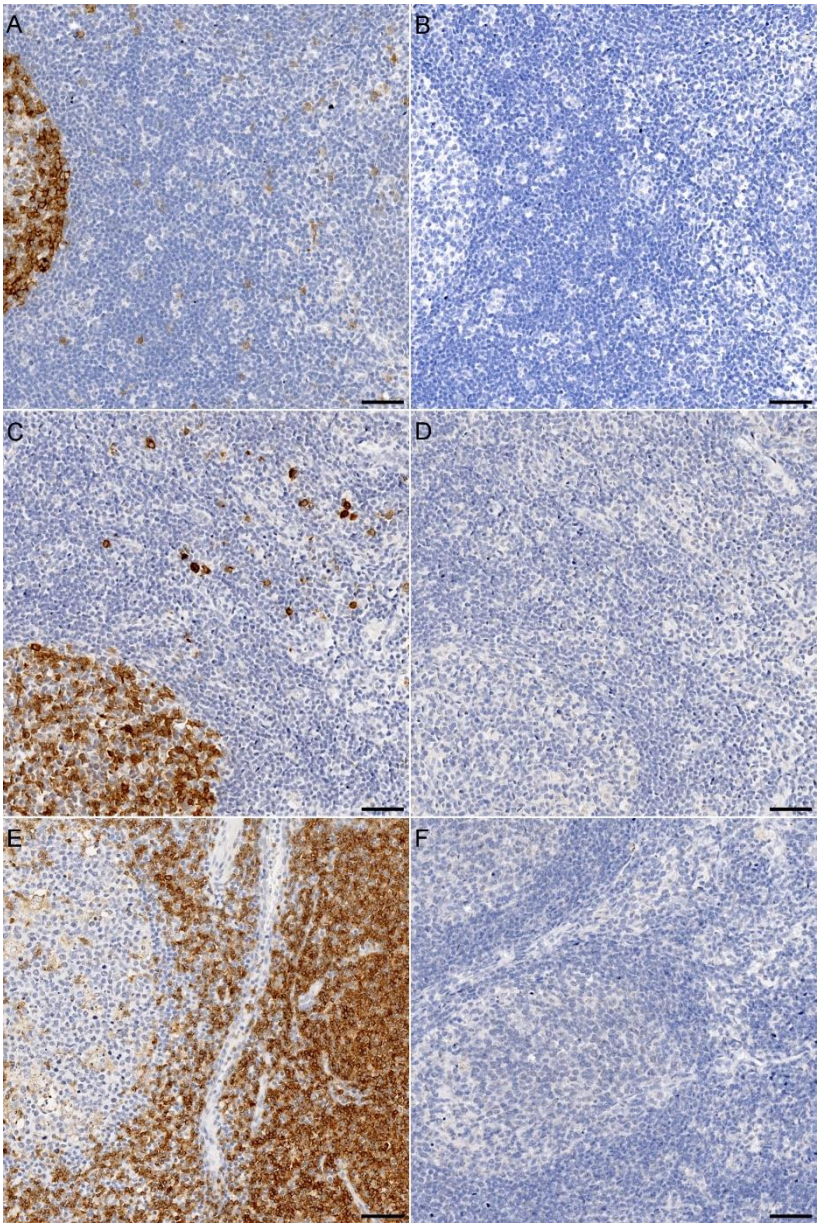

Figure 7. CD4 (SP35) antibody specifically marks CAR^{+} cells with no immunoreactivity to the endogenous macaque CD4. Mesenteric lymph node sections from CAR2 (**A**) and Control 1 (**C**) show specific immunoreactivity in the germinal center, with sparse marking in the parafollicular zone, when labeled with the CD4 (SP35) antibody clone. Brown indicates immunoreactivity for human CD4CAR; blue indicates hematoxylin counterstain. No immunoreactivity was seen in paired adjacent tissue sections labeled with an isotype control (**B** and **D**). CD4 (SP35) labeling of a human tonsil section (**E**) shows specific immunoreactivity, which is predominately in the parafollicular zone; the pattern is consistent with CD4^{+} T-cell marking in the parafollicular T-cell zone. No Specific immunoreactivity is seen in the control mesenteric lymph node section from a CAR^{-} macaque (**F**), indicating that the CD4 (SP35) antibody clone does not cross-react with the endogenous pigtail macaque CD4 antigen. Scale: 50μm.

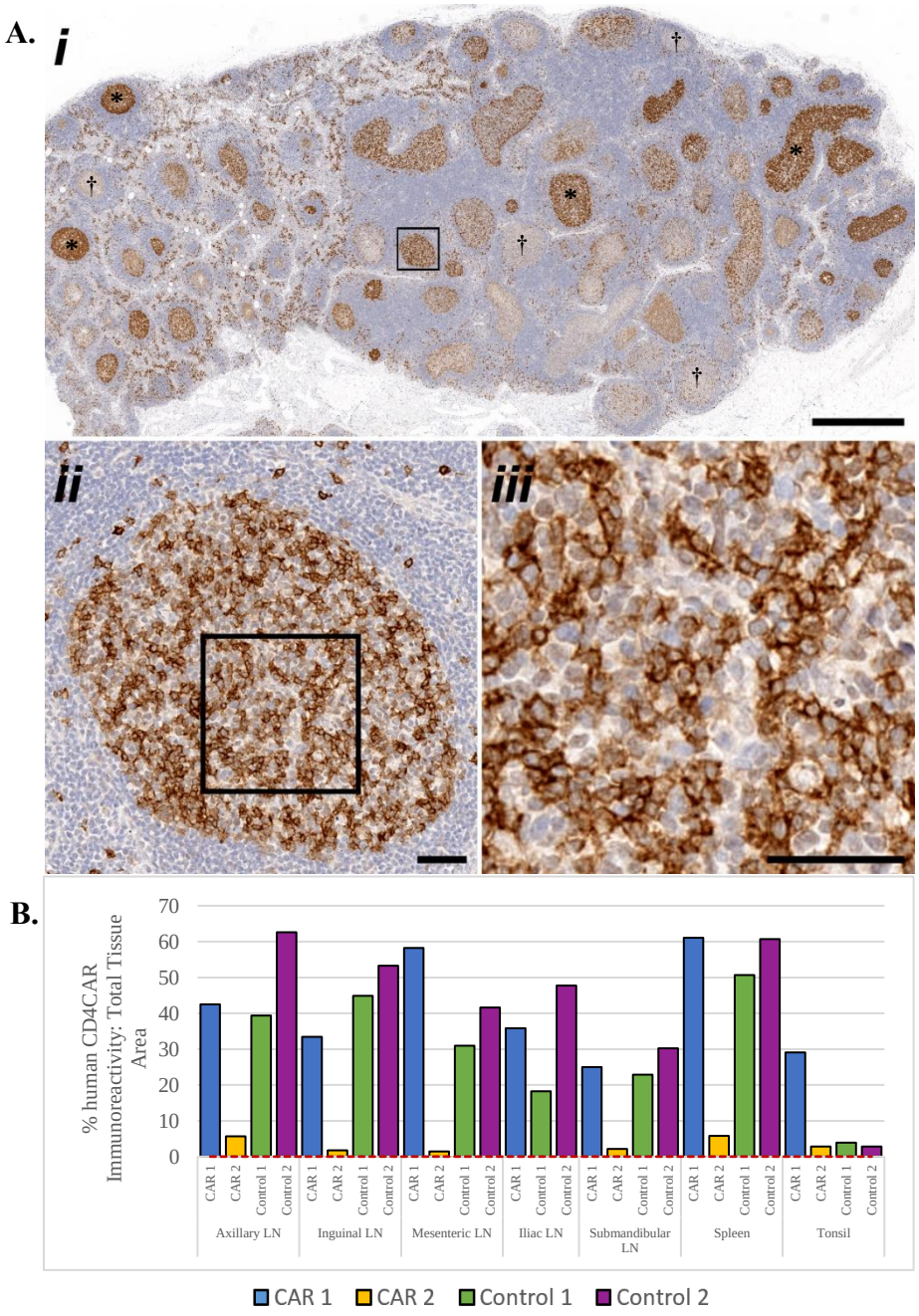

Figure 8. HSPC-derived CAR$^+$ cells localize to the GCs in central and peripheral lymphoid tissues. **A)** Low (*i*.), medium (*ii*.), and high magnification (iii) photomicrographs of the CAR1 iliac LN, illustrating CAR$^+$ cells localizing in the germinal centers. Brown indicates immunoreactivity for human CD4CAR; blue indicates hematoxylin counterstain. The lymphoid GC's have varying degrees of CD4CAR immunoreactivity, ranging from germinal centers with high levels of CD4CAR immunoreactivity (*) to germinal centers with minimal to no CAR immunoreactivity (†). **B)** The amount of CD4CAR-labeled lymphoid GC's as a percentage of the total lymphoid GC tissue area in both CAR and Control macaques. The dotted red line indicates that average % CD4CAR GC marking in representative lymphoid tissues from macaques that did not receive a CAR (0.0031%). Scale: (*i*.) 1mm; (*ii*. *iii*.) 50µm.

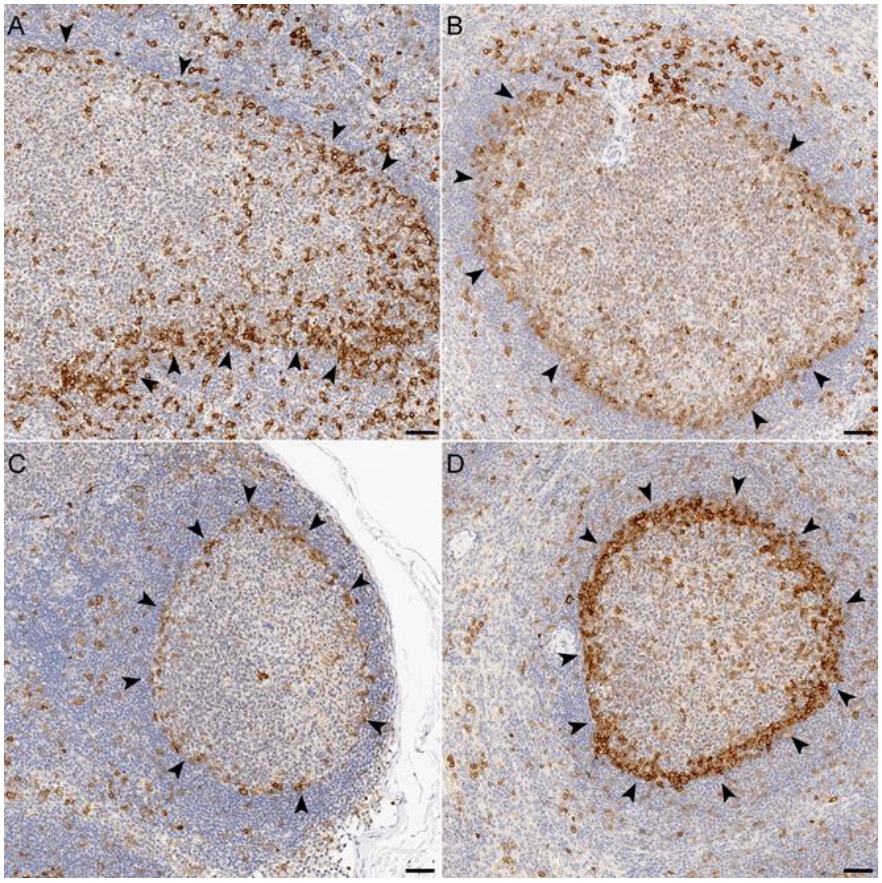

Figure 9. Subsets of HSPC-derived CD4CAR expressing cells localize to the GC margins in CAR animals. Brightfield photomicrographs illustrating CAR^{+} cells localizing to the margins of GCs in CAR 1 (**A**: tonsil; **B**: spleen) and CAR 2 (**C:** submandibular lymph node; **D**: spleen). Arrowheads outline the germinal center margins, with associated CAR immunoreactivity. Brown indicates immunoreactivity for human CD4CAR; blue indicates hematoxylin counterstain. This marginal staining pattern was not observed in any of the lymphoid tissues from the control animals. Scale: 50µm.

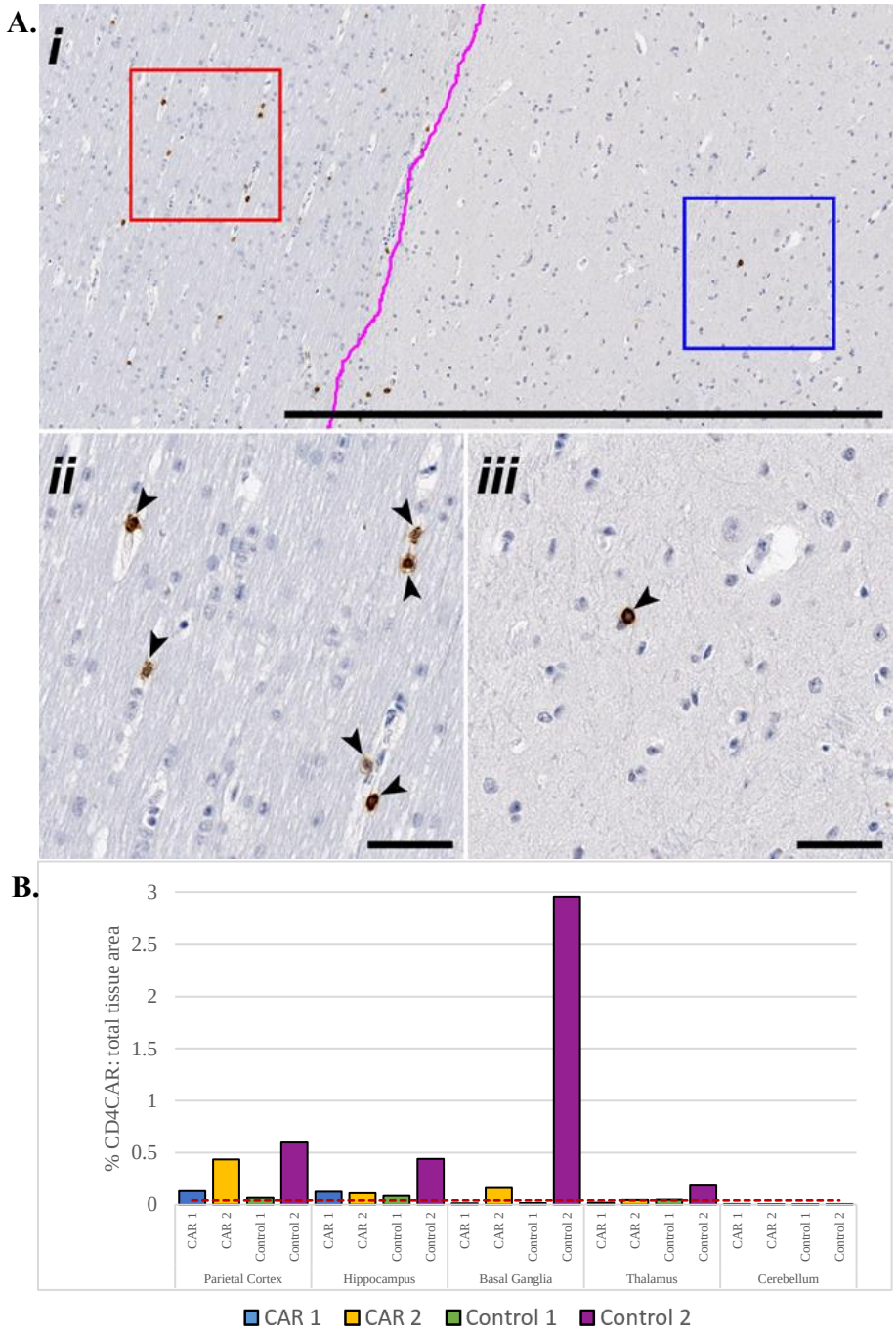

Figure 10. **HSPC-derived CD4^{+} cells localize to the CNS. A)** Low (*i.*) and high (*ii.* and *iii.*) magnification photomicrographs of the Control 2 basal ganglia, illustrating CD4CAR^{+} cells localizing to the white (*ii*. Red inset) and gray (*iii*. Blue inset) matter in the CNS (arrowheads). Brown indicates immunoreactivity for human CD4CAR; blue indicates hematoxylin counterstain. The magenta line demarcates the margin between the gray and white matter in the basal ganglia. **B)** The amount of CD4CAR-labeled CNS tissue (gray and white matter) as a percentage of the total CNS tissue area in both CAR and Control macaques. The dotted red line indicates that average % CD4CAR marking in representative CNS sections from CAR^{-} animals (0.04%). Scale: (*i.*) 1mm; (*ii*. *iii*.) 50µm.

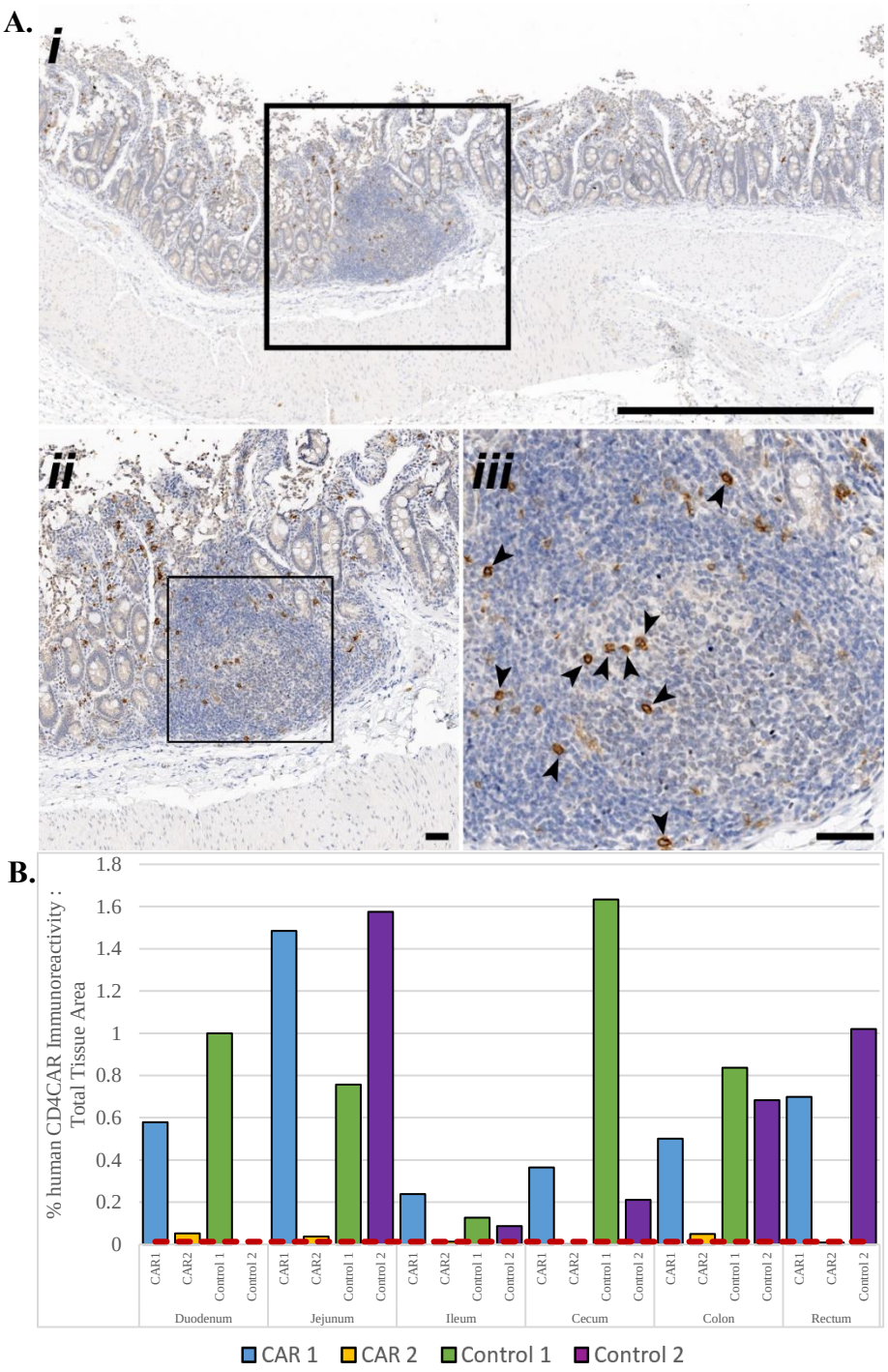

Figure 11. **HSPC-derived CD4^{+} cells localize to the GIT. A)** Low (*i.*) and high (*ii.* and *iii.*) magnification photomicrographs of the jejunum from CAR 1, illustrating CD4CAR^{+} cells localizing to the GALT (arrowheads). Brown indicates immunoreactivity for human CD4CAR; blue indicates hematoxylin counterstain. CAR^{+} cells are also visible in the adjacent submucosa. **B)** The amount of CD4CAR marking in the GALT and associated submucosa as a percentage of the tissue area. The dotted red line indicates that average % CD4CAR marking in representative GIT sections from CAR^{-} animals (0.013%). Scale: (*i.*) 1mm; (*ii. iii.*) 50µm.

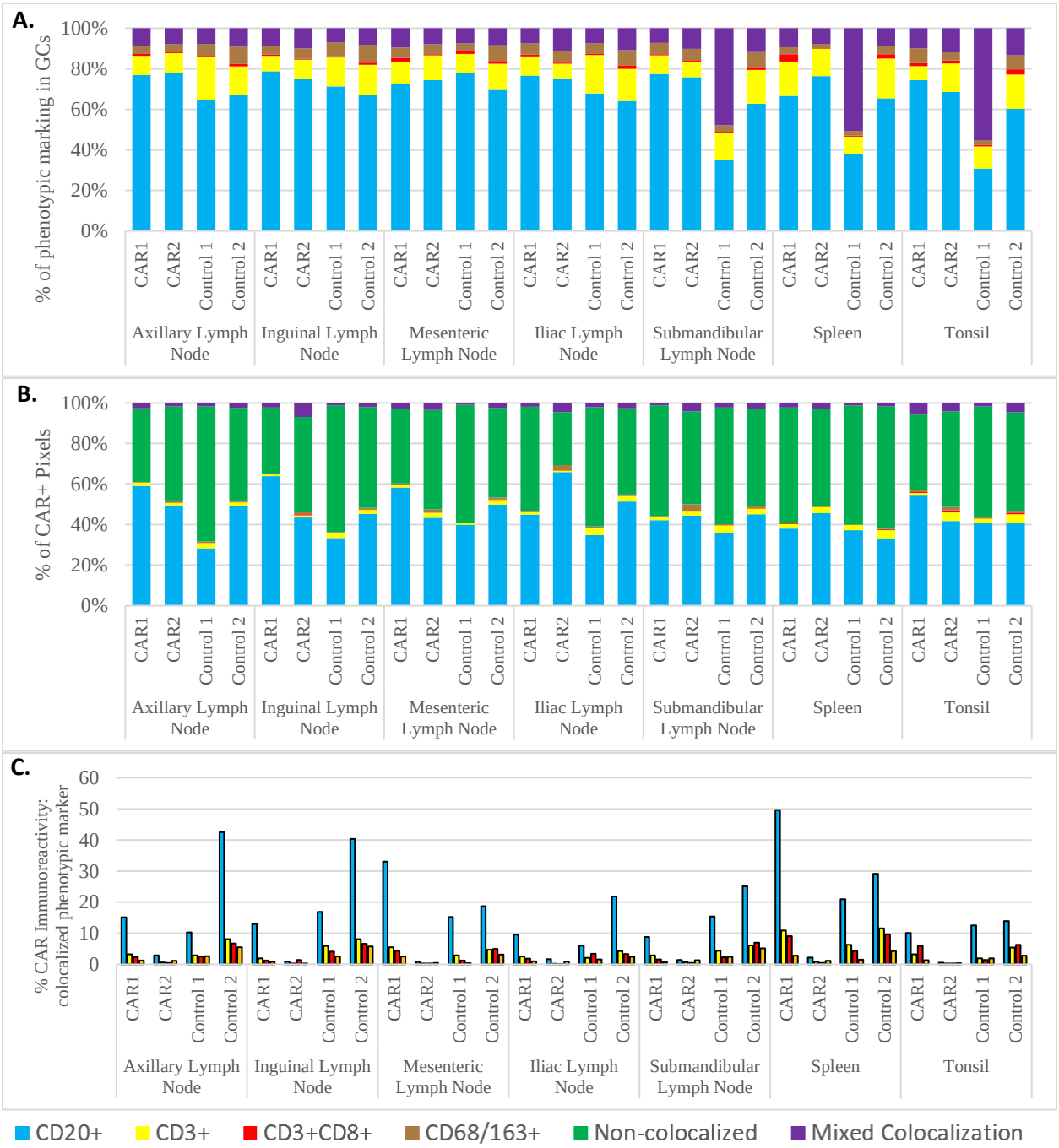

Figure 12. **Multilineage engraftment of HSPC-derived CAR$^+$ cells in GCs. A)** Percentages of total B-cell (CD20$^+$), T-cell (CD3$^+$), CTL (CD3$^+$CD8$^+$), and monocyte/macrophage (CD68/CD163$^+$) marking that that colocalized with CD4CAR immunoreactivity in GCs. **B)** Quantitation of CAR$^+$ pixel colocalization within GCs. **C)** Distribution of total phenotypic marking (colocalized and non-colocalized with the CAR) within the GCs.

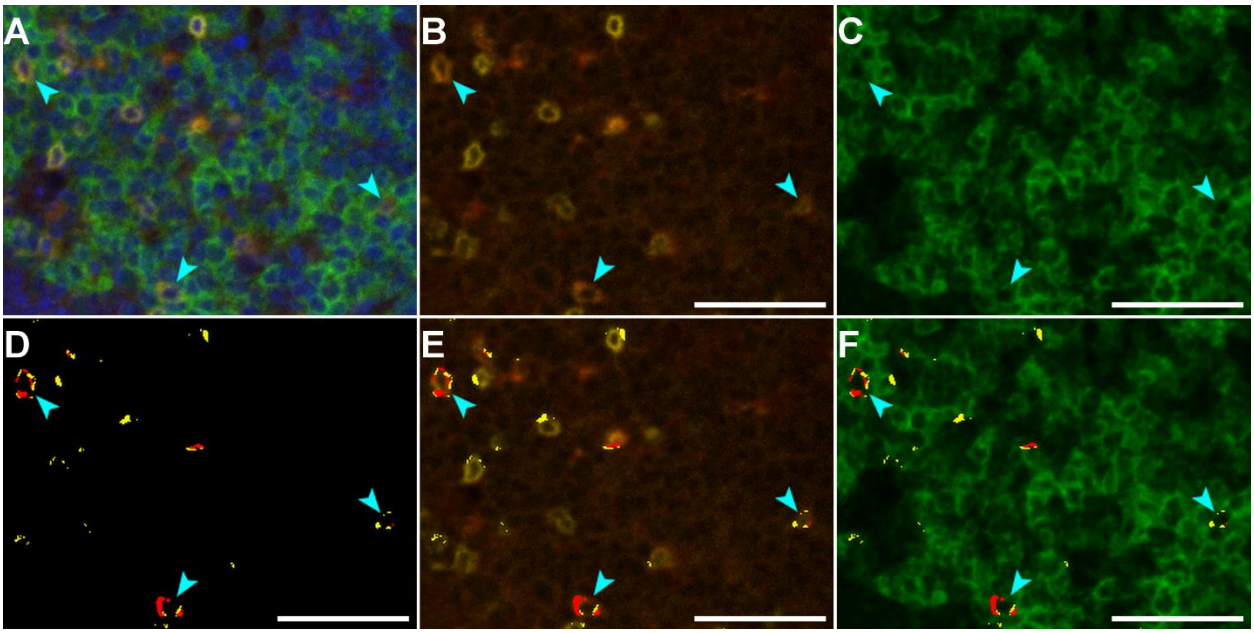

Figure 13. **HSCP-derived CAR^{+} T-cells traffic to GCs. A)** Composite fluorescent mIHC photomicrograph showing CD3 (yellow), CD8 (red), and CD4CAR (green) immunoreactivity, with DAPI (blue) counterstain; from CAR 1 mesenteric LN. **B and C)** Photomicrographs of separated phenotypic markers (**B**: CD3 and CD8; **C**: CD4CAR). **D)** Composite binarized micrograph that illustrates CAR colocalization with CD3 (yellow), and colocalization with CD3 and CD8 (red), without colocalization with CD20 or CD68/163. **E and F)** Separated fluorescent micrographs (**E**: CD3 and CD8; **F**: CD4CAR) overlayed with the binarized micrographs. Arrowheads indicate CAR^{+} T-cells within the GC. Scale: 50µm.

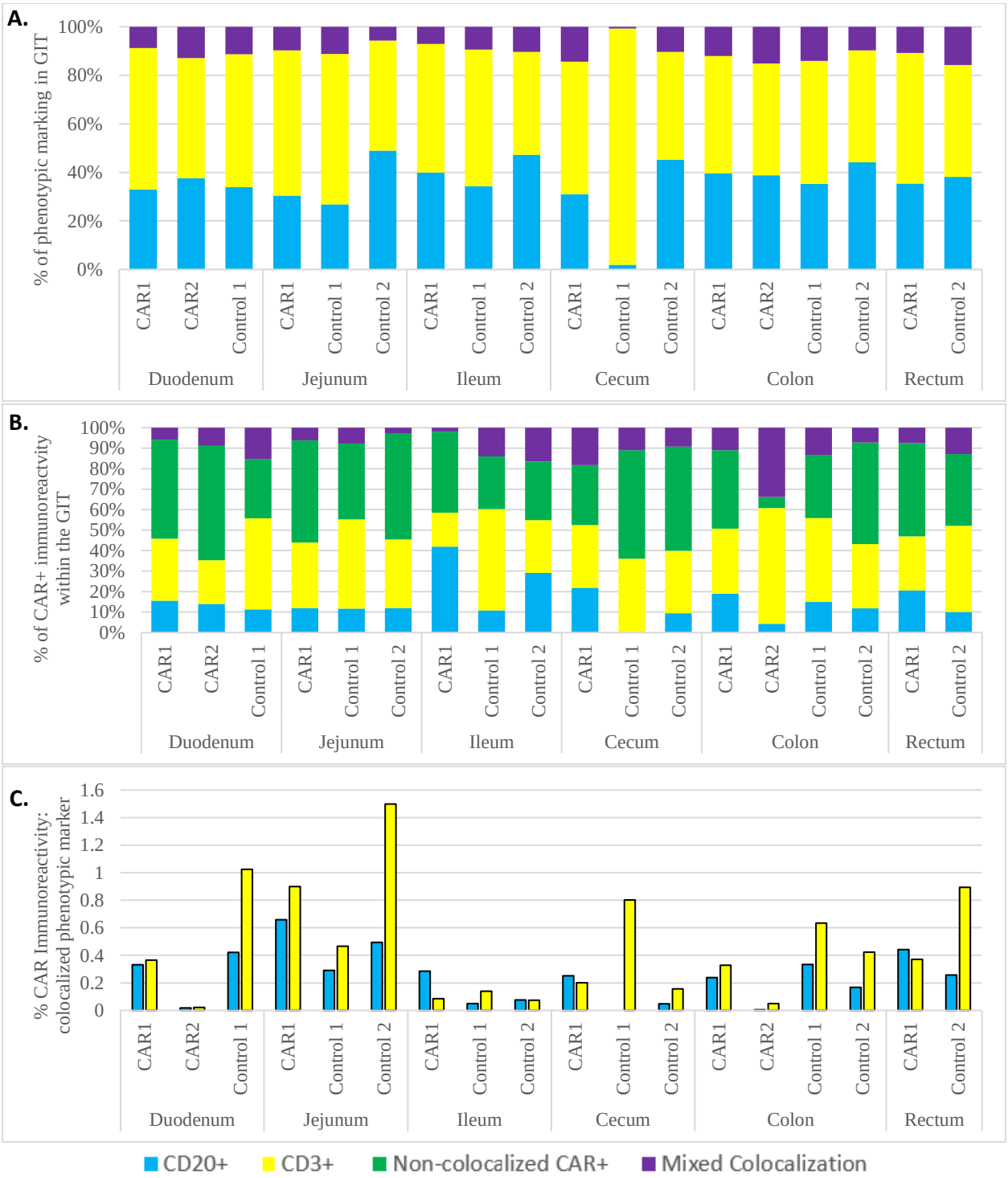

Figure 14. **Multilineage engraftment of HSPC-derived CAR$^+$ cells in the GIT. A)** Percentages of total B-cell (CD20$^+$) and T-cell (CD3$^+$) immunoreactivity that colocalized with CD4CAR immunoreactivity. **B)** Quantitation of CAR$^+$ pixel colocalization within GCs. **C)** Distribution of total phenotypic marking (colocalized and non-colocalized with the CAR) in the GIT.

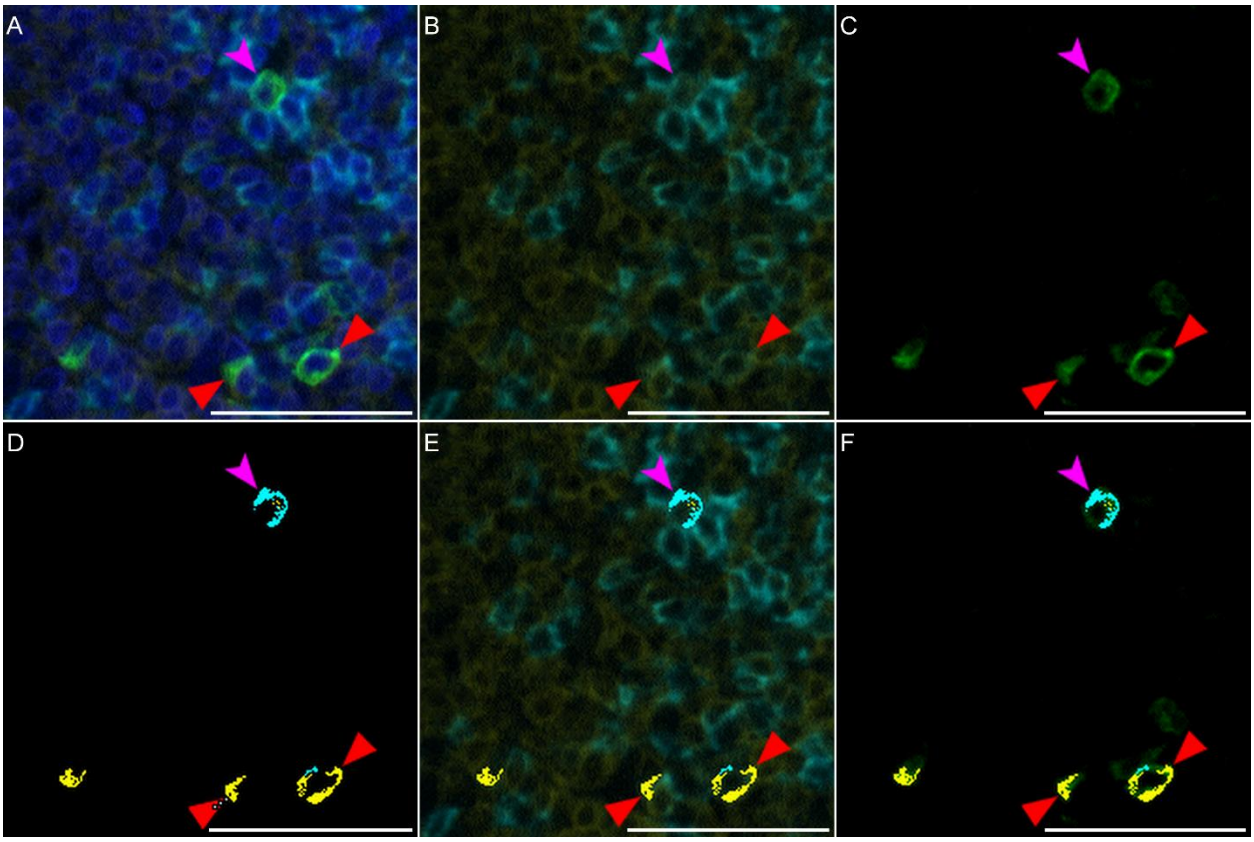

Figure 15. **HSCP-derived CAR$^+$ T-cells and B-cells traffic to the GIT. A)** Composite fluorescent mIHC photomicrograph showing CD3 (yellow), CD20 (Cyan), and CD4CAR (green) immunoreactivity, with DAPI (blue) counterstain; from Control 1 ileum. **B and C)** Photomicrographs of separated phenotypic markers (**B**: CD3 and CD20; **C**: CD4CAR). **D)** Composite binarized micrograph that illustrates CAR colocalization with CD3 (yellow), and CD20 (Cyan), without colocalization without CD3-CD20 double positive colocalization. **E and F)** Separated fluorescent micrographs (**E**: CD3 and CD20; **F**: CD4CAR) overlayed with the binarized micrographs. Red arrowheads indicate CAR$^+$ T-cells, and the magenta arrowhead indicates a CAR$^+$ B-cell. Scale: 50µm.

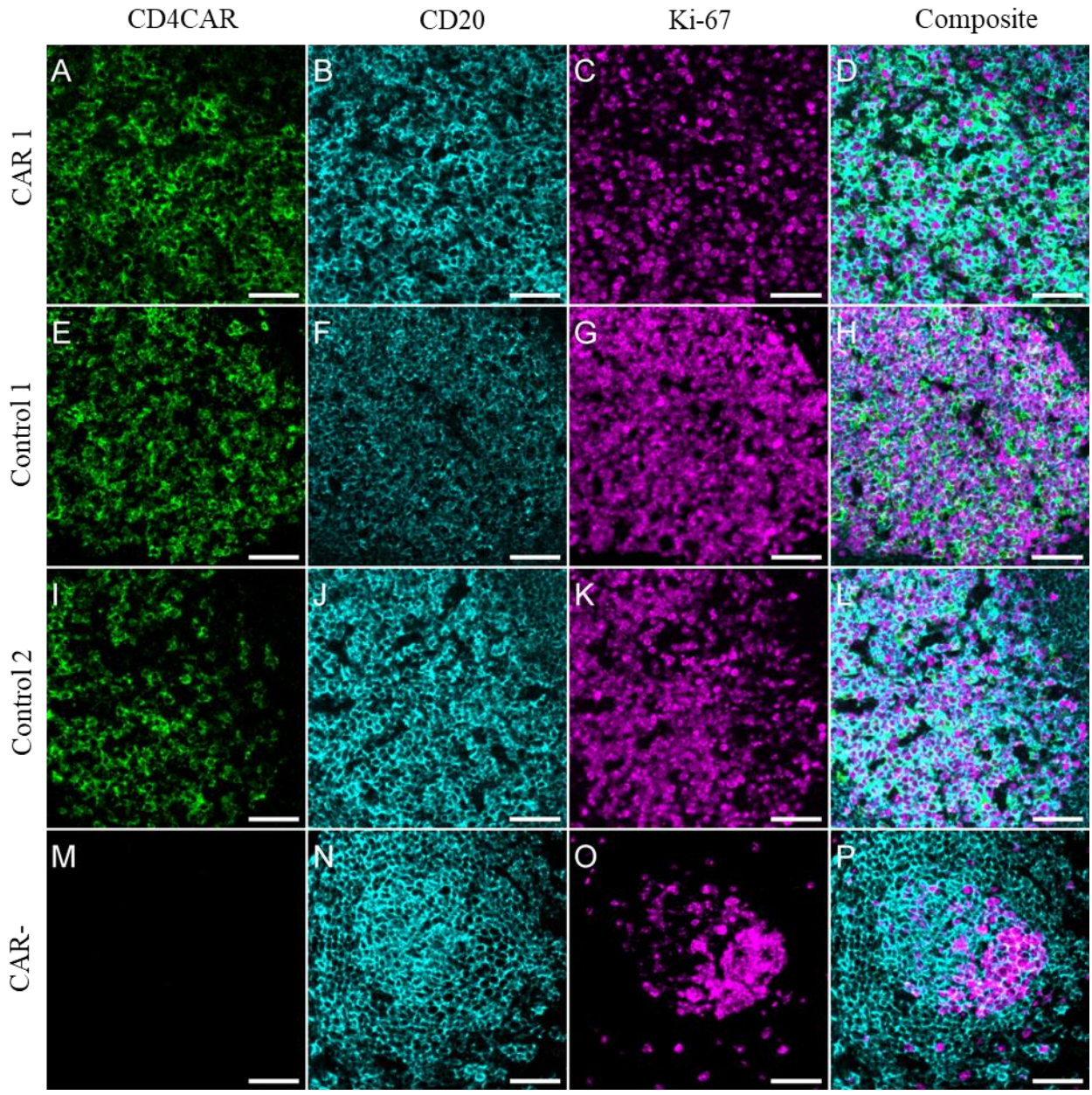

Figure 16: HSPC-derived CAR^{+} cells in the lymphoid GC are Ki-67^{+}, indicative of cell cycle activity. Colocalization of CD4CAR (column 1), CD20 (column 2), and Ki-67 (column 3) are apparent in lymphoid GC's from CAR 1 (A-D), control 1 (E-H), and control 2 (I-L). Ki-67^{+} CD20^{+} B-cells are visible in the GC of the CAR^{-} section (N-P). However, no CAR immunoreactivity is present within the CAR^{-} section (M). Scale: 50μm.

	Gross Lesions	Histologic Lesions
CAR 1	• Testicular atrophy/ hypoplasia	• Mild to moderate, diffuse, eosinophilic, lymphoplasmacytic and histiocytic gastro-entero-colitis with enteric villar blunting and fusion • Extensive, diffuse testicular hypoplasia • Renal adenoma "in-situ" with atypia
CAR 2	• Testicular atrophy/ hypoplasia	• Mild to moderate, diffuse, eosinophilic, lymphoplasmacytic and histiocytic gastro-entero-colitis with enteric villar blunting and fusion • Extensive, diffuse testicular hypoplasia
Control 1	• Testicular atrophy/ hypoplasia	• Mild to moderate, diffuse, eosinophilic, lymphoplasmacytic and histiocytic gastro-entero-colitis with enteric villar blunting and fusion • Extensive, diffuse testicular hypoplasia
Control 2	• Testicular atrophy/ hypoplasia	• Mild, multifocal, granulomatous meningoencephalitis • Mild to moderate, diffuse, eosinophilic, lymphoplasmacytic and histiocytic gastro-entero-colitis with enteric villar blunting and fusion • Extensive, diffuse testicular hypoplasia

Table 5. No evidence of toxicity associated with CAR lentiviral modified HSPC transduction. Summary of the major gross and histologic changes identified on postmortem evaluation of both CAR and control macaques.

A. MHC (HLA) class II, α2 chain [residues 125-131]			
Species	**Sequence ID**	**Sequence**	**% Homology**
Homo sapien	**P01906.2**	**LGQPNTL**	**100%**
Macaca nemistrina	**XP_011727361.1**	**LGQPNTL**	**100%**
Mus musculus	**AAA39614.1**	**LGQPNTL**	**100%**

B. MHC (HLA) class II, β1 chain [residues 41-56]			
Species	**Sequence ID**	**Sequence**	**% Homology**
Homo sapien	**P01920.2**	**YQFKAMCYFTNGTERV**	**100%**
Macaca nemistrina	**NP_001292858.1**	**HQFKFMCYFVNGTERV**	**81.3%**
Mus musculus	**AAC17911.1**	**FQFKGECYFTNGTQRI**	**68.8%**

C. MHC (HLA) class II, β2 chain [residues 134-155]			
Species	**Sequence ID**	**Sequence**	**% Homology**
Homo sapien	**P05538.2**	**PSRTEALNHHNLLVCSVTDFYP**	**100%**
Macaca nemistrina	**NP_001292858.1**	**PSRTEALNHHNLLVCSVTDFYP**	**100%**
Mus musculus	**NP_996988.2**	**SRTEALNHHNTLVCSVTDFYP**	**95.2%**

Figure 17. CD4 coreceptor binding sites on MHC class II antigen chains maintain moderate to high amino acid sequence homology across species. Comparison of the CD4 coreceptor binding domains on the HLA Class II α2 (**A**), β1 (**B**), and β2 chains to the pigtail macaque and mouse homologs. High homology is maintained across all 3 species in the α2 and β2. There is high amino acid sequence homology between the human and pigtail macaque β1 domain, with moderate sequence homology between the human and the mouse.

References

1. Hütter, G., Nowak, D., Mossner, M., Ganepola, S., Müßig, A., Allers, K., Schneider, T., Hofmann, J., Kücherer, C., Blau, O., Blau, I. W., Hofmann, W. K. & Thiel, E. Long-Term Control of HIV by CCR5 Delta32/Delta32 Stem-Cell Transplantation. *New Engl J Medicine* **360,** 692–698 (2009).

2. Allers, K., Hütter, G., Hofmann, J., Loddenkemper, C., Rieger, K., Thiel, E. & Schneider, T. Evidence for the cure of HIV infection by CCR5Δ32/Δ32 stem cell transplantation. *Blood* **117,** 2791–2799 (2011).

3. Hütter, G. & Ganepola, S. Eradication of HIV by Transplantation of CCR5-Deficient Hematopoietic Stem Cells. *Sci World J* **11,** 1068–1076 (2011).

4. Gupta, R. K., Abdul-Jawad, S., McCoy, L. E., Mok, H. P., Peppa, D., Salgado, M., Martinez-Picado, J., Nijhuis, M., Wensing, A. M., Lee, H., Grant, P., Nastouli, E., Lambert, J., Pace, M., Salasc, F., Monit, C., Innes, A. J., Muir, L., Waters, L., Frater, J., Lever, A. M., Edwards, S. G., Gabriel, I. H. & Olavarria, E. HIV-1 remission following CCR5Δ32/Δ32 haematopoietic stem-cell transplantation. *Nature* **568,** 244–248 (2019).

5. Hütter, G., Neumann, M., Nowak, D., Klein, S., Klüter, H. & Hofmann, W.-K. The effect of the CCR5-delta32 deletion on global gene expression considering immune response and inflammation. *J Inflamm* **8,** 29 (2011).

6. Liu, R., Paxton, W. A., Choe, S., Ceradini, D., Martin, S. R., Horuk, R., MacDonald, M. E., Stuhlmann, H., Koup, R. A. & Landau, N. R. Homozygous Defect in HIV-1 Coreceptor Accounts for Resistance of Some Multiply-Exposed Individuals to HIV-1 Infection. *Cell* **86,** 367–377 (1996).

7. Samson, M., Libert, F., Doranz, B. J., Rucker, J., Liesnard, C., Farber, C.-M., Saragosti, S., Lapouméroulie, C., Cognaux, J., Forceille, C., Muyldermans, G., Verhofstede, C., Burtonboy, G., Georges, M., Imai, T., Rana, S., Yi, Y., Smyth, R. J., Collman, R. G., Doms, R. W., Vassart, G. & Parmentier, M. Resistance to HIV-1 infection in Caucasian individuals bearing mutant alleles of the CCR-5 chemokine receptor gene. *Nature* **382,** 722 (1996).

8. an, Carrington, M., Winkler, C., Huttley, G., Smith, M., Allikmets, R., Goedert, J., Buchbinder, S., Vittinghoff, E., Gomperts, E., Donfield, S., Vlahov, D., Kaslow, R., Saah, A., Rinaldo, C., Detels, R., and Study, H., Study, M., Study, M., Cohort, S., Study, A. & O'Brien, S. Genetic Restriction of HIV-1 Infection and Progression to AIDS by a Deletion Allele of the CKR5 Structural Gene. *Science* **273,** 1856–1862 (1996).

16. Dragic, T., Litwin, V., Allaway, G. P., Martin, S. R., Huang, Y., Nagashima, K. A., Cayanan, C., Maddon, P. J., Koup, R. A., Moore, J. P. & Paxton, W. A. HIV-1 entry into CD4+ cells is mediated by the chemokine receptor CC-CKR-5. *Nature* **381,** 381667a0 (1996).

17. Deng, H., Liu, R., Ellmeier, W., Choe, S., Unutmaz, D., Burkhart, M., Marzio, P., Marmon, S., Sutton, R. E., Hill, M. C., Davis, C. B., Peiper, S. C., Schall, T. J., Littman, D. R. & Landau,

N. R. Identification of a major co-receptor for primary isolates of HIV-1. *Nature* **381,** 661–666 (1996).

18. Alkhatib, G., Combadiere, C., Broder, C. C., Feng, Y., Kennedy, P. E., Murphy, P. M. & Berger, E. A. CC CKR5: A RANTES, MIP-1α, MIP-1 Receptor as a Fusion Cofactor for Macrophage-Tropic HIV-1. *Science* **272,** 1955–1958 (1996).

19. Eugen-Olsen, J., Iversen, A., Garred, P., Koppelhus, U., Pedersen, C., Benfield, T. L., Sorensen, A. M., Katzenstein, T., Dickmeiss, E., Gerstoft, J., Skinhøj, P., Svejgaard, A., Nielsen, J. O. & Hofmann, B. Heterozygosity for a deletion in the CKR-5 gene leads to prolonged AIDS-free survival and slower CD4 T-cell decline in a cohort of HIV-seropositive individuals. *Aids* **11,** 305–310 (1997).

20. Henrich, T. J., Hu, Z., Li, J. Z., Sciaranghella, G., Busch, M. P., Keating, S. M., Gallien, S., Lin, N. H., Giguel, F. F., Lavoie, L., Ho, V. T., Armand, P., Soiffer, R. J., Sagar, M., LaCasce, A. S. & Kuritzkes, D. R. Long-Term Reduction in Peripheral Blood HIV Type 1 Reservoirs Following Reduced-Intensity Conditioning Allogeneic Stem Cell Transplantation. *The Journal of Infectious Diseases* **207,** 1694–1702 (2013).

14. Trajkovska, I., Georgievski, B., Cevreska, L., Gacovski, A., Hasan, T. & Nedeska-Minova, N. Early and Late Complications in Patients with Allogeneic Transplantation of Hematopoietic Stem Cell – Case Report. *Open Access Macedonian J Medical Sci* **0,** 340–343 (2017).

21. Tabbara, I. A., Zimmerman, K., Morgan, C. & Nahleh, Z. Allogeneic Hematopoietic Stem Cell Transplantation: Complications and Results. *Arch Intern Med* **162,** 1558–1566 (2002).

22. Kwon, M., Bailén, R., Balsalobre, P., Jurado, M., Bermudez, A., Badiola, J., Esquirol, A., Miralles, P., López-Fernández, E., Sanz, J., Yanez, L., Colorado, M., Piñana, J., Dorado, N., Solán, L., Laperche, C., Anguita, J., Serrano, D., Díez-Martin, J. & de y (GETH), G. Allogeneic stem cell transplantation in HIV-1 infected patients with high-risk hematological disorders. *Aids Lond Engl* 1 (2019). doi:10.1097/qad.0000000000002209

23. Martinson, J. J., Chapman, N. H., Rees, D. C., Liu, Y.-T. & Clegg, J. B. Global distribution of the CCR5 gene 32-basepair deletion. *Nat Genet* **16,** ng0597-100 (1997).

24. Nkenfou, C., Mekue, L., Nana, C. & Kuiate, J. Distribution of CCR5-Delta32, CCR5 promoter 59029 A/G, CCR2-64I and SDF1-3'A genetic polymorphisms in HIV-1 infected and uninfected patients in the West Region of Cameroon. *Bmc Res Notes* **6,** 288 (2013).

25. Rahimi, H., Farajollahi, M. M. & Hosseini, A. Distribution of the mutated delta 32 allele of CCR5 co-receptor gene in Iranian population. *Medical J Islamic Repub Iran* **28,** 140 (2014).

2. Zhang, C., Fu, S., Xue, Y., Wang, Q., Huang, X., Wang, B., Liu, A., Ma, L., Yu, Y., Shi, R., Lv, F., Shi, Z., Zhang, Y., Cheng, W., Ai, Q., Xu, F., Huang, C., Chen, B., Kang, X., Sun, Y., Zhang, G. & Li, P. Distribution of the CCR5 gene 32-basepair deletion in 11 Chinese populations. *Anthropologischer Anzeiger Bericht Über Die Biologisch-anthropologische Literatur* **60,** 267–71 (2002).

21. Yudin, N., Sergey, V. V., Potapova, T. A., Naykova, T. M., Sitnikova, V. V., Kulikov, I. V., Khasnulin, V. I., Konchuk, C., Vloschinskii, P. E., Ivanov, S. V., Kobzev, V. F., Romaschenko, A. G. & Voevoda, M. I. Distribution of CCR5-delta 32 gene deletion across the Russian part of Eurasia. *Human Genetics* **102,** 695–698 (1998).

22. Su, Q., Mai, Z., Zang, N., Wu, S., Xiao, X. & Liang, H. Distribution of CCR5-Δ32, CCR2-64I, and SDF1-3'A in Guangxi Zhuang Population. *J Int Assoc Physicians Aids Care* **9,** 145–149 (2010).

23. Hütter, G., Blüthgen, C., Elvers-Hornung, S., Klüter, H. & Bugert, P. Distribution of the CCR5-delta32 deletion in Southwest Germany. *Hütter Gero* **72,** 303-309(7) (2015).

24. Wei, X. & Nielsen, R. CCR5-Δ32 is deleterious in the homozygous state in humans. *Nat Med* 1–2 (2019). doi:10.1038/s41591-019-0459-6

25. Kordelas, L., Verheyen, J., Beelen, D. W., Horn, P. A., Heinold, A., Kaiser, R., Trenschel, R., Schadendorf, D., Dittmer, U., Esser, S. & Group, E. H. A. Shift of HIV Tropism in Stem-Cell Transplantation with CCR5 Delta32 Mutation. *New Engl J Medicine* **371,** 880–882 (2014).

26. Verheyen, J., Esser, S. & Kordelas, L. More on Shift of HIV Tropism in Stem-Cell Transplantation with CCR5 Delta32/Delta32 Mutation. *New Engl J Medicine* **371,** 2437–2438 (2014).

27. Archer, J., Braverman, M. S., Taillon, B. E., Desany, B., James, I., Harrigan, R. P., Lewis, M. & Robertson, D. L. Detection of low-frequency pretherapy chemokine (CXC motif) receptor 4 (CXCR4)-using HIV-1 with ultra-deep pyrosequencing. *Aids* **23,** 1209–1218 (2009).

28. Westby, M., Lewis, M., Whitcomb, J., Youle, M., Pozniak, A. L., James, I. T., Jenkins, T. M., Perros, M. & van der Ryst, E. Emergence of CXCR4-Using Human Immunodeficiency Virus Type 1 (HIV-1) Variants in a Minority of HIV-1-Infected Patients following Treatment with the CCR5 Antagonist Maraviroc Is from a Pretreatment CXCR4-Using Virus Reservoir. *J Virol* **80,** 4909–4920 (2006).

29. Henrich, T. J., Hanhauser, E., Hu, Z., Stellbrink, H.-J., Noah, C., Martin, J. N., Deeks, S. G., Kuritzkes, D. R. & Pereyra, F. Viremic control and viral coreceptor usage in two HIV-1-infected persons homozygous for CCR5 &Dgr;32. *Aids* **29,** 867–876 (2015).

30. Gray, L., Churchill, M. J., Keane, N., Sterjovski, J., Ellett, A. M., Purcell, D. F., Poumbourios, P., Kol, C., Wang, B., Saksena, N. K., Wesselingh, S. L., Price, P., French, M., Gabuzda, D. & Gorry, P. R. Genetic and Functional Analysis of R5X4 Human Immunodeficiency Virus Type 1 Envelope Glycoproteins Derived from Two Individuals Homozygous for the CCR5Δ32 Allele. *J Virol* **80,** 3684–3691 (2006).

31. Egelhofer, M., Brandenburg, G., Martinius, H., Schult-Dietrich, P., Melikyan, G., Kunert, R., Baum, C., Choi, I., Alexandrov, A. & von Laer, D. Inhibition of Human Immunodeficiency Virus Type 1 Entry in Cells Expressing gp41-Derived Peptides. *J Virol* **78,** 568–575 (2004).

32. Hildinger, M., Dittmar, M. T., Schult-Dietrich, P., Fehse, B., Schnierle, B. S., Thaler, S., Stiegler, G., Welker, R. & von Laer, D. Membrane-Anchored Peptide Inhibits Human Immunodeficiency Virus Entry. *J Virol* **75,** 3038–3042 (2001).

33. Wild, C., Shugars, D., Greenwell, T., nal, C. & Matthews, T. Peptides corresponding to a predictive alpha-helical domain of human immunodeficiency virus type 1 gp41 are potent inhibitors of virus infection. *Proc National Acad Sci* **91,** 9770–9774 (1994).

34. Wild, C., Dubay, J., Greenwell, T., Baird, T., Oas, T., nal, C., Hunter, E. & Matthews, T. Propensity for a leucine zipper-like domain of human immunodeficiency virus type 1 gp41 to form oligomers correlates with a role in virus-induced fusion rather than assembly of the glycoprotein complex. *Proc National Acad Sci* **91,** 12676–12680 (1994).

35. Dubay, J., Roberts, S., Brody, B. & Hunter, E. Mutations in the leucine zipper of the human immunodeficiency virus type 1 transmembrane glycoprotein affect fusion and infectivity. *J Virol* **66,** 4748–56 (1992).

36. Chen, S., Lee, S., Hao, H. & Chuang, C. Mutations in the leucine zipper-like heptad repeat sequence of human immunodeficiency virus type 1 gp41 dominantly interfere with wild-type virus infectivity. *J Virol* **72,** 4765–74 (1998).

37. Chen, S., Lee, C., Lee, W., McIntosh, K. & Lee, T. Mutational analysis of the leucine zipper-like motif of the human immunodeficiency virus type 1 envelope transmembrane glycoprotein. *J Virol* **67,** 3615–9 (1993).

38. Ding, X., Zhang, X., Chong, H., Zhu, Y., Wei, H., Wu, X., He, J., Wang, X. & He, Y. Enfuvirtide (T20)-Based Lipopeptide Is a Potent HIV-1 Cell Fusion Inhibitor: Implications for Viral Entry and Inhibition. *J Virol* **91,** e00831-17 (2017).

39. He, Y., Xiao, Y., Song, H., Liang, Q., Ju, D., Chen, X., Lu, H., Jing, W., Jiang, S. & Zhang, L. Design and Evaluation of Sifuvirtide, a Novel HIV-1 Fusion Inhibitor. *J Biol Chem* **283,** 11126–11134 (2008).

40. Eggink, D., Berkhout, B. & Sanders, R. W. Inhibition of HIV-1 by Fusion Inhibitors. *Curr Pharm Design* **16,** 3716–3728 (2010).

41. van Lunzen, J., Glaunsinger, T., Stahmer, I., von Baehr, V., Baum, C., Schilz, A., Kuehlcke, K., Naundorf, S., Martinius, H., Hermann, F., Giroglou, T., Newrzela, S., Müller, I., Brauer, F., Brandenburg, G., Alexandrov, A. & von Laer, D. Transfer of Autologous Gene-modified T Cells in HIV-infected Patients with Advanced Immunodeficiency and Drug-resistant Virus. *Mol Ther* **15,** 1024–1033 (2007).

42. Qin, H., Cho, M., Haso, W., Zhang, L., Tasian, S. K., Oo, H., Negri, G., Lin, Y., Zou, J., Mallon, B. S., Maude, S., Teachey, D. T., Barrett, D. M., Orentas, R. J., Daugaard, M., Sorensen, P. H., Grupp, S. A. & Fry, T. J. Eradication of B-ALL using chimeric antigen receptor–expressing T cells targeting the TSLPR oncoprotein. *Blood* **126,** 629–639 (2015).

43. Kochenderfer, J. N., Wilson, W. H., Janik, J. E., Dudley, M. E., Stetler-Stevenson, M.,

Feldman, S. A., Maric, I., Raffeld, M., Nathan, D.-A. N., Lanier, B. J., Morgan, R. A. & Rosenberg, S. A. Eradication of B-lineage cells and regression of lymphoma in a patient treated with autologous T cells genetically engineered to recognize CD19. *Blood* **116,** 4099–4102 (2010).

44. Maude, S. L., Frey, N., Shaw, P. A., Aplenc, R., Barrett, D. M., Bunin, N. J., Chew, A., Gonzalez, V. E., Zheng, Z., Lacey, S. F., Mahnke, Y. D., Melenhorst, J. J., Rheingold, S. R., Shen, A., Teachey, D. T., Levine, B. L., June, C. H., Porter, D. L. & Grupp, S. A. Chimeric Antigen Receptor T Cells for Sustained Remissions in Leukemia. *New Engl J Medicine* **371,** 1507–1517 (2014).

45. Till, B. G., Jensen, M. C., Wang, J., Qian, X., Gopal, A. K., Maloney, D. G., Lindgren, C. G., Lin, Y., Pagel, J. M., Budde, L. E., Raubitschek, A., Forman, S. J., Greenberg, P. D., Riddell, S. R. & Press, O. W. CD20-specific adoptive immunotherapy for lymphoma using a chimeric antigen receptor with both CD28 and 4-1BB domains: pilot clinical trial results. *Blood* **119,** 3940–3950 (2012).

46. Porter, D. L., Hwang, W.-T., Frey, N. V., Lacey, S. F., Shaw, P. A., Loren, A. W., Bagg, A., Marcucci, K. T., Shen, A., Gonzalez, V., Ambrose, D., Grupp, S. A., Chew, A., Zheng, Z., Milone, M. C., Levine, B. L., Melenhorst, J. J. & June, C. H. Chimeric antigen receptor T cells persist and induce sustained remissions in relapsed refractory chronic lymphocytic leukemia. *Sci Transl Med* **7,** 303ra139-303ra139 (2015).

47. Porter, D. L., Levine, B. L., Kalos, M., Bagg, A. & June, C. H. Chimeric Antigen Receptor–

Modified T Cells in Chronic Lymphoid Leukemia. *New Engl J Medicine* **365,** 725–733 (2011).

48. Lamers, C., Sleijfer, S., Vulto, A. G., Kruit, W., Kliffen, M., Debets, R., Gratama, J. W., Stoter, G. & Oosterwijk, E. Treatment of Metastatic Renal Cell Carcinoma With Autologous T-Lymphocytes Genetically Retargeted Against Carbonic Anhydrase IX: First Clinical Experience. *J Clin Oncol* **24,** e20–e22 (2006).

49. Luskin, M. R. & DeAngelo, D. J. Chimeric Antigen Receptor Therapy in Acute Lymphoblastic Leukemia Clinical Practice. *Curr Hematol Malig R* **12,** 370–379 (2017).

50. Yu, S., Li, A., Liu, Q., Li, T., Yuan, X., Han, X. & Wu, K. Chimeric antigen receptor T cells: a novel therapy for solid tumors. *J Hematol Oncol* **10,** 78 (2017).

51. Ramos, C. A., Savoldo, B. & Dotti, G. CD19-CAR Trials. *Cancer J* **20,** 112–118 (2014).

52. Qasim, W., Zhan, H., Samarasinghe, S., Adams, S., Amrolia, P., Stafford, S., Butler, K., Rivat, C., Wright, G., Somana, K., Ghorashian, S., Pinner, D., Ahsan, G., Gilmour, K., Lucchini, G., Inglott, S., Mifsud, W., Chiesa, R., Peggs, K. S., Chan, L., Farzeneh, F., Thrasher, A. J., Vora, A., Pule, M. & Veys, P. Molecular remission of infant B-ALL after infusion of universal TALEN gene-edited CAR T cells. *Sci Transl Med* **9,** eaaj2013 (2017).

53. Roberts, M. R., Qin, L., Zhang, D., Smith, D. H., Tran, A. C., Dull, T. J., Groopman, J. E., Capon, D. J., Byrn, R. A. & Finer, M. H. Targeting of human immunodeficiency virus-infected cells by CD8+ T lymphocytes armed with universal T-cell receptors. *Blood* **84,** 2878–89 (1994).

54. Yang, O. O., Tran, A.-C., Kalams, S. A., Johnson, R. P., Roberts, M. R. & Walker, B. D. Lysis of HIV-1-infected cells and inhibition of viral replication by universal receptor T cells. *Proc National Acad Sci* **94,** 11478–11483 (1997).

55. Scheppler, J., Nicholson, J., Swan, D., Ahmed-Ansari, A. & ugal, J. Down-modulation of MHC-I in a CD4+ T cell line, CEM-E5, after HIV-1 infection. *J Immunol Baltim Md 1950* **143,** 2858–66 (1989).

56. KERKAU, T., SCHMITT-LANDGRAF, R., SCHIMPL, A. & WECKER, E. Downregulation of HLA Class I Antigens in HIV-1-Infected Cells. *Aids Res Hum Retrov* **5,** 613–620 (1989).

57. Deeks, S. G., Wagner, B., Anton, P. A., Mitsuyasu, R. T., Scadden, D. T., Huang, C., Macken, C., Richman, D. D., Christopherson, C., June, C. H., Lazar, R., Broad, D. F., Jalali, S. & Hege, K. M. A Phase II Randomized Study of HIV-Specific T-Cell Gene Therapy in Subjects with Undetectable Plasma Viremia on Combination Antiretroviral Therapy. *Mol Ther* **5,** 788–797 (2002).

58. Scholler, J., Brady, T. L., Binder-Scholl, G., Hwang, W.-T., Plesa, G., Hege, K. M., Vogel, A. N., Kalos, M., Riley, J. L., Deeks, S. G., Mitsuyasu, R. T., Bernstein, W. B., Aronson, N. E., Levine, B. L., Bushman, F. D. & June, C. H. Decade-Long Safety and Function of Retroviral-Modified Chimeric Antigen Receptor T Cells. *Sci Transl Med* **4,** 132ra53-132ra53 (2012).

59. Walker, R., Bechtel, C., Natarajan, V., Baseler, M., Hege, K., Metcalf, J., Stevens, R., Hazen, A., Blaese, R., Chen, C., Leitman, S., Palensky, J., Wittes, J., Davey, R., Falloon, J., Polis, M., Kovacs, J., Broad, D., Levine, B., Roberts, M., Masur, H. & Lane, H. Long-term in vivo survival of receptor-modified syngeneic T cells in patients with human immunodeficiency virus infection. *Blood* **96,** 467–74 (2000).

60. Mitsuyasu, R., Anton, P., Deeks, S., Scadden, D., Connick, E., Downs, M., Bakker, A., Roberts, M., June, C., Jalali, S., Lin, A., Pennathur-Das, R. & Hege, K. Prolonged survival and tissue trafficking following adoptive transfer of CD4zeta gene-modified autologous CD4(+) and CD8(+) T cells in human immunodeficiency virus-infected subjects. *Blood* **96,** 785–93 (2000).

61. Oliveira, S., Ryan, C., Giannoni, F., Hardee, C. L., Tremcinska, I., Katebian, B., Wherley, J., Sahaghian, A., Tu, A., Grogan, T., Elashoff, D., Cooper, L. J., Hollis, R. P. & Kohn, D. B. Modification of Hematopoietic Stem/Progenitor Cells with CD19-Specific Chimeric Antigen Receptors as a Novel Approach for Cancer Immunotherapy. *Hum Gene Ther* **24,** 824–839 (2013).

62. Savoldo, B., Ramos, C., Liu, E., Mims, M. P., Keating, M. J., Carrum, G., Kamble, R. T., Bollard, C. M., Gee, A. P., Mei, Z., Liu, H., Grilley, B., Rooney, C. M., Heslop, H. E., Brenner, M. K. & Dotti, G. CD28 costimulation improves expansion and persistence of chimeric antigen receptor–modified T cells in lymphoma patients. *J Clin Invest* **121,** 1822–1826 (2011).

63. Gschweng, E., Oliveira, S. & Kohn, D. B. Hematopoietic stem cells for cancer immunotherapy. *Immunol Rev* **257,** 237–249 (2014).

64. Larson, S. & Oliveira, S. N. Gene-modified hematopoietic stem cells for cancer immunotherapy. *Hum Vacc Immunother* **10,** 982–985 (2014).

65. Zhen, A., Kamata, M., Rezek, V., Rick, J., Levin, B., Kasparian, S., Chen, I. S., Yang, O. O., Zack, J. A. & Kitchen, S. G. HIV-specific Immunity Derived From Chimeric Antigen Receptor-engineered Stem Cells. *Mol Ther* **23,** 1358–1367 (2015).

66. Zhen, A., Peterson, C. W., Carrillo, M. A., Reddy, S. S., Youn, C. S., Lam, B. B., Chang, N. Y., Martin, H. A., Rick, J. W., Kim, J., Neel, N. C., Rezek, V. K., Kamata, M., Chen, I. S. Y., Zack, J. A., Kiem, H.-P. & Kitchen, S. G. Long-term persistence and function of hematopoietic stem cell-derived chimeric antigen receptor T cells in a nonhuman primate model of HIV/AIDS. *Plos Pathog* **13,** e1006753 (2017).

67. Badowski, M. S., Zhang, T., Tsang, T. C. & Harris, D. T. Chimeric antigen receptors for stem cell based immunotherapy. *J Exp Ther Oncol* **8,** 53–63 (2009).

68. Tran, A., Zhang, D., Byrn, R. & Roberts, M. Chimeric zeta-receptors direct human natural killer (NK) effector function to permit killing of NK-resistant tumor cells and HIV-infected T lymphocytes. *J Immunol Baltim Md 1950* **155,** 1000–9 (1995).

69. Schirrmann, T. & Pecher, G. Specific targeting of CD33+ leukemia cells by a natural killer cell line modified with a chimeric receptor. *Leukemia Res* **29,** 301–306 (2005).

70. Li, L., Liu, L., Feller, S., Allen, C., Shivakumar, R., Fratantoni, J., Wolfraim, L., Fujisaki, H., Campana, D., Chopas, N., Dzekunov, S. & Peshwa, M. Expression of chimeric antigen receptors in natural killer cells with a regulatory-compliant non-viral method. *Cancer Gene Ther* **17,** 147 (2010).

71. Hege, K. M., Cooke, K. S., Finer, M. H., Zsebo, K. M. & Roberts, M. R. Systemic T Cell–independent Tumor Immunity after Transplantation of Universal Receptor–modified Bone Marrow into SCID Mice. *J Exp Medicine* **184,** 2261–2270 (1996).

72. Han, J., Chu, J., Chan, W., Zhang, J., Wang, Y., Cohen, J. B., Victor, A., Meisen, W. H., Kim, S., Grandi, P., Wang, Q.-E., He, X., Nakano, I., Chiocca, A. E., III, J. C., Kaur, B., Caligiuri, M. A. & Yu, J. CAR-Engineered NK Cells Targeting Wild-Type EGFR and EGFRvIII Enhance Killing of Glioblastoma and Patient-Derived Glioblastoma Stem Cells. *Sci Rep-uk* **5,** 11483 (2015).

73. Roberts, M., Cooke, K., Tran, A., Smith, K., Lin, W., Wang, M., Dull, T., Farson, D., Zsebo, K. & Finer, M. Antigen-specific cytolysis by neutrophils and NK cells expressing chimeric immune receptors bearing zeta or gamma signaling domains. *J Immunol Baltim Md 1950* **161,** 375–84 (1998).

74. Fox, C. H., Tenner-Rácz, K., Rácz, P., Firpo, A., Pizzo, P. A. & Fauci, A. S. Lymphoid germinal centers are reservoirs of human immunodeficiency virus type 1 RNA. *J Infect Dis* **164,** 1051–7 (1991).

75. Miles, B. & Connick, E. TFH in HIV Latency and as Sources of Replication-Competent Virus. *Trends Microbiol* **24,** 338–344 (2016).

76. Fukazawa, Y., Lum, R., Okoye, A. A., Park, H., Matsuda, K., Bae, J. Y., Hagen, S. I., Shoemaker, R., Deleage, C., Lucero, C., Morcock, D., Swanson, T., Legasse, A. W., Axthelm, M. K., Hesselgesser, J., Geleziunas, R., Hirsch, V. M., Edlefsen, P. T., Jr, M. P., Estes, J. D., Lifson, J. D. & Picker, L. J. B cell follicle sanctuary permits persistent productive simian immunodeficiency virus infection in elite controllers. *Nat Med* **21,** 132–139 (2015).

77. Aid, M., Dupuy, F. P., Moysi, E., Moir, S., Haddad, E. K., Estes, J. D., Sekaly, R., Petrovas, C. & Ribeiro, S. Follicular CD4 T Helper Cells As a Major HIV Reservoir Compartment: A Molecular Perspective. *Front Immunol* **9,** 895 (2018).

78. Bronnimann, M. P., Skinner, P. J. & Connick, E. The B-Cell Follicle in HIV Infection: Barrier to a Cure. *Frontiers in Immunology* **9,** 20 (2018).

79. Barton, K., Winckelmann, A. & Palmer, S. HIV-1 Reservoirs During Suppressive Therapy. *Trends Microbiol* **24,** 345–355 (2016).

80. Smith, M. Z., Wightman, F. & Lewin, S. R. HIV Reservoirs and Strategies for Eradication. *Curr Hiv-aids Rep* **9,** 5–15 (2012).

81. Hellmuth, J., Valcour, V. & Spudich, S. CNS reservoirs for HIV: implications for eradication. *J Virus Erad* **1,** 67–71 (2015).

82. Thompson, K. A., Cherry, C. L., Bell, J. E. & McLean, C. A. Brain Cell Reservoirs of Latent Virus in Presymptomatic HIV-Infected Individuals. *Am J Pathology* **179,** 1623–1629 (2011).

83. Gama, L., Abreu, C. M., Shirk, E. N., Price, S. L., Li, M., Laird, G. M., Pate, K. A. M., Wietgrefe, S. W., O'Connor, S. L., Pianowski, L., Haase, A. T., Van Lint, C., Siliciano, R. F., Clements, J. E. & Group, T. L.-S. S. Reactivation of simian immunodeficiency virus reservoirs in the brain of virally suppressed macaques. *Aids* **31,** 5 (2017).

84. Bednar, M. M., Sturdevant, C., Tompkins, L. A., Arrildt, K., Dukhovlinova, E., Kincer, L. P. & Swanstrom, R. Compartmentalization, Viral Evolution, and Viral Latency of HIV in the CNS. *Curr Hiv-aids Rep* **12,** 262–271 (2015).

85. Petito, C. K., Chen, H., Mastri, A. R., Torres-Munoz, J., Roberts, B. & Wood, C. HIV infection of choroid plexus in AIDS and asymptomatic HIV-infected patients suggests that the choroid plexus may be a reservoir of productive infection. *J Neurovirol* **5,** 670–677 (1999).

86. Chaillon, A., Gianella, S., Wertheim, J. O., Richman, D. D., Mehta, S. R. & Smith, D. M. HIV Migration Between Blood and Cerebrospinal Fluid or Semen Over Time. *J Infect Dis* **209,** 1642–1652 (2014).

87. Chun, T.-W., Nickle, D. C., Justement, J. S., Meyers, J. H., Roby, G., Hallahan, C. W., Kottilil, S., Moir, S., Mican, J. M., Mullins, J. I., Ward, D. J., A., K. J., Mannon, P. J. & Fauci, A. S. Persistence of HIV in Gut-Associated Lymphoid Tissue despite Long-Term Antiretroviral

Therapy. *J Infect Dis* **197,** 714–720 (2008).

88. Lampinen, T. M., Critchlow, C. W., Kuypers, J. M., Hurt, C. S., Nelson, P. J., Hawes, S. E., Coombs, R. W., Holmes, K. K. & Kiviat, N. B. Association of antiretroviral therapy with detection of HIV-1 RNA and DNA in the anorectal mucosa of homosexual men. *Aids* **14,** F69 (2000).

89. Lerner, P., Guadalupe, M., Donovan, R., Hung, J., Flamm, J., Prindiville, T., Sankaran-Walters, S., Syvanen, M., Wong, J. K., George, M. D. & Dandekar, S. The Gut Mucosal Viral Reservoir in HIV-Infected Patients Is Not the Major Source of Rebound Plasma Viremia following Interruption of Highly Active Antiretroviral Therapy. *J Virol* **85,** 4772–4782 (2011).

90. Poles, M. A., Boscardin, W. J., Elliott, J., Taing, P., Fuerst, M. M. P., McGowan, I., Brown, S. & Anton, P. A. Lack of Decay of HIV-1 in Gut-Associated Lymphoid Tissue Reservoirs in Maximally Suppressed Individuals. *Jaids J Acquir Immune Defic Syndromes* **43,** 65 (2006).

91. Di Stefano, M., Favia, A., Monno, L., Lopalco, P., Caputi, O., Scardigno, A. C., Pastore, G., Fiore, J. R. & Angarano, G. Intracellular and cell-free (infectious) HIV-1 in rectal mucosa. *J Med Virol* **65,** 637–643 (2001).

92. Dandekar, S. Pathogenesis of HIV in the gastrointestinal tract. *Curr Hiv-aids Rep* **4,** 10–15 (2007).

93. Smith, P. D., Meng, G., Salazar-Gonzalez, J. F. & Shaw, G. M. Macrophage HIV-1 infection

and the gastrointestinal tract reservoir. *J Leukocyte Biol* **74,** 642–649 (2003).

94. Yukl, S. A., Gianella, S., Sinclair, E., Epling, L., Li, Q., Duan, L., Choi, A. L. M., Girling, V., Ho, T., Li, P., Fujimoto, K., Lampiris, H., Hare, C. B., Pandori, M., Haase, A. T., Günthard, H. F., Fischer, M., Shergill, A. K., McQuaid, K., Havlir, D. V. & Wong, J. K. Differences in HIV Burden and Immune Activation within the Gut of HIV-Positive Patients Receiving Suppressive Antiretroviral Therapy. *J Infect Dis* **202,** 1553–1561 (2010).

95. Belmonte, L., Olmos, M., Fanin, A., Parodi, C., Baré, P., Concetti, H., Pérez, H., de Bracco, M. M. E. & Cahn, P. The intestinal mucosa as a reservoir of HIV-1 infection after successful HAART. *Aids* **21,** 2106 (2007).

96. Brown, D. & Mattapallil, J. J. Gastrointestinal Tract and the Mucosal Macrophage Reservoir in HIV Infection. *Clin Vaccine Immunol* **21,** 1469–1473 (2014).

97. Hlavacek, W. S., Stilianakis, N. I. & Perelson, A. S. Influence of follicular dendritic cells on HIV dynamics. *Philosophical Transactions Royal Soc Lond Ser B Biological Sci* **355,** 1051–1058 (2000).

98. Smith, B. A., Gartner, S., Liu, Y., Perelson, A. S., Stilianakis, N. I., Keele, B. F., Kerkering, T. M., Ferreira-Gonzalez, A., Szakal, A. K., Tew, J. G. & Burton, G. F. Persistence of Infectious HIV on Follicular Dendritic Cells. *J Immunol* **166,** 690–696 (2001).

99. Heesters, B. A., Lindqvist, M., Vagefi, P. A., Scully, E. P., Schildberg, F. A., Altfeld, M.,

Walker, B. D., Kaufmann, D. E. & Carroll, M. C. Follicular Dendritic Cells Retain Infectious HIV in Cycling Endosomes. *Plos Pathog* **11,** e1005285 (2015).

100. Zhang, J. & Perelson, A. S. Contribution of Follicular Dendritic Cells to Persistent HIV Viremia. *J Virol* **87,** 7893–7901 (2013).

101. Brauer, F., Schmidt, K., Zahn, R. C., Richter, C., Radeke, H. H., Schmitz, J. E., von Laer, D. & Egerer, L. A Rationally Engineered Anti-HIV Peptide Fusion Inhibitor with Greatly Reduced Immunogenicity. *Antimicrob Agents Ch* **57,** 679–688 (2013).

102. Song, R., Chenine, A.-L., Rasmussen, R., Ruprecht, C., Mirshahidi, S., Grisson, R., Xu, W., Whitney, J., Goins, L., Ong, H., Li, P.-L., Shai-Kobiler, E., Wang, T., McCann, C., Zhang, H., Wood, C., Kankasa, C., Secor, W., McClure, H., Strobert, E., Else, J. & Ruprecht, R. Molecularly Cloned SHIV-1157ipd3N4: a Highly Replication- Competent, Mucosally Transmissible R5 Simian-Human Immunodeficiency Virus Encoding HIV Clade C env. *J Virol* **80,** 8729–8738 (2006).

103. Peterson, C. W., Younan, P., Polacino, P. S., Maurice, N. J., Miller, H. W., Prlic, M., Jerome, K. R., Woolfrey, A. E., Hu, S. & Kiem, H. Robust suppression of env-SHIV viremia in Macaca nemestrina by 3-drug ART is independent of timing of initiation during chronic infection. *Journal of Medical Primatology* **42,** 237–246 (2013).

104. Peterson, C. W., Haworth, K. G., Burke, B. P., Polacino, P., Norman, K. K., Adair, J. E., Hu, S.-L., Bartlett, J. S., Symonds, G. P. & Kiem, H.-P. Multilineage polyclonal engraftment of

Cal-1 gene-modified cells and in vivo selection after SHIV infection in a nonhuman primate model of AIDS. *Mol Ther - Methods Clin Dev* **3,** 16007 (2016).

105. Stack, E. C., Wang, C., Roman, K. A. & Hoyt, C. C. Multiplexed immunohistochemistry, imaging, and quantitation: A review, with an assessment of Tyramide signal amplification, multispectral imaging and multiplex analysis. *Methods* **70,** 46–58 (2014).

106. Snyder, J. M., Washington, I. M., Birkland, T., Chang, M. Y. & Frevert, C. W. Correlation of Versican Expression, Accumulation, and Degradation during Embryonic Development by Quantitative Immunohistochemistry. *J Histochem Cytochem* **63,** 952–967 (2015).

107. Bankhead, P., Loughrey, M. B., Fernández, J. A., Dombrowski, Y., McArt, D. G., Dunne, P. D., McQuaid, S., Gray, R. T., Murray, L. J., Coleman, H. G., James, J. A., Salto-Tellez, M. & Hamilton, P. W. QuPath: Open source software for digital pathology image analysis. *Sci Rep-uk* **7,** 16878 (2017).

108. Rueden, C. T., Schindelin, J., Hiner, M. C., DeZonia, B. E., Walter, A. E., Arena, E. T. & Eliceiri, K. W. ImageJ2: ImageJ for the next generation of scientific image data. *BMC Bioinformatics* **18,** 529 (2017).

109. Schneider, C. A., Rasband, W. S. & Eliceiri, K. W. NIH Image to ImageJ: 25 years of image analysis. *Nature methods* **9,** 671–5 (2012).

110. Schindelin, J., Arganda-Carreras, I., Frise, E., Kaynig, V., Longair, M., Pietzsch, T.,

Preibisch, S., Rueden, C., Saalfeld, S., Schmid, B., Tinevez, J.-Y., White, D., Hartenstein, V., Eliceiri, K., Tomancak, P. & Cardona, A. Fiji: an open-source platform for biological-image analysis. *Nature Methods* **9,** 676 (2012).

111. MUTTERER, J. & ZINCK, E. Quick-and-clean article figures with FigureJ. *Journal of Microscopy* **252,** 89–91 (2013).

112. Estes, J. D., Harris, L. D., Klatt, N. R., Tabb, B., Pittaluga, S., Paiardini, M., Barclay, R. G., Smedley, J., Pung, R., Oliveira, K. M., Hirsch, V. M., Silvestri, G., Douek, D. C., Miller, C. J., Haase, A. T., Lifson, J. & Brenchley, J. M. Damaged Intestinal Epithelial Integrity Linked to Microbial Translocation in Pathogenic Simian Immunodeficiency Virus Infections. *Plos Pathog* **6,** e1001052 (2010).

113. Camp, R. L., Chung, G. G. & Rimm, D. L. Automated subcellular localization and quantification of protein expression in tissue microarrays. *Nat Med* **8,** nm791 (2002).

114. Sternberg, S. R. Biomedical Image Processing. *Computer* **16,** 22–34 (1983).

115. Otsu, N. A Threshold Selection Method from Gray-Level Histograms. *IEEE Transactions on Systems, Man, and Cybernetics* **9,** 62–66 (1979).

116. Shah, N. J., Mao, A. S., Shih, T.-Y. Y., Kerr, M. D., Sharda, A., Raimondo, T. M., Weaver, J. C., Vrbanac, V. D., Deruaz, M., Tager, A. M., Mooney, D. J. & Scadden, D. T. An injectable bone marrow-like scaffold enhances T cell immunity after hematopoietic stem cell

transplantation. *Nature biotechnology* **37,** 293–302 (2019).

117. Silva, N. S. & Klein, U. Dynamics of B cells in germinal centres. *Nat Rev Immunol* **15,** 137–148 (2015).

118. Victora, G. D. & Mesin, L. Clonal and cellular dynamics in germinal centers. *Curr Opin Immunol* **28,** 90–96 (2014).

119. Scaradavou, A. HIV-related thrombocytopenia. *Blood Rev* **16,** 73–76 (2002).

120. Gill, A. F., Ahsan, M. H., Lackner, A. A. & Veazey, R. S. Hematologic abnormalities associated with simian immunodeficieny virus (SIV) infection mimic those in HIV infection. *J Med Primatol* **41,** 214–224 (2012).

121. Hacein-Bey-Abina, S., Deist, F., Carlier, F., Bouneaud, C., Hue, C., Villartay, J.-P., Thrasher, A. J., Wulffraat, N., Sorensen, R., Dupuis-Girod, S., Fischer, A., Davies, G. E., Kuis, W., Leiva, L. & Cavazzana-Calvo, M. Sustained Correction of X-Linked Severe Combined Immunodeficiency by ex Vivo Gene Therapy. *New Engl J Medicine* **346,** 1185–1193 (2002).

122. Baum, C., Düllmann, J., Li, Z., Fehse, B., Meyer, J., Williams, D. A. & von Kalle, C. Side effects of retroviral gene transfer into hematopoietic stem cells. *Blood* **101,** 2099–2113 (2003).

123. Kohn, D. B., Sadelain, M. & Glorioso, J. C. Occurrence of leukaemia following gene therapy of X-linked SCID. *Nat Rev Cancer* **3,** 477–488 (2003).

124. Hacein-Bey-Abina, S., von Kalle, C., Schmidt, M., Deist, F., Wulffraat, N., McIntyre, E., Radford, I., Villeval, J.-L., Fraser, C. C., Cavazzana-Calvo, M. & Fischer, A. A Serious Adverse Event after Successful Gene Therapy for X-Linked Severe Combined Immunodeficiency. *New Engl J Medicine* **348,** 255–256 (2003).

125. Hacein-Bey-Abina, S., Kalle, V. C., Schmidt, M., McCormack, M., Wulffraat, N., Leboulch, P., Lim, A., Osborne, C., Pawliuk, R., Morillon, E., Sorensen, R., Forster, A., Fraser, P., Cohen, J., de Basile, S. G., Alexander, I., Wintergerst, U., Frebourg, T., Aurias, A., Stoppa-Lyonnet, D., Romana, S., Radford-Weiss, I., Gross, F., Valensi, F., Delabesse, E., Macintyre, E., Sigaux, F., Soulier, J., Leiva, L., Wissler, M., Prinz, C., Rabbitts, T., Deist, L. F., Fischer, A. & Cavazzana-Calvo, M. LMO2-Associated Clonal T Cell Proliferation in Two Patients after Gene Therapy for SCID-X1. *Science* **302,** 415–419 (2003).

126. Romano, G. Development of Safer Gene Delivery Systems to Minimize the Risk of Insertional Mutagenesis-Related Malignancies: A Critical Issue for the Field of Gene Therapy. *Isrn Oncol* **2012,** 616310 (2012).

127. Edelstein, M. L., Abedi, M. R. & Wixon, J. Gene therapy clinical trials worldwide to 2007—an update. *J Gene Medicine* **9,** 833–842 (2007).

128. Baum, C. Gene Therapy for SCID-X1: Focus on Clinical Data. *Mol Ther* **19,** 2103–2104 (2011).

129. Cavazzana-Calvo, M. & Fischer, A. Gene therapy for severe combined immunodeficiency: are we there yet? *J Clin Invest* **117,** 1456–1465 (2007).

130. Hacein-Bey-Abina, S., Garrigue, A., Wang, G. P., Soulier, J., Lim, A., Morillon, E., Clappier, E., Caccavelli, L., Delabesse, E., Beldjord, K., Asnafi, V., MacIntyre, E., Cortivo, L., Radford, I., Brousse, N., Sigaux, F., Moshous, D., Hauer, J., Borkhardt, A., Belohradsky, B. H., Wintergerst, U., Velez, M. C., Leiva, L., Sorensen, R., Wulffraat, N., Blanche, S., Bushman, F. D., Fischer, A. & Cavazzana-Calvo, M. Insertional oncogenesis in 4 patients after retrovirus-mediated gene therapy of SCID-X1. *J Clin Invest* **118,** 3132–3142 (2008).

131. Howe, S. J., Mansour, M. R., Schwarzwaelder, K., Bartholomae, C., Hubank, M., Kempski, H., Brugman, M. H., Pike-Overzet, K., Chatters, S. J., de Ridder, D., Gilmour, K. C., Adams, S., Thornhill, S. I., Parsley, K. L., Staal, F., Gale, R. E., Linch, D. C., Bayford, J., Brown, L., Quaye, M., Kinnon, C., Ancliff, P., Webb, D. K., Schmidt, M., von Kalle, C., Gaspar, B. H. & Thrasher, A. J. Insertional mutagenesis combined with acquired somatic mutations causes leukemogenesis following gene therapy of SCID-X1 patients. *J Clin Invest* **118,** 3143–3150 (2008).

132. Pike-Overzet, K., van der Burg, M., Wagemaker, G., van Dongen, J. J. & Staal, F. J. New Insights and Unresolved Issues Regarding Insertional Mutagenesis in X-linked SCID Gene Therapy. *Mol Ther* **15,** 1910–1916 (2007).

133. Chinen, J. & Puck, J. M. Successes and risks of gene therapy in primary immunodeficiencies. *J Allergy Clin Immun* **113,** 595–603 (2004).

134. David, R. M. & Doherty, A. T. Viral Vectors: The Road to Reducing Genotoxicity. *Toxicol Sci* **155,** 315–325 (2017).

135. Schambach, A., Zychlinski, D., Ehrnstroem, B. & Baum, C. Biosafety Features of Lentiviral Vectors. *Hum Gene Ther* **24,** 132–142 (2013).

136. Kroese, F. G., Wubbena, A. S., Seijen, H. G. & Nieuwenhuis, P. Germinal centers develop oligoclonally. *European Journal of Immunology* **17,** 1069–1072 (1987).

137. Eglitis, M. A. & Mezey, É. Hematopoietic cells differentiate into both microglia and macroglia in the brains of adult mice. *Proceedings of the National Academy of Sciences* **94,** 4080–4085 (1997).

138. Prinz, M., Erny, D. & Hagemeyer, N. Ontogeny and homeostasis of CNS myeloid cells. *Nat Immunol* **18,** 385–392 (2017).

139. Kierdorf, K., Katzmarski, N., Haas, C. A. & Prinz, M. Bone Marrow Cell Recruitment to the Brain in the Absence of Irradiation or Parabiosis Bias. *Plos One* **8,** e58544 (2013).

140. Filip, S., Mokrý, J., Vávrová, J., Šinkorová, Z., Mičuda, S., Šponer, P., Filipová, A., Hrebíková, H. & Dayanithi, G. The peripheral chimerism of bone marrow–derived stem cells after transplantation: regeneration of gastrointestinal tissues in lethally irradiated mice. *J Cell Mol Med* **18,** 832–843 (2014).

141. Linderman, J. A. & Shizuru, J. A. Rapid Reconstitution of Antibody Responses Following Transplantation of Purified Allogeneic Hematopoietic Stem Cells. *J Immunol* **186,** 4191–4199 (2011).

142. Goldmann, T., Wieghofer, P., Jordão, M., Prutek, F., Hagemeyer, N., Frenzel, K., Amann, L., Staszewski, O., Kierdorf, K., Krueger, M., Locatelli, G., Hochgerner, H., Zeiser, R., Epelman, S., Geissmann, F., Priller, J., Rossi, F. M., Bechmann, I., Kerschensteiner, M., Linnarsson, S., Jung, S. & Prinz, M. Origin, fate and dynamics of macrophages at central nervous system interfaces. *Nat Immunol* **17,** 797–805 (2016).

143. Ajami, B., Bennett, J. L., Krieger, C., Tetzlaff, W. & Rossi, F. M. Local self-renewal can sustain CNS microglia maintenance and function throughout adult life. *Nat Neurosci* **10,** nn2014 (2007).

144. Priller, J., Flügel, A., Wehner, T., Boentert, M., Haas, C. A., Prinz, M., Fernández-Klett, F., Prass, K., Bechmann, I., de Boer, B. A., Frotscher, M., Kreutzberg, G. W., Persons, D. A. & Dirnagl, U. Targeting gene-modified hematopoietic cells to the central nervous system: Use of green fluorescent protein uncovers microglial engraftment. *Nat Med* **7,** nm1201-1356 (2001).

145. Massengale, M., Wagers, A. J., Vogel, H. & Weissman, I. L. Hematopoietic cells maintain hematopoietic fates upon entering the brain. *J Exp Medicine* **201,** 1579–1589 (2005).

146. Mildner, A., Schmidt, H., Nitsche, M., Merkler, D., Hanisch, U.-K., Mack, M., Heikenwalder, M., Brück, W., Priller, J. & Prinz, M. Microglia in the adult brain arise from Ly-

6ChiCCR2+ monocytes only under defined host conditions. *Nat Neurosci* **10,** nn2015 (2007).

147. Mildner, A., Schlevogt, B., Kierdorf, K., Böttcher, C., Erny, D., Kummer, M. P., Quinn, M., Brück, W., Bechmann, I., Heneka, M. T., Priller, J. & Prinz, M. Distinct and Non-Redundant Roles of Microglia and Myeloid Subsets in Mouse Models of Alzheimer's Disease. *J Neurosci* **31,** 11159–11171 (2011).

148. Lampron, A., Lessard, M. & Rivest, S. Effects of Myeloablation, Peripheral Chimerism, and Whole-Body Irradiation on the Entry of Bone Marrow-Derived Cells into the Brain. *Cell Transplant* **21,** 1149–1159 (2011).

149. Diserbo, M., Agin, A., Lamproglou, I., Mauris, J., Staali, F., Multon, E. & Amourette, C. Blood-brain barrier permeability after gamma whole-body irradiation: an in vivo microdialysis study. *Can J Physiol Pharm* **80,** 670–678 (2002).

150. Yuan, H., Gaber, M. W., McColgan, T., Naimark, M. D., Kiani, M. F. & Merchant, T. E. Radiation-induced permeability and leukocyte adhesion in the rat blood–brain barrier: modulation with anti-ICAM-1 antibodies. *Brain Res* **969,** 59–69 (2003).

151. Kaya, M., Palanduz, A., Kalayci, R., Kemikler, G., Simsek, G., Bilgic, B., Ahishali, B., Arican, N., Kocyildiz, Z., Elmas, I., Kucuk, M. & Karadeniz, A. Effects of lipopolysaccharide on the radiation-induced changes in the blood–brain barrier and the astrocytes. *Brain Res* **1019,** 105–112 (2004).

152. Li, Y.-Q., Chen, P., Jain, V., Reilly, R. M. & Wong, S. C. Early Radiation-Induced Endothelial Cell Loss and Blood–Spinal Cord Barrier Breakdown in the Rat Spinal Cord. *Radiat Res* **181,** 143–152 (2004).

153. Garvin, A. M., Davis, C. B., Littman, D. R., Carlow, D. A., Teh, H.-S., Forbush, K. A. & Perlmutter, R. M. Participation of CD4 coreceptor molecules in T-cell repertoire selection. *Nature* **349,** 241 (1991).

1. Hütter, G., Nowak, D., Mossner, M., Ganepola, S., Müßig, A., Allers, K., Schneider, T., Hofmann, J., Kücherer, C., Blau, O., Blau, I. W., Hofmann, W. K. & Thiel, E. Long-Term Control of HIV by CCR5 Delta32/Delta32 Stem-Cell Transplantation. New Engl J Medicine 360, 692–698 (2009).

2. Allers, K., Hütter, G., Hofmann, J., Loddenkemper, C., Rieger, K., Thiel, E. & Schneider, T. Evidence for the cure of HIV infection by CCR5Δ32/Δ32 stem cell transplantation. Blood 117, 2791–2799 (2011).

3. Hütter, G. & Ganepola, S. Eradication of HIV by Transplantation of CCR5-Deficient Hematopoietic Stem Cells. Sci World J 11, 1068–1076 (2011).

4. Gupta, R. K., Abdul-Jawad, S., McCoy, L. E., Mok, H. P., Peppa, D., Salgado, M., Martinez-Picado, J., Nijhuis, M., Wensing, A. M., Lee, H., Grant, P., Nastouli, E., Lambert, J., Pace, M., Salasc, F., Monit, C., Innes, A. J., Muir, L., Waters, L., Frater, J., Lever, A. M., Edwards, S. G., Gabriel, I. H. & Olavarria, E. HIV-1 remission following CCR5Δ32/Δ32 haematopoietic stem-cell transplantation. Nature 568, 244–248 (2019).

5. Hütter, G., Neumann, M., Nowak, D., Klein, S., Klüter, H. & Hofmann, W.-K. The effect of the CCR5-delta32 deletion on global gene expression considering immune response and inflammation. J Inflamm 8, 29 (2011).

6. Liu, R., Paxton, W. A., Choe, S., Ceradini, D., Martin, S. R., Horuk, R., MacDonald, M. E., Stuhlmann, H., Koup, R. A. & Landau, N. R. Homozygous Defect in HIV-1 Coreceptor Accounts for Resistance of Some Multiply-Exposed Individuals to HIV-1 Infection. Cell 86, 367–377 (1996).

7. Samson, M., Libert, F., Doranz, B. J., Rucker, J., Liesnard, C., Farber, C.-M., Saragosti, S., Lapouméroulie, C., Cognaux, J., Forceille, C., Muyldermans, G., Verhofstede, C., Burtonboy, G., Georges, M., Imai, T., Rana, S., Yi, Y., Smyth, R. J., Collman, R. G., Doms, R. W., Vassart, G. & Parmentier, M. Resistance to HIV-1 infection in Caucasian individuals bearing mutant alleles of the CCR-5 chemokine receptor gene. Nature 382, 722 (1996).

8. an, Carrington, M., Winkler, C., Huttley, G., Smith, M., Allikmets, R., Goedert, J., Buchbinder, S., Vittinghoff, E., Gomperts, E., Donfield, S., Vlahov, D., Kaslow, R., Saah, A., Rinaldo, C., Detels, R., and Study, H., Study, M., Study, M., Cohort, S., Study, A. & O'Brien, S. Genetic Restriction of HIV-1 Infection and Progression to AIDS by a Deletion Allele of the CKR5 Structural Gene. Science 273, 1856–1862 (1996).

9. Smiley, S. T., Singh, A., Read, S. W., Sharma, O. K., Finzi, D., Lane, C. & Rice, J. S. Progress Toward Curing HIV Infections With Hematopoietic Stem Cell Transplantation. Clin Infect Dis 60, 292–297 (2015).

10. Peterson, C. W. & Kiem, H.-P. Lessons from London and Berlin: Designing A Scalable Gene Therapy Approach for HIV Cure. Cell Stem Cell 24, 685–687 (2019).

11. Pitman, M. C. & Lewin, S. R. Towards a cure for human immunodeficiency virus. Intern Med J 48, 12–15 (2018).

12. Hütter, G. & Ganepola, S. Eradication of HIV by Transplantation of CCR5-Deficient Hematopoietic Stem Cells. Sci World J 11, 1068–1076 (2011).

13. Hütter, G. & Zaia, J. A. Allogeneic haematopoietic stem cell transplantation in patients with human immunodeficiency virus: the experiences of more than 25 years. Clin Exp Immunol 163, 284–295 (2011).

14. Horowitz, M., Gale, R., ndel, P., Goldman, J., Kersey, J., Kolb, H., Rimm, A., Ringdén, O., Rozman, C. & Speck, B. Graft-versus-leukemia reactions after bone marrow transplantation. Blood 75, 555–62 (1990).

15. Dickinson, A. M., Norden, J., Li, S., Hromadnikova, I., Schmid, C., Schmetzer, H. & Jochem-Kolb, H. Graft-versus-Leukemia Effect Following Hematopoietic Stem Cell Transplantation for Leukemia. Front Immunol 8, 496 (2017).

16. Dragic, T., Litwin, V., Allaway, G. P., Martin, S. R., Huang, Y., Nagashima, K. A., Cayanan, C., Maddon, P. J., Koup, R. A., Moore, J. P. & Paxton, W. A. HIV-1 entry into CD4+ cells is mediated by the chemokine receptor CC-CKR-5. Nature 381, 381667a0 (1996).

17. Deng, H., Liu, R., Ellmeier, W., Choe, S., Unutmaz, D., Burkhart, M., Marzio, P., Marmon, S., Sutton, R. E., Hill, M. C., Davis, C. B., Peiper, S. C., Schall, T. J., Littman, D. R. & Landau, N. R. Identification of a major co-receptor for primary isolates of HIV-1. Nature 381, 661–666 (1996).

18. Alkhatib, G., Combadiere, C., Broder, C. C., Feng, Y., Kennedy, P. E., Murphy, P. M. & Berger, E. A. CC CKR5: A RANTES, MIP-1α, MIP-1 Receptor as a Fusion Cofactor for Macrophage-Tropic HIV-1. Science 272, 1955–1958 (1996).

19. Eugen-Olsen, J., Iversen, A., Garred, P., Koppelhus, U., Pedersen, C., Benfield, T. L., Sorensen, A. M., Katzenstein, T., Dickmeiss, E., Gerstoft, J., Skinhøj, P., Svejgaard, A., Nielsen, J. O. & Hofmann, B. Heterozygosity for a deletion in the CKR-5 gene leads to prolonged AIDS-free survival and slower CD4 T-cell decline in a cohort of HIV-seropositive individuals. Aids 11, 305–310 (1997).

20. Henrich, T. J., Hu, Z., Li, J. Z., Sciaranghella, G., Busch, M. P., Keating, S. M., Gallien, S., Lin, N. H., Giguel, F. F., Lavoie, L., Ho, V. T., Armand, P., Soiffer, R. J., Sagar, M., LaCasce, A. S. & Kuritzkes, D. R. Long-Term Reduction in Peripheral Blood HIV Type 1 Reservoirs Following Reduced-Intensity Conditioning Allogeneic Stem Cell Transplantation. The Journal of Infectious Diseases 207, 1694–1702 (2013).

21. Trajkovska, I., Georgievski, B., Cevreska, L., Gacovski, A., Hasan, T. & Nedeska-Minova, N. Early and Late Complications in Patients with Allogeneic Transplantation of Hematopoietic Stem Cell – Case Report. Open Access Macedonian J Medical Sci 0, 340–343 (2017).

22. Tabbara, I. A., Zimmerman, K., Morgan, C. & Nahleh, Z. Allogeneic Hematopoietic Stem Cell Transplantation: Complications and Results. Arch Intern Med 162, 1558–1566 (2002).

23. Kwon, M., Bailén, R., Balsalobre, P., Jurado, M., Bermudez, A., Badiola, J., Esquirol, A., Miralles, P., López-Fernández, E., Sanz, J., Yanez, L., Colorado, M., Piñana, J., Dorado, N., Solán, L., Laperche, C., Anguita, J., Serrano, D., Díez-Martin, J. & de y (GETH), G. Allogeneic stem cell transplantation in HIV-1 infected patients with high-risk hematological disorders. Aids Lond Engl 1 (2019). doi:10.1097/qad.0000000000002209

24. Martinson, J. J., Chapman, N. H., Rees, D. C., Liu, Y.-T. & Clegg, J. B. Global distribution of the CCR5 gene 32-basepair deletion. Nat Genet 16, ng0597-100 (1997).

25. Nkenfou, C., Mekue, L., Nana, C. & Kuiate, J. Distribution of CCR5-Delta32, CCR5 promoter 59029 A/G, CCR2-64I and SDF1-3'A genetic polymorphisms in HIV-1 infected and uninfected patients in the West Region of Cameroon. Bmc Res Notes 6, 288 (2013).

26. Rahimi, H., Farajollahi, M. M. & Hosseini, A. Distribution of the mutated delta 32 allele of CCR5 co-receptor gene in Iranian population. Medical J Islamic Repub Iran 28, 140 (2014).

27. Zhang, C., Fu, S., Xue, Y., Wang, Q., Huang, X., Wang, B., Liu, A., Ma, L., Yu, Y., Shi, R., Lv, F., Shi, Z., Zhang, Y., Cheng, W., Ai, Q., Xu, F., Huang, C., Chen, B., Kang, X., Sun, Y.,

Zhang, G. & Li, P. Distribution of the CCR5 gene 32-basepair deletion in 11 Chinese populations. Anthropologischer Anzeiger Bericht Über Die Biologisch-anthropologische Literatur 60, 267–71 (2002).

28. Yudin, N., Sergey, V. V., Potapova, T. A., Naykova, T. M., Sitnikova, V. V., Kulikov, I. V., Khasnulin, V. I., Konchuk, C., Vloschinskii, P. E., Ivanov, S. V., Kobzev, V. F., Romaschenko, A. G. & Voevoda, M. I. Distribution of CCR5-delta 32 gene deletion across the Russian part of Eurasia. Human Genetics 102, 695–698 (1998).

29. Su, Q., Mai, Z., Zang, N., Wu, S., Xiao, X. & Liang, H. Distribution of CCR5-Δ32, CCR2-64I, and SDF1-3'A in Guangxi Zhuang Population. J Int Assoc Physicians Aids Care 9, 145–149 (2010).

30. Hütter, G., Blüthgen, C., Elvers-Hornung, S., Klüter, H. & Bugert, P. Distribution of the CCR5-delta32 deletion in Southwest Germany. Hütter Gero 72, 303-309(7) (2015).

31. Wei, X. & Nielsen, R. CCR5-Δ32 is deleterious in the homozygous state in humans. Nat Med 1–2 (2019). doi:10.1038/s41591-019-0459-6

32. Kordelas, L., Verheyen, J., Beelen, D. W., Horn, P. A., Heinold, A., Kaiser, R., Trenschel, R., Schadendorf, D., Dittmer, U., Esser, S. & Group, E. H. A. Shift of HIV Tropism in Stem-Cell Transplantation with CCR5 Delta32 Mutation. New Engl J Medicine 371, 880–882 (2014).

33. Verheyen, J., Esser, S. & Kordelas, L. More on Shift of HIV Tropism in Stem-Cell Transplantation with CCR5 Delta32/Delta32 Mutation. New Engl J Medicine 371, 2437–2438 (2014).

34. Archer, J., Braverman, M. S., Taillon, B. E., Desany, B., James, I., Harrigan, R. P., Lewis, M. & Robertson, D. L. Detection of low-frequency pretherapy chemokine (CXC motif) receptor 4 (CXCR4)-using HIV-1 with ultra-deep pyrosequencing. Aids 23, 1209–1218 (2009).

35. Westby, M., Lewis, M., Whitcomb, J., Youle, M., Pozniak, A. L., James, I. T., Jenkins, T. M., Perros, M. & van der Ryst, E. Emergence of CXCR4-Using Human Immunodeficiency Virus Type 1 (HIV-1) Variants in a Minority of HIV-1-Infected Patients following Treatment with the CCR5 Antagonist Maraviroc Is from a Pretreatment CXCR4-Using Virus Reservoir. J Virol 80, 4909–4920 (2006).

36. Henrich, T. J., Hanhauser, E., Hu, Z., Stellbrink, H.-J., Noah, C., Martin, J. N., Deeks, S. G., Kuritzkes, D. R. & Pereyra, F. Viremic control and viral coreceptor usage in two HIV-1-infected persons homozygous for CCR5 &Dgr;32. Aids 29, 867–876 (2015).

37. Gray, L., Churchill, M. J., Keane, N., Sterjovski, J., Ellett, A. M., Purcell, D. F., Poumbourios, P., Kol, C., Wang, B., Saksena, N. K., Wesselingh, S. L., Price, P., French, M., Gabuzda, D. & Gorry, P. R. Genetic and Functional Analysis of R5X4 Human Immunodeficiency Virus Type 1 Envelope Glycoproteins Derived from Two Individuals Homozygous for the CCR5Δ32 Allele. J Virol 80, 3684–3691 (2006).

38. Egelhofer, M., Brandenburg, G., Martinius, H., Schult-Dietrich, P., Melikyan, G., Kunert, R., Baum, C., Choi, I., Alexandrov, A. & von Laer, D. Inhibition of Human Immunodeficiency Virus Type 1 Entry in Cells Expressing gp41-Derived Peptides. J Virol 78, 568–575 (2004).

39. Hildinger, M., Dittmar, M. T., Schult-Dietrich, P., Fehse, B., Schnierle, B. S., Thaler, S., Stiegler, G., Welker, R. & von Laer, D. Membrane-Anchored Peptide Inhibits Human Immunodeficiency Virus Entry. J Virol 75, 3038–3042 (2001).

40. Wild, C., Shugars, D., Greenwell, T., nal, C. & Matthews, T. Peptides corresponding to a predictive alpha-helical domain of human immunodeficiency virus type 1 gp41 are potent inhibitors of virus infection. Proc National Acad Sci 91, 9770–9774 (1994).

41. Wild, C., Dubay, J., Greenwell, T., Baird, T., Oas, T., nal, C., Hunter, E. & Matthews, T. Propensity for a leucine zipper-like domain of human immunodeficiency virus type 1 gp41 to

form oligomers correlates with a role in virus-induced fusion rather than assembly of the glycoprotein complex. Proc National Acad Sci 91, 12676–12680 (1994).

42. Dubay, J., Roberts, S., Brody, B. & Hunter, E. Mutations in the leucine zipper of the human immunodeficiency virus type 1 transmembrane glycoprotein affect fusion and infectivity. J Virol 66, 4748–56 (1992).

43. Chen, S., Lee, S., Hao, H. & Chuang, C. Mutations in the leucine zipper-like heptad repeat sequence of human immunodeficiency virus type 1 gp41 dominantly interfere with wild-type virus infectivity. J Virol 72, 4765–74 (1998).

44. Chen, S., Lee, C., Lee, W., McIntosh, K. & Lee, T. Mutational analysis of the leucine zipper-like motif of the human immunodeficiency virus type 1 envelope transmembrane glycoprotein. J Virol 67, 3615–9 (1993).

45. Ding, X., Zhang, X., Chong, H., Zhu, Y., Wei, H., Wu, X., He, J., Wang, X. & He, Y. Enfuvirtide (T20)-Based Lipopeptide Is a Potent HIV-1 Cell Fusion Inhibitor: Implications for Viral Entry and Inhibition. J Virol 91, e00831-17 (2017).

46. He, Y., Xiao, Y., Song, H., Liang, Q., Ju, D., Chen, X., Lu, H., Jing, W., Jiang, S. & Zhang, L. Design and Evaluation of Sifuvirtide, a Novel HIV-1 Fusion Inhibitor. J Biol Chem 283, 11126–11134 (2008).

47. Eggink, D., Berkhout, B. & Sanders, R. W. Inhibition of HIV-1 by Fusion Inhibitors. Curr Pharm Design 16, 3716–3728 (2010).

48. van Lunzen, J., Glaunsinger, T., Stahmer, I., von Baehr, V., Baum, C., Schilz, A., Kuehlcke, K., Naundorf, S., Martinius, H., Hermann, F., Giroglou, T., Newrzela, S., Müller, I., Brauer, F., Brandenburg, G., Alexandrov, A. & von Laer, D. Transfer of Autologous Gene-modified T Cells in HIV-infected Patients with Advanced Immunodeficiency and Drug-resistant Virus. Mol Ther 15, 1024–1033 (2007).

49. Qin, H., Cho, M., Haso, W., Zhang, L., Tasian, S. K., Oo, H., Negri, G., Lin, Y., Zou, J., Mallon, B. S., Maude, S., Teachey, D. T., Barrett, D. M., Orentas, R. J., Daugaard, M., Sorensen, P. H., Grupp, S. A. & Fry, T. J. Eradication of B-ALL using chimeric antigen receptor–expressing T cells targeting the TSLPR oncoprotein. Blood 126, 629–639 (2015).

50. Kochenderfer, J. N., Wilson, W. H., Janik, J. E., Dudley, M. E., Stetler-Stevenson, M., Feldman, S. A., Maric, I., Raffeld, M., Nathan, D.-A. N., Lanier, B. J., Morgan, R. A. & Rosenberg, S. A. Eradication of B-lineage cells and regression of lymphoma in a patient treated

with autologous T cells genetically engineered to recognize CD19. Blood 116, 4099–4102 (2010).

51. Maude, S. L., Frey, N., Shaw, P. A., Aplenc, R., Barrett, D. M., Bunin, N. J., Chew, A., Gonzalez, V. E., Zheng, Z., Lacey, S. F., Mahnke, Y. D., Melenhorst, J. J., Rheingold, S. R., Shen, A., Teachey, D. T., Levine, B. L., June, C. H., Porter, D. L. & Grupp, S. A. Chimeric Antigen Receptor T Cells for Sustained Remissions in Leukemia. New Engl J Medicine 371, 1507–1517 (2014).

52. Till, B. G., Jensen, M. C., Wang, J., Qian, X., Gopal, A. K., Maloney, D. G., Lindgren, C. G., Lin, Y., Pagel, J. M., Budde, L. E., Raubitschek, A., Forman, S. J., Greenberg, P. D., Riddell, S. R. & Press, O. W. CD20-specific adoptive immunotherapy for lymphoma using a chimeric antigen receptor with both CD28 and 4-1BB domains: pilot clinical trial results. Blood 119, 3940–3950 (2012).

53. Porter, D. L., Hwang, W.-T., Frey, N. V., Lacey, S. F., Shaw, P. A., Loren, A. W., Bagg, A., Marcucci, K. T., Shen, A., Gonzalez, V., Ambrose, D., Grupp, S. A., Chew, A., Zheng, Z., Milone, M. C., Levine, B. L., Melenhorst, J. J. & June, C. H. Chimeric antigen receptor T cells persist and induce sustained remissions in relapsed refractory chronic lymphocytic leukemia. Sci Transl Med 7, 303ra139-303ra139 (2015).

54. Porter, D. L., Levine, B. L., Kalos, M., Bagg, A. & June, C. H. Chimeric Antigen Receptor–Modified T Cells in Chronic Lymphoid Leukemia. New Engl J Medicine 365, 725–733 (2011).

55. Lamers, C., Sleijfer, S., Vulto, A. G., Kruit, W., Kliffen, M., Debets, R., Gratama, J. W., Stoter, G. & Oosterwijk, E. Treatment of Metastatic Renal Cell Carcinoma With Autologous T-Lymphocytes Genetically Retargeted Against Carbonic Anhydrase IX: First Clinical Experience. J Clin Oncol 24, e20–e22 (2006).

56. Luskin, M. R. & DeAngelo, D. J. Chimeric Antigen Receptor Therapy in Acute Lymphoblastic Leukemia Clinical Practice. Curr Hematol Malig R 12, 370–379 (2017).

57. Yu, S., Li, A., Liu, Q., Li, T., Yuan, X., Han, X. & Wu, K. Chimeric antigen receptor T cells: a novel therapy for solid tumors. J Hematol Oncol 10, 78 (2017).

58. Ramos, C. A., Savoldo, B. & Dotti, G. CD19-CAR Trials. Cancer J 20, 112–118 (2014).

59. Qasim, W., Zhan, H., Samarasinghe, S., Adams, S., Amrolia, P., Stafford, S., Butler, K., Rivat, C., Wright, G., Somana, K., Ghorashian, S., Pinner, D., Ahsan, G., Gilmour, K., Lucchini, G., Inglott, S., Mifsud, W., Chiesa, R., Peggs, K. S., Chan, L., Farzeneh, F., Thrasher, A. J., Vora, A., Pule, M. & Veys, P. Molecular remission of infant B-ALL after infusion of universal TALEN gene-edited CAR T cells. Sci Transl Med 9, eaaj2013 (2017).

60. Roberts, M. R., Qin, L., Zhang, D., Smith, D. H., Tran, A. C., Dull, T. J., Groopman, J. E., Capon, D. J., Byrn, R. A. & Finer, M. H. Targeting of human immunodeficiency virus-infected cells by CD8+ T lymphocytes armed with universal T-cell receptors. Blood 84, 2878–89 (1994).

61. Yang, O. O., Tran, A.-C., Kalams, S. A., Johnson, R. P., Roberts, M. R. & Walker, B. D. Lysis of HIV-1-infected cells and inhibition of viral replication by universal receptor T cells. Proc National Acad Sci 94, 11478–11483 (1997).

62. Scheppler, J., Nicholson, J., Swan, D., Ahmed-Ansari, A. & ugal, J. Down-modulation of MHC-I in a CD4+ T cell line, CEM-E5, after HIV-1 infection. J Immunol Baltim Md 1950 143, 2858–66 (1989).

63. KERKAU, T., SCHMITT-LANDGRAF, R., SCHIMPL, A. & WECKER, E. Downregulation of HLA Class I Antigens in HIV-1-Infected Cells. Aids Res Hum Retrov 5, 613–620 (1989).

64. Deeks, S. G., Wagner, B., Anton, P. A., Mitsuyasu, R. T., Scadden, D. T., Huang, C., Macken, C., Richman, D. D., Christopherson, C., June, C. H., Lazar, R., Broad, D. F., Jalali, S. & Hege, K. M. A Phase II Randomized Study of HIV-Specific T-Cell Gene Therapy in Subjects

with Undetectable Plasma Viremia on Combination Antiretroviral Therapy. Mol Ther 5, 788–797 (2002).

65. Scholler, J., Brady, T. L., Binder-Scholl, G., Hwang, W.-T., Plesa, G., Hege, K. M., Vogel, A. N., Kalos, M., Riley, J. L., Deeks, S. G., Mitsuyasu, R. T., Bernstein, W. B., Aronson, N. E., Levine, B. L., Bushman, F. D. & June, C. H. Decade-Long Safety and Function of Retroviral-Modified Chimeric Antigen Receptor T Cells. Sci Transl Med 4, 132ra53-132ra53 (2012).

66. Walker, R., Bechtel, C., Natarajan, V., Baseler, M., Hege, K., Metcalf, J., Stevens, R., Hazen, A., Blaese, R., Chen, C., Leitman, S., Palensky, J., Wittes, J., Davey, R., Falloon, J., Polis, M., Kovacs, J., Broad, D., Levine, B., Roberts, M., Masur, H. & Lane, H. Long-term in vivo survival of receptor-modified syngeneic T cells in patients with human immunodeficiency virus infection. Blood 96, 467–74 (2000).

67. Mitsuyasu, R., Anton, P., Deeks, S., Scadden, D., Connick, E., Downs, M., Bakker, A., Roberts, M., June, C., Jalali, S., Lin, A., Pennathur-Das, R. & Hege, K. Prolonged survival and tissue trafficking following adoptive transfer of CD4zeta gene-modified autologous CD4(+) and CD8(+) T cells in human immunodeficiency virus-infected subjects. Blood 96, 785–93 (2000).

68. Oliveira, S., Ryan, C., Giannoni, F., Hardee, C. L., Tremcinska, I., Katebian, B., Wherley, J., Sahaghian, A., Tu, A., Grogan, T., Elashoff, D., Cooper, L. J., Hollis, R. P. & Kohn, D. B.

Modification of Hematopoietic Stem/Progenitor Cells with CD19-Specific Chimeric Antigen Receptors as a Novel Approach for Cancer Immunotherapy. Hum Gene Ther 24, 824–839 (2013).

69. Savoldo, B., Ramos, C., Liu, E., Mims, M. P., Keating, M. J., Carrum, G., Kamble, R. T., Bollard, C. M., Gee, A. P., Mei, Z., Liu, H., Grilley, B., Rooney, C. M., Heslop, H. E., Brenner, M. K. & Dotti, G. CD28 costimulation improves expansion and persistence of chimeric antigen receptor–modified T cells in lymphoma patients. J Clin Invest 121, 1822–1826 (2011).

70. Gschweng, E., Oliveira, S. & Kohn, D. B. Hematopoietic stem cells for cancer immunotherapy. Immunol Rev 257, 237–249 (2014).

71. Larson, S. & Oliveira, S. N. Gene-modified hematopoietic stem cells for cancer immunotherapy. Hum Vacc Immunother 10, 982–985 (2014).

72. Zhen, A., Kamata, M., Rezek, V., Rick, J., Levin, B., Kasparian, S., Chen, I. S., Yang, O. O., Zack, J. A. & Kitchen, S. G. HIV-specific Immunity Derived From Chimeric Antigen Receptor-engineered Stem Cells. Mol Ther 23, 1358–1367 (2015).

73. Zhen, A., Peterson, C. W., Carrillo, M. A., Reddy, S. S., Youn, C. S., Lam, B. B., Chang, N. Y., Martin, H. A., Rick, J. W., Kim, J., Neel, N. C., Rezek, V. K., Kamata, M., Chen, I. S. Y.,

Zack, J. A., Kiem, H.-P. & Kitchen, S. G. Long-term persistence and function of hematopoietic stem cell-derived chimeric antigen receptor T cells in a nonhuman primate model of HIV/AIDS. Plos Pathog 13, e1006753 (2017).

74. Badowski, M. S., Zhang, T., Tsang, T. C. & Harris, D. T. Chimeric antigen receptors for stem cell based immunotherapy. J Exp Ther Oncol 8, 53–63 (2009).

75. Tran, A., Zhang, D., Byrn, R. & Roberts, M. Chimeric zeta-receptors direct human natural killer (NK) effector function to permit killing of NK-resistant tumor cells and HIV-infected T lymphocytes. J Immunol Baltim Md 1950 155, 1000–9 (1995).

76. Schirrmann, T. & Pecher, G. Specific targeting of CD33+ leukemia cells by a natural killer cell line modified with a chimeric receptor. Leukemia Res 29, 301–306 (2005).

77. Li, L., Liu, L., Feller, S., Allen, C., Shivakumar, R., Fratantoni, J., Wolfraim, L., Fujisaki, H., Campana, D., Chopas, N., Dzekunov, S. & Peshwa, M. Expression of chimeric antigen receptors in natural killer cells with a regulatory-compliant non-viral method. Cancer Gene Ther 17, 147 (2010).

78. Hege, K. M., Cooke, K. S., Finer, M. H., Zsebo, K. M. & Roberts, M. R. Systemic T Cell–independent Tumor Immunity after Transplantation of Universal Receptor–modified Bone Marrow into SCID Mice. J Exp Medicine 184, 2261–2270 (1996).

79. Han, J., Chu, J., Chan, W., Zhang, J., Wang, Y., Cohen, J. B., Victor, A., Meisen, W. H., Kim, S., Grandi, P., Wang, Q.-E., He, X., Nakano, I., Chiocca, A. E., III, J. C., Kaur, B., Caligiuri, M. A. & Yu, J. CAR-Engineered NK Cells Targeting Wild-Type EGFR and EGFRvIII Enhance Killing of Glioblastoma and Patient-Derived Glioblastoma Stem Cells. Sci Rep-uk 5, 11483 (2015).

80. Roberts, M., Cooke, K., Tran, A., Smith, K., Lin, W., Wang, M., Dull, T., Farson, D., Zsebo, K. & Finer, M. Antigen-specific cytolysis by neutrophils and NK cells expressing chimeric immune receptors bearing zeta or gamma signaling domains. J Immunol Baltim Md 1950 161, 375–84 (1998).

81. Fox, C. H., Tenner-Rácz, K., Rácz, P., Firpo, A., Pizzo, P. A. & Fauci, A. S. Lymphoid germinal centers are reservoirs of human immunodeficiency virus type 1 RNA. J Infect Dis 164, 1051–7 (1991).

82. Miles, B. & Connick, E. TFH in HIV Latency and as Sources of Replication-Competent Virus. Trends Microbiol 24, 338–344 (2016).

83. Fukazawa, Y., Lum, R., Okoye, A. A., Park, H., Matsuda, K., Bae, J. Y., Hagen, S. I., Shoemaker, R., Deleage, C., Lucero, C., Morcock, D., Swanson, T., Legasse, A. W., Axthelm, M. K., Hesselgesser, J., Geleziunas, R., Hirsch, V. M., Edlefsen, P. T., Jr, M. P., Estes, J. D., Lifson, J. D. & Picker, L. J. B cell follicle sanctuary permits persistent productive simian immunodeficiency virus infection in elite controllers. Nat Med 21, 132–139 (2015).

84. Aid, M., Dupuy, F. P., Moysi, E., Moir, S., Haddad, E. K., Estes, J. D., Sekaly, R., Petrovas, C. & Ribeiro, S. Follicular CD4 T Helper Cells As a Major HIV Reservoir Compartment: A Molecular Perspective. Front Immunol 9, 895 (2018).

85. Bronnimann, M. P., Skinner, P. J. & Connick, E. The B-Cell Follicle in HIV Infection: Barrier to a Cure. Frontiers in Immunology 9, 20 (2018).

86. Barton, K., Winckelmann, A. & Palmer, S. HIV-1 Reservoirs During Suppressive Therapy. Trends Microbiol 24, 345–355 (2016).

87. Smith, M. Z., Wightman, F. & Lewin, S. R. HIV Reservoirs and Strategies for Eradication. Curr Hiv-aids Rep 9, 5–15 (2012).

88. Hellmuth, J., Valcour, V. & Spudich, S. CNS reservoirs for HIV: implications for eradication. J Virus Erad 1, 67–71 (2015).

89. Thompson, K. A., Cherry, C. L., Bell, J. E. & McLean, C. A. Brain Cell Reservoirs of Latent Virus in Presymptomatic HIV-Infected Individuals. Am J Pathology 179, 1623–1629 (2011).

90. Gama, L., Abreu, C. M., Shirk, E. N., Price, S. L., Li, M., Laird, G. M., Pate, K. A. M., Wietgrefe, S. W., O'Connor, S. L., Pianowski, L., Haase, A. T., Van Lint, C., Siliciano, R. F., Clements, J. E. & Group, T. L.-S. S. Reactivation of simian immunodeficiency virus reservoirs in the brain of virally suppressed macaques. Aids 31, 5 (2017).

91. Bednar, M. M., Sturdevant, C., Tompkins, L. A., Arrildt, K., Dukhovlinova, E., Kincer, L. P. & Swanstrom, R. Compartmentalization, Viral Evolution, and Viral Latency of HIV in the CNS. Curr Hiv-aids Rep 12, 262–271 (2015).

92. Petito, C. K., Chen, H., Mastri, A. R., Torres-Munoz, J., Roberts, B. & Wood, C. HIV infection of choroid plexus in AIDS and asymptomatic HIV-infected patients suggests that the choroid plexus may be a reservoir of productive infection. J Neurovirol 5, 670–677 (1999).

93. Chaillon, A., Gianella, S., Wertheim, J. O., Richman, D. D., Mehta, S. R. & Smith, D. M. HIV Migration Between Blood and Cerebrospinal Fluid or Semen Over Time. J Infect Dis 209, 1642–1652 (2014).

94. Chun, T.-W., Nickle, D. C., Justement, J. S., Meyers, J. H., Roby, G., Hallahan, C. W., Kottilil, S., Moir, S., Mican, J. M., Mullins, J. I., Ward, D. J., A., K. J., Mannon, P. J. & Fauci, A. S. Persistence of HIV in Gut-Associated Lymphoid Tissue despite Long-Term Antiretroviral Therapy. J Infect Dis 197, 714–720 (2008).

95. Lampinen, T. M., Critchlow, C. W., Kuypers, J. M., Hurt, C. S., Nelson, P. J., Hawes, S. E., Coombs, R. W., Holmes, K. K. & Kiviat, N. B. Association of antiretroviral therapy with detection of HIV-1 RNA and DNA in the anorectal mucosa of homosexual men. Aids 14, F69 (2000).

96. Lerner, P., Guadalupe, M., Donovan, R., Hung, J., Flamm, J., Prindiville, T., Sankaran-Walters, S., Syvanen, M., Wong, J. K., George, M. D. & Dandekar, S. The Gut Mucosal Viral Reservoir in HIV-Infected Patients Is Not the Major Source of Rebound Plasma Viremia following Interruption of Highly Active Antiretroviral Therapy. J Virol 85, 4772–4782 (2011).

97. Poles, M. A., Boscardin, W. J., Elliott, J., Taing, P., Fuerst, M. M. P., McGowan, I., Brown, S. & Anton, P. A. Lack of Decay of HIV-1 in Gut-Associated Lymphoid Tissue Reservoirs in Maximally Suppressed Individuals. Jaids J Acquir Immune Defic Syndromes 43, 65 (2006).

98. Di Stefano, M., Favia, A., Monno, L., Lopalco, P., Caputi, O., Scardigno, A. C., Pastore, G., Fiore, J. R. & Angarano, G. Intracellular and cell-free (infectious) HIV-1 in rectal mucosa. J Med Virol 65, 637–643 (2001).

99. Dandekar, S. Pathogenesis of HIV in the gastrointestinal tract. Curr Hiv-aids Rep 4, 10–15 (2007).

100. Smith, P. D., Meng, G., Salazar-Gonzalez, J. F. & Shaw, G. M. Macrophage HIV-1 infection and the gastrointestinal tract reservoir. J Leukocyte Biol 74, 642–649 (2003).

101. Yukl, S. A., Gianella, S., Sinclair, E., Epling, L., Li, Q., Duan, L., Choi, A. L. M., Girling, V., Ho, T., Li, P., Fujimoto, K., Lampiris, H., Hare, C. B., Pandori, M., Haase, A. T., Günthard, H. F., Fischer, M., Shergill, A. K., McQuaid, K., Havlir, D. V. & Wong, J. K. Differences in HIV Burden and Immune Activation within the Gut of HIV-Positive Patients Receiving Suppressive Antiretroviral Therapy. J Infect Dis 202, 1553–1561 (2010).

102. Belmonte, L., Olmos, M., Fanin, A., Parodi, C., Baré, P., Concetti, H., Pérez, H., de Bracco, M. M. E. & Cahn, P. The intestinal mucosa as a reservoir of HIV-1 infection after successful HAART. Aids 21, 2106 (2007).

103. Brown, D. & Mattapallil, J. J. Gastrointestinal Tract and the Mucosal Macrophage Reservoir in HIV Infection. Clin Vaccine Immunol 21, 1469–1473 (2014).

104. Hlavacek, W. S., Stilianakis, N. I. & Perelson, A. S. Influence of follicular dendritic cells on HIV dynamics. Philosophical Transactions Royal Soc Lond Ser B Biological Sci 355, 1051–1058 (2000).

105. Smith, B. A., Gartner, S., Liu, Y., Perelson, A. S., Stilianakis, N. I., Keele, B. F., Kerkering, T. M., Ferreira-Gonzalez, A., Szakal, A. K., Tew, J. G. & Burton, G. F. Persistence of Infectious HIV on Follicular Dendritic Cells. J Immunol 166, 690–696 (2001).

106. Heesters, B. A., Lindqvist, M., Vagefi, P. A., Scully, E. P., Schildberg, F. A., Altfeld, M., Walker, B. D., Kaufmann, D. E. & Carroll, M. C. Follicular Dendritic Cells Retain Infectious HIV in Cycling Endosomes. Plos Pathog 11, e1005285 (2015).

107. Zhang, J. & Perelson, A. S. Contribution of Follicular Dendritic Cells to Persistent HIV Viremia. J Virol 87, 7893–7901 (2013).

108. Brauer, F., Schmidt, K., Zahn, R. C., Richter, C., Radeke, H. H., Schmitz, J. E., von Laer, D. & Egerer, L. A Rationally Engineered Anti-HIV Peptide Fusion Inhibitor with Greatly Reduced Immunogenicity. Antimicrob Agents Ch 57, 679–688 (2013).

109. Song, R., Chenine, A.-L., Rasmussen, R., Ruprecht, C., Mirshahidi, S., Grisson, R., Xu, W., Whitney, J., Goins, L., Ong, H., Li, P.-L., Shai-Kobiler, E., Wang, T., McCann, C., Zhang, H., Wood, C., Kankasa, C., Secor, W., McClure, H., Strobert, E., Else, J. & Ruprecht, R. Molecularly Cloned SHIV-1157ipd3N4: a Highly Replication- Competent, Mucosally Transmissible R5 Simian-Human Immunodeficiency Virus Encoding HIV Clade C env. J Virol 80, 8729–8738 (2006).

110. Peterson, C. W., Younan, P., Polacino, P. S., Maurice, N. J., Miller, H. W., Prlic, M., Jerome, K. R., Woolfrey, A. E., Hu, S. & Kiem, H. Robust suppression of env-SHIV viremia in Macaca nemestrina by 3-drug ART is independent of timing of initiation during chronic infection. Journal of Medical Primatology 42, 237–246 (2013).

111. Peterson, C. W., Haworth, K. G., Burke, B. P., Polacino, P., Norman, K. K., Adair, J. E., Hu, S.-L., Bartlett, J. S., Symonds, G. P. & Kiem, H.-P. Multilineage polyclonal engraftment of Cal-1 gene-modified cells and in vivo selection after SHIV infection in a nonhuman primate model of AIDS. Mol Ther - Methods Clin Dev 3, 16007 (2016).

112. Stack, E. C., Wang, C., Roman, K. A. & Hoyt, C. C. Multiplexed immunohistochemistry, imaging, and quantitation: A review, with an assessment of Tyramide signal amplification, multispectral imaging and multiplex analysis. Methods 70, 46–58 (2014).

113. Snyder, J. M., Washington, I. M., Birkland, T., Chang, M. Y. & Frevert, C. W. Correlation of Versican Expression, Accumulation, and Degradation during Embryonic Development by Quantitative Immunohistochemistry. J Histochem Cytochem 63, 952–967 (2015).

114. Bankhead, P., Loughrey, M. B., Fernández, J. A., Dombrowski, Y., McArt, D. G., Dunne, P. D., McQuaid, S., Gray, R. T., Murray, L. J., Coleman, H. G., James, J. A., Salto-Tellez, M. & Hamilton, P. W. QuPath: Open source software for digital pathology image analysis. Sci Rep-uk 7, 16878 (2017).

115. Rueden, C. T., Schindelin, J., Hiner, M. C., DeZonia, B. E., Walter, A. E., Arena, E. T. & Eliceiri, K. W. ImageJ2: ImageJ for the next generation of scientific image data. BMC Bioinformatics 18, 529 (2017).

116. Schneider, C. A., Rasband, W. S. & Eliceiri, K. W. NIH Image to ImageJ: 25 years of image analysis. Nature methods 9, 671–5 (2012).

117. Schindelin, J., Arganda-Carreras, I., Frise, E., Kaynig, V., Longair, M., Pietzsch, T., Preibisch, S., Rueden, C., Saalfeld, S., Schmid, B., Tinevez, J.-Y., White, D., Hartenstein, V., Eliceiri, K., Tomancak, P. & Cardona, A. Fiji: an open-source platform for biological-image analysis. Nature Methods 9, 676 (2012).

118. MUTTERER, J. & ZINCK, E. Quick-and-clean article figures with FigureJ. Journal of Microscopy 252, 89–91 (2013).

119. Estes, J. D., Harris, L. D., Klatt, N. R., Tabb, B., Pittaluga, S., Paiardini, M., Barclay, R. G., Smedley, J., Pung, R., Oliveira, K. M., Hirsch, V. M., Silvestri, G., Douek, D. C., Miller, C. J., Haase, A. T., Lifson, J. & Brenchley, J. M. Damaged Intestinal Epithelial Integrity Linked to Microbial Translocation in Pathogenic Simian Immunodeficiency Virus Infections. Plos Pathog 6, e1001052 (2010).

120. Camp, R. L., Chung, G. G. & Rimm, D. L. Automated subcellular localization and quantification of protein expression in tissue microarrays. Nat Med 8, nm791 (2002).

121. Sternberg, S. R. Biomedical Image Processing. Computer 16, 22–34 (1983).

122. Otsu, N. A Threshold Selection Method from Gray-Level Histograms. IEEE Transactions on Systems, Man, and Cybernetics 9, 62–66 (1979).

123. Shah, N. J., Mao, A. S., Shih, T.-Y. Y., Kerr, M. D., Sharda, A., Raimondo, T. M., Weaver, J. C., Vrbanac, V. D., Deruaz, M., Tager, A. M., Mooney, D. J. & Scadden, D. T. An injectable bone marrow-like scaffold enhances T cell immunity after hematopoietic stem cell transplantation. Nature biotechnology 37, 293–302 (2019).

124. Silva, N. S. & Klein, U. Dynamics of B cells in germinal centres. Nat Rev Immunol 15, 137–148 (2015).

125. Victora, G. D. & Mesin, L. Clonal and cellular dynamics in germinal centers. Curr Opin Immunol 28, 90–96 (2014).

126. Scaradavou, A. HIV-related thrombocytopenia. Blood Rev 16, 73–76 (2002).

127. Gill, A. F., Ahsan, M. H., Lackner, A. A. & Veazey, R. S. Hematologic abnormalities associated with simian immunodeficieny virus (SIV) infection mimic those in HIV infection. J Med Primatol 41, 214–224 (2012).

128. Hacein-Bey-Abina, S., Deist, F., Carlier, F., Bouneaud, C., Hue, C., Villartay, J.-P., Thrasher, A. J., Wulffraat, N., Sorensen, R., Dupuis-Girod, S., Fischer, A., Davies, G. E., Kuis,

W., Leiva, L. & Cavazzana-Calvo, M. Sustained Correction of X-Linked Severe Combined Immunodeficiency by ex Vivo Gene Therapy. New Engl J Medicine 346, 1185–1193 (2002).

129. Baum, C., Düllmann, J., Li, Z., Fehse, B., Meyer, J., Williams, D. A. & von Kalle, C. Side effects of retroviral gene transfer into hematopoietic stem cells. Blood 101, 2099–2113 (2003).

130. Kohn, D. B., Sadelain, M. & Glorioso, J. C. Occurrence of leukaemia following gene therapy of X-linked SCID. Nat Rev Cancer 3, 477–488 (2003).

131. Hacein-Bey-Abina, S., von Kalle, C., Schmidt, M., Deist, F., Wulffraat, N., McIntyre, E., Radford, I., Villeval, J.-L., Fraser, C. C., Cavazzana-Calvo, M. & Fischer, A. A Serious Adverse Event after Successful Gene Therapy for X-Linked Severe Combined Immunodeficiency. New Engl J Medicine 348, 255–256 (2003).

132. Hacein-Bey-Abina, S., Kalle, V. C., Schmidt, M., McCormack, M., Wulffraat, N., Leboulch, P., Lim, A., Osborne, C., Pawliuk, R., Morillon, E., Sorensen, R., Forster, A., Fraser, P., Cohen, J., de Basile, S. G., Alexander, I., Wintergerst, U., Frebourg, T., Aurias, A., Stoppa-Lyonnet, D., Romana, S., Radford-Weiss, I., Gross, F., Valensi, F., Delabesse, E., Macintyre, E., Sigaux, F., Soulier, J., Leiva, L., Wissler, M., Prinz, C., Rabbitts, T., Deist, L. F., Fischer, A. & Cavazzana-Calvo, M. LMO2-Associated Clonal T Cell Proliferation in Two Patients after Gene Therapy for SCID-X1. Science 302, 415–419 (2003).

133. Romano, G. Development of Safer Gene Delivery Systems to Minimize the Risk of Insertional Mutagenesis-Related Malignancies: A Critical Issue for the Field of Gene Therapy. Isrn Oncol 2012, 616310 (2012).

134. Edelstein, M. L., Abedi, M. R. & Wixon, J. Gene therapy clinical trials worldwide to 2007—an update. J Gene Medicine 9, 833–842 (2007).

135. Baum, C. Gene Therapy for SCID-X1: Focus on Clinical Data. Mol Ther 19, 2103–2104 (2011).

136. Cavazzana-Calvo, M. & Fischer, A. Gene therapy for severe combined immunodeficiency: are we there yet? J Clin Invest 117, 1456–1465 (2007).

137. Hacein-Bey-Abina, S., Garrigue, A., Wang, G. P., Soulier, J., Lim, A., Morillon, E., Clappier, E., Caccavelli, L., Delabesse, E., Beldjord, K., Asnafi, V., MacIntyre, E., Cortivo, L., Radford, I., Brousse, N., Sigaux, F., Moshous, D., Hauer, J., Borkhardt, A., Belohradsky, B. H., Wintergerst, U., Velez, M. C., Leiva, L., Sorensen, R., Wulffraat, N., Blanche, S., Bushman, F. D., Fischer, A. & Cavazzana-Calvo, M. Insertional oncogenesis in 4 patients after retrovirus-mediated gene therapy of SCID-X1. J Clin Invest 118, 3132–3142 (2008).

138. Howe, S. J., Mansour, M. R., Schwarzwaelder, K., Bartholomae, C., Hubank, M., Kempski, H., Brugman, M. H., Pike-Overzet, K., Chatters, S. J., de Ridder, D., Gilmour, K. C., Adams, S., Thornhill, S. I., Parsley, K. L., Staal, F., Gale, R. E., Linch, D. C., Bayford, J., Brown, L., Quaye, M., Kinnon, C., Ancliff, P., Webb, D. K., Schmidt, M., von Kalle, C., Gaspar, B. H. & Thrasher, A. J. Insertional mutagenesis combined with acquired somatic mutations causes leukemogenesis following gene therapy of SCID-X1 patients. J Clin Invest 118, 3143–3150 (2008).

139. Pike-Overzet, K., van der Burg, M., Wagemaker, G., van Dongen, J. J. & Staal, F. J. New Insights and Unresolved Issues Regarding Insertional Mutagenesis in X-linked SCID Gene Therapy. Mol Ther 15, 1910–1916 (2007).

140. Chinen, J. & Puck, J. M. Successes and risks of gene therapy in primary immunodeficiencies. J Allergy Clin Immun 113, 595–603 (2004).

141. Murnane, R., Zhang, X., Hukkanen, R., Vogel, K., Kelley, S. & Kiem, H. Myelodysplasia in 2 Pig-Tailed Macaques (Macaca nemestrina) Associated With Retroviral Vector–Mediated Insertional Mutagenesis and Overexpression of HOXB4. Vet Pathol 48, 999–1001 (2011).

142. David, R. M. & Doherty, A. T. Viral Vectors: The Road to Reducing Genotoxicity. Toxicol Sci 155, 315–325 (2017).

143. Schambach, A., Zychlinski, D., Ehrnstroem, B. & Baum, C. Biosafety Features of Lentiviral Vectors. Hum Gene Ther 24, 132–142 (2013).

144. Marktel, S., Scaramuzza, S., Cicalese, M., Giglio, F., Galimberti, S., Lidonnici, M., Calbi, V., Assanelli, A., Bernardo, M., Rossi, C., Calabria, A., Milani, R., Gattillo, S., Benedicenti, F., Spinozzi, G., Aprile, A., Bergami, A., Casiraghi, M., Consiglieri, G., Masera, N., D'Angelo, E., Mirra, N., Origa, R., Tartaglione, I., Perrotta, S., Winter, R., Coppola, M., Viarengo, G., Santoleri, L., Graziadei, G., Gabaldo, M., Valsecchi, M., Montini, E., Naldini, L., Cappellini, M., Ciceri, F., Aiuti, A. & Ferrari, G. Intrabone hematopoietic stem cell gene therapy for adult and pediatric patients affected by transfusion-dependent ß-thalassemia. Nat Med 25, 234–241 (2019).

145. Thompson, A. A., Walters, M. C., Kwiatkowski, J., Rasko, J., Ribeil, J.-A., Hongeng, S., Magrin, E., Schiller, G. J., Payen, E., Semeraro, M., Moshous, D., Lefrere, F., Puy, H., Bourget, P., Magnani, A., Caccavelli, L., Diana, J.-S., Suarez, F., Monpoux, F., Brousse, V., Poirot, C., Brouzes, C., Meritet, J.-F., Pondarré, C., Beuzard, Y., Chrétien, S., Lefebvre, T., Teachey, D. T., Anurathapan, U., Ho, J. P., von Kalle, C., Kletzel, M., Vichinsky, E., Soni, S., Veres, G., Negre, O., Ross, R. W., Davidson, D., Petrusich, A., Sandler, L., Asmal, M., Hermine, O., Montalembert, M., Hacein-Bey-Abina, S., Blanche, S., Leboulch, P. & Cavazzana, M. Gene Therapy in Patients with Transfusion-Dependent β-Thalassemia. New Engl J Medicine 378, 1479–1493 (2018).

146. Cavazzana-Calvo, M., Payen, E., Negre, O., Wang, G., Hehir, K., Fusil, F., Down, J., Denaro, M., Brady, T., Westerman, K., Cavallesco, R., Gillet-Legrand, B., Caccavelli, L., Sgarra, R., Maouche-Chrétien, L., Bernaudin, F., Girot, R., Dorazio, R., Mulder, G.-J., Polack, A., Bank, A., Soulier, J., Larghero, J., Kabbara, N., Dalle, B., Gourmel, B., Socie, G., Chrétien, S., Cartier, N., Aubourg, P., Fischer, A., Cornetta, K., Galacteros, F., Beuzard, Y., Gluckman, E., Bushman, F., Hacein-Bey-Abina, S. & Leboulch, P. Transfusion independence and HMGA2 activation after gene therapy of human β-thalassaemia. Nature 467, 318 (2010).

147. Eichler, F., Duncan, C., Musolino, P. L., Orchard, P. J., Oliveira, S., Thrasher, A. J., Armant, M., Dansereau, C., Lund, T. C., Miller, W. P., Raymond, G. V., Sankar, R., Shah, A. J., Sevin, C., Gaspar, B. H., Gissen, P., Amartino, H., Bratkovic, D., Smith, N., Paker, A. M., Shamir, E., O'Meara, T., Davidson, D., Aubourg, P. & Williams, D. A. Hematopoietic Stem-Cell Gene Therapy for Cerebral Adrenoleukodystrophy. New Engl J Medicine 377, 1630–1638 (2017).

148. Cartier, N., Hacein-Bey-Abina, S., Bartholomae, C. C., Veres, G., Schmidt, M., Kutschera, I., Vidaud, M., Abel, U., Dal-Cortivo, L., Caccavelli, L., Mahlaoui, N., Kiermer, V., Mittelstaedt, D., Bellesme, C., Lahlou, N., Lefrère, F., Blanche, S., Audit, M., Payen, E., Leboulch, P., l'Homme, B., Bougnères, P., Kalle, C., Fischer, A., Cavazzana-Calvo, M. & Aubourg, P. Hematopoietic Stem Cell Gene Therapy with a Lentiviral Vector in X-Linked Adrenoleukodystrophy. Science 326, 818–823 (2009).

149. Morris, E. C., Fox, T., Chakraverty, R., Tendeiro, R., Snell, K., Rivat, C., Grace, S., Gilmour, K., Workman, S., Buckland, K., Butler, K., Chee, R., Salama, A. D., Ibrahim, H., Hara, H., Duret, C., Mavilio, F., Male, F., Bushman, F. D., Galy, A., Burns, S. O., Gaspar, B. H. & Thrasher, A. J. Gene therapy for Wiskott-Aldrich syndrome in a severely affected adult. Blood 130, 1327–1335 (2017).

150. Abina, S., Gaspar, B. H., Blondeau, J., Caccavelli, L., Charrier, S., Buckland, K., Picard, C., Six, E., Himoudi, N., Gilmour, K., McNicol, A.-M., Hara, H., Xu-Bayford, J., Rivat, C., Touzot, F., Mavilio, F., Lim, A., Treluyer, J.-M., Héritier, S., Lefrère, F., Magalon, J., Pengue-Koyi, I., Honnet, G., Blanche, S., Sherman, E. A., Male, F., Berry, C., Malani, N., Bushman, F. D., Fischer, A., Thrasher, A. J., Galy, A. & Cavazzana, M. Outcomes Following Gene Therapy in Patients With Severe Wiskott-Aldrich Syndrome. Jama 313, 1550–1563 (2015).

151. Aiuti, A., Biasco, L., Scaramuzza, S., Ferrua, F., Cicalese, M., Baricordi, C., Dionisio, F., Calabria, A., Giannelli, S., Castiello, M., Bosticardo, M., Evangelio, C., Assanelli, A., Casiraghi, M., Nunzio, S., Callegaro, L., Benati, C., Rizzardi, P., Pellin, D., Serio, C., Schmidt, M., Kalle, C., Gardner, J., Mehta, N., Neduva, V., Dow, D. J., Galy, A., Miniero, R., Finocchi, A., Metin, A., Banerjee, P. P., Orange, J. S., Galimberti, S., Valsecchi, M., Biffi, A., Montini, E., Villa, A., Ciceri, F., Roncarolo, M. & Naldini, L. Lentiviral Hematopoietic Stem Cell Gene Therapy in Patients with Wiskott-Aldrich Syndrome. Science 341, 1233151 (2013).

152. Ravin, S., Wu, X., Moir, S., Kardava, L., Anaya-O'Brien, S., Kwatemaa, N., Littel, P., Theobald, N., Choi, U., Su, L., Marquesen, M., Hilligoss, D., Lee, J., Buckner, C. M., Zarember, K. A., O'Connor, G., McVicar, D., Kuhns, D., Throm, R. E., Zhou, S., Notarangelo, L. D., Hanson, C. I., Cowan, M. J., Kang, E., Hadigan, C., Meagher, M., Gray, J. T., Sorrentino, B. P. & Malech, H. L. Lentiviral hematopoietic stem cell gene therapy for X-linked severe combined immunodeficiency. Sci Transl Med 8, 335ra57-335ra57 (2016).

153. Mamcarz, E., Zhou, S., Lockey, T., Abdelsamed, H., Cross, S. J., Kang, G., Ma, Z., Condori, J., Dowdy, J., Triplett, B., Li, C., Maron, G., Becerra, J. C., Church, J. A., Dokmeci, E., Love, J. T., da Ain, A. C., van der Watt, H., Tang, X., Janssen, W., Ryu, B. Y., Ravin, S., Weiss, M. J., Youngblood, B., Long-Boyle, J. R., Gottschalk, S., Meagher, M. M., Malech, H. L., Puck, J. M., Cowan, M. J. & Sorrentino, B. P. Lentiviral Gene Therapy Combined with Low-Dose Busulfan in Infants with SCID-X1. New Engl J Med 380, 1525–1534 (2019).

154. Aiuti, A., Cattaneo, F., Galimberti, S., Benninghoff, U., Cassani, B., Callegaro, L., Scaramuzza, S., Andolfi, G., Mirolo, M., Brigida, I., Tabucchi, A., Carlucci, F., Eibl, M., Aker, M., Slavin, S., Al-Mousa, H., Ghonaium, A., Ferster, A., Duppenthaler, A., Notarangelo, L., Wintergerst, U., Buckley, R. H., Bregni, M., Marktel, S., Valsecchi, M., Rossi, P., Ciceri, F., Miniero, R., Bordignon, C. & Roncarolo, M.-G. Gene Therapy for Immunodeficiency Due to Adenosine Deaminase Deficiency. New Engl J Medicine 360, 447–458 (2009).

155. Biffi, A., Montini, E., Lorioli, L., Cesani, M., Fumagalli, F., Plati, T., Baldoli, C., Martino, S., Calabria, A., Canale, S., Benedicenti, F., Vallanti, G., Biasco, L., Leo, S., Kabbara, N., Zanetti, G., Rizzo, W. B., Mehta, N. A., Cicalese, M., Casiraghi, M., Boelens, J. J., Carro, U., Dow, D. J., Schmidt, M., Assanelli, A., Neduva, V., Serio, C., Stupka, E., Gardner, J., von Kalle, C., Bordignon, C., Ciceri, F., Rovelli, A., Roncarolo, M., Aiuti, A., Sessa, M. & Naldini, L. Lentiviral Hematopoietic Stem Cell Gene Therapy Benefits Metachromatic Leukodystrophy. Science 341, 1233158 (2013).

156. Shaw, K. L., Garabedian, E., Mishra, S., Barman, P., Davila, A., Carbonaro, D., Shupien, S., Silvin, C., Geiger, S., Nowicki, B., Smogorzewska, M. E., Brown, B., Wang, X., de Oliveira, S., Choi, Y., Ikeda, A., Terrazas, D., Fu, P.-Y., Yu, A., Fernandez, B., Cooper, A. R., Engel, B., Podsakoff, G., Balamurugan, A., Anderson, S., Muul, L., Jagadeesh, J. G., Kapoor, N., Tse, J., Moore, T. B., Purdy, K., Rishi, R., Mohan, K., Skoda-Smith, S., Buchbinder, D., Abraham, R. S., Scharenberg, A., Yang, O. O., Cornetta, K., Gjertson, D., Hershfield, M., Sokolic, R., Candotti, F. & Kohn, D. B. Clinical efficacy of gene-modified stem cells in adenosine deaminase–deficient immunodeficiency. J Clin Invest 127, 1689–1699 (2017).

157. Kroese, F. G., Wubbena, A. S., Seijen, H. G. & Nieuwenhuis, P. Germinal centers develop oligoclonally. European Journal of Immunology 17, 1069–1072 (1987).

158. Eglitis, M. A. & Mezey, É. Hematopoietic cells differentiate into both microglia and macroglia in the brains of adult mice. Proceedings of the National Academy of Sciences 94, 4080–4085 (1997).

159. Prinz, M., Erny, D. & Hagemeyer, N. Ontogeny and homeostasis of CNS myeloid cells. Nat Immunol 18, 385–392 (2017).

160. Kierdorf, K., Katzmarski, N., Haas, C. A. & Prinz, M. Bone Marrow Cell Recruitment to the Brain in the Absence of Irradiation or Parabiosis Bias. Plos One 8, e58544 (2013).

161. Filip, S., Mokrý, J., Vávrová, J., Šinkorová, Z., Mičuda, S., Šponer, P., Filipová, A., Hrebíková, H. & Dayanithi, G. The peripheral chimerism of bone marrow–derived stem cells after transplantation: regeneration of gastrointestinal tissues in lethally irradiated mice. J Cell Mol Med 18, 832–843 (2014).

162. Linderman, J. A. & Shizuru, J. A. Rapid Reconstitution of Antibody Responses Following Transplantation of Purified Allogeneic Hematopoietic Stem Cells. J Immunol 186, 4191–4199 (2011).

163. Goldmann, T., Wieghofer, P., Jordão, M., Prutek, F., Hagemeyer, N., Frenzel, K., Amann, L., Staszewski, O., Kierdorf, K., Krueger, M., Locatelli, G., Hochgerner, H., Zeiser, R.,

Epelman, S., Geissmann, F., Priller, J., Rossi, F. M., Bechmann, I., Kerschensteiner, M., Linnarsson, S., Jung, S. & Prinz, M. Origin, fate and dynamics of macrophages at central nervous system interfaces. Nat Immunol 17, 797–805 (2016).

164. Ajami, B., Bennett, J. L., Krieger, C., Tetzlaff, W. & Rossi, F. M. Local self-renewal can sustain CNS microglia maintenance and function throughout adult life. Nat Neurosci 10, nn2014 (2007).

165. Priller, J., Flügel, A., Wehner, T., Boentert, M., Haas, C. A., Prinz, M., Fernández-Klett, F., Prass, K., Bechmann, I., de Boer, B. A., Frotscher, M., Kreutzberg, G. W., Persons, D. A. & Dirnagl, U. Targeting gene-modified hematopoietic cells to the central nervous system: Use of green fluorescent protein uncovers microglial engraftment. Nat Med 7, nm1201-1356 (2001).

166. Massengale, M., Wagers, A. J., Vogel, H. & Weissman, I. L. Hematopoietic cells maintain hematopoietic fates upon entering the brain. J Exp Medicine 201, 1579–1589 (2005).

167. Mildner, A., Schmidt, H., Nitsche, M., Merkler, D., Hanisch, U.-K., Mack, M., Heikenwalder, M., Brück, W., Priller, J. & Prinz, M. Microglia in the adult brain arise from Ly-6ChiCCR2+ monocytes only under defined host conditions. Nat Neurosci 10, nn2015 (2007).

168. Mildner, A., Schlevogt, B., Kierdorf, K., Böttcher, C., Erny, D., Kummer, M. P., Quinn, M., Brück, W., Bechmann, I., Heneka, M. T., Priller, J. & Prinz, M. Distinct and Non-Redundant Roles of Microglia and Myeloid Subsets in Mouse Models of Alzheimer's Disease. J Neurosci 31, 11159–11171 (2011).

169. Lampron, A., Lessard, M. & Rivest, S. Effects of Myeloablation, Peripheral Chimerism, and Whole-Body Irradiation on the Entry of Bone Marrow-Derived Cells into the Brain. Cell Transplant 21, 1149–1159 (2011).

170. Diserbo, M., Agin, A., Lamproglou, I., Mauris, J., Staali, F., Multon, E. & Amourette, C. Blood-brain barrier permeability after gamma whole-body irradiation: an in vivo microdialysis study. Can J Physiol Pharm 80, 670–678 (2002).

171. Yuan, H., Gaber, M. W., McColgan, T., Naimark, M. D., Kiani, M. F. & Merchant, T. E. Radiation-induced permeability and leukocyte adhesion in the rat blood–brain barrier: modulation with anti-ICAM-1 antibodies. Brain Res 969, 59–69 (2003).

172. Kaya, M., Palanduz, A., Kalayci, R., Kemikler, G., Simsek, G., Bilgic, B., Ahishali, B., Arican, N., Kocyildiz, Z., Elmas, I., Kucuk, M. & Karadeniz, A. Effects of lipopolysaccharide on the radiation-induced changes in the blood–brain barrier and the astrocytes. Brain Res 1019, 105–112 (2004).

173. Li, Y.-Q., Chen, P., Jain, V., Reilly, R. M. & Wong, S. C. Early Radiation-Induced Endothelial Cell Loss and Blood–Spinal Cord Barrier Breakdown in the Rat Spinal Cord. Radiat Res 181, 143–152 (2004).

174. Garvin, A. M., Davis, C. B., Littman, D. R., Carlow, D. A., Teh, H.-S., Forbush, K. A. & Perlmutter, R. M. Participation of CD4 coreceptor molecules in T-cell repertoire selection. Nature 349, 241 (1991).

175. Norment, A. M., Forbush, K. A., Nguyen, N., Malissen, M. & Perlmutter, R. M. Replacement of Pre-T Cell Receptor Signaling Functions by the CD4 Coreceptor. The Journal of Experimental Medicine 185, 121–130 (1997).

176. Lin, W. & Roberts, M. R. Developmental dissociation of T cells from B, NK, and myeloid cells revealed by MHC class II–specific chimeric immune receptors bearing TCR-ζ or FcR-γ chain signaling domains. Blood 100, 3045–3048 (2002).

177. Brogdon, J., Eckels, D., Davies, C., White, S. & Doyle, C. A site for CD4 binding in the beta 1 domain of the MHC class II protein HLA-DR1. Journal of immunology (Baltimore, Md. : 1950) 161, 5472–80 (1998).

178. König, R., Shen, X. & Germain, R. Involvement of both major histocompatibility complex class II alpha and beta chains in CD4 function indicates a role for ordered oligomerization in T cell activation. J Exp Medicine 182, 779–787 (1995).

179. Scheirle, A., Takacs, B., Doran, D. M., Sinigaglia, F., Cammarota, G., Guardiola, J., Knorr, R. & Bannwarth, W. Identification of a CD4 binding site on the β2 domain of HLA-DR molecules. Nature 356, 799 (1992).

180. Coordinators, N. Database resources of the National Center for Biotechnology Information. Nucleic Acids Res 42, D7–D17 (2014).

181. Hagn, M. & Jahrsdörfer, B. Why do human B cells secrete granzyme B? Insights into a novel B-cell differentiation pathway. Oncoimmunology 1, 1368–1375 (2012).

182. Hagn, M., Schwesinger, E., Ebel, V., Sontheimer, K., Maier, J., Beyer, T., Syrovets, T., Laumonnier, Y., Fabricius, D., Simmet, T. & Jahrsdörfer, B. Human B Cells Secrete Granzyme B When Recognizing Viral Antigens in the Context of the Acute Phase Cytokine IL-21. J Immunol 183, 1838–1845 (2009).

183. Lindner, S., Dahlke, K., Sontheimer, K., Hagn, M., Kaltenmeier, C., Barth, T. F. E., Beyer, T., Reister, F., Fabricius, D., Lotfi, R., Lunov, O., Nienhaus, G. U., Simmet, T., Kreienberg, R.,

Möller, P., Schrezenmeier, H. & Jahrsdörfer, B. Interleukin 21–Induced Granzyme B–Expressing B Cells Infiltrate Tumors and Regulate T Cells. Cancer Res 73, 2468–2479 (2013).

184. Hagn, M., Panikkar, A., Smith, C., Jr, H. H. B., Khanna, R., Voskoboinik, I. & Trapani, J. A. B cell-derived circulating granzyme B is a feature of acute infectious mononucleosis. Clin Transl Immunol 4, e38 (2015).

185. Hagn, M., Sontheimer, K., Dahlke, K., Brueggemann, S., Kaltenmeier, C., Beyer, T., Hofmann, S., Lunov, O., Barth, T. F., Fabricius, D., Tron, K., Nienhaus, G. U., Simmet, T., Schrezenmeier, H. & Jahrsdörfer, B. Human B cells differentiate into granzyme B-secreting cytotoxic B lymphocytes upon incomplete T-cell help. Immunol Cell Biol 90, 457 (2012).

186. Long, A. H., Haso, W. M., Shern, J. F., Wanhainen, K. M., Murgai, M., Ingaramo, M., Smith, J. P., Walker, A. J., Kohler, E. M., Venkateshwara, V. R., Kaplan, R. N., Patterson, G. H., Fry, T. J., Orentas, R. J. & Mackall, C. L. 4-1BB costimulation ameliorates T cell exhaustion induced by tonic signaling of chimeric antigen receptors. Nat Med 21, 581–590 (2015).

187. Imai, C., Mihara, K., Andreansky, M., Nicholson, I., Pui, C.-H., Geiger, T. & Campana, D. Chimeric receptors with 4-1BB signaling capacity provoke potent cytotoxicity against acute lymphoblastic leukemia. Leukemia 18, 2403302 (2004).

188. Loskog, A., Giandomenico, V., Rossig, C., Pule, M., Dotti, G. & Brenner, M. Addition of the CD28 signaling domain to chimeric T-cell receptors enhances chimeric T-cell resistance to T regulatory cells. Leukemia 20, 2404366 (2006).

189. Wang, J., Jensen, M., Lin, Y., Sui, X., Chen, E., Lindgren, C. G., Till, B., Raubitschek, A., Forman, S. J., Qian, X., James, S., Greenberg, P., Riddell, S. & Press, O. W. Optimizing Adoptive Polyclonal T Cell Immunotherapy of Lymphomas, Using a Chimeric T Cell Receptor Possessing CD28 and CD137 Costimulatory Domains. Hum Gene Ther 18, 712–725 (2007).

190. Chmielewski, M. & Abken, H. TRUCKs: the fourth generation of CARs. Expert Opin Biol Th 15, 1145–1154 (2015).

191. Milone, M. C., Fish, J. D., Carpenito, C., Carroll, R. G., Binder, G. K., Teachey, D., Samanta, M., Lakhal, M., Gloss, B., Danet-Desnoyers, G., Campana, D., Riley, J. L., Grupp, S. A. & June, C. H. Chimeric Receptors Containing CD137 Signal Transduction Domains Mediate Enhanced Survival of T Cells and Increased Antileukemic Efficacy In Vivo. Mol Ther 17, 1453–1464 (2009).

192. Joseph, A., Zheng, J. H., Chen, K., Dutta, M., Chen, C., Stiegler, G., Kunert, R., Follenzi, A. & Goldstein, H. Inhibition of In Vivo HIV Infection in Humanized Mice by Gene Therapy of

Human Hematopoietic Stem Cells with a Lentiviral Vector Encoding a Broadly Neutralizing Anti-HIV Antibody. J Virol 84, 6645–6653 (2010).

193. Kuhlmann, A.-S., Haworth, K. G., Barber-Axthelm, I. M., Ironside, C., Giese, M. A., Peterson, C. W. & Kiem, H.-P. Long-Term Persistence of Anti-HIV Broadly Neutralizing Antibody-Secreting Hematopoietic Cells in Humanized Mice. Mol Ther (2018). doi:10.1016/j.ymthe.2018.09.017

194. Padte, N. N., Yu, J., Huang, Y. & Ho, D. D. Engineering multi-specific antibodies against HIV-1. Retrovirology 15, 60 (2018).